FIRE RESISTANCE OF EPOXIED STEEL RODS IN GLULAM TIMBER

A report submitted in partial fulfilment of the requirements for the degree of Master of Engineering at the University of Canterbury, Christchurch, New Zealand.

by

David J. Barber

February, 1994.

ABSTRACT

Timber connections using threaded rods epoxied in glulam timber are becoming more prevalent in use throughout the construction industry and as such their fire resistance must be investigated.

The research conducted here was based on finding how strength and stiffness of the cured epoxy was affected by elevated temperatures. Testing was carried out using an oven to simulate heat exposure and with full scale furnace tests.

Results show that the epoxies tested lost stiffness at approximately 45 to 55°C. As temperatures rise the strength of the connection becomes less dependent on embedment length and more dependent on the temperature within the epoxy. Steel rods epoxied into the ends of glulam members can achieve a 30 minute fire rating with at least 50 to 60mm timber cover.

ACKNOWLEDGEMENTS

The research in this report was carried out at the Civil Engineering Department, University of Canterbury, Christchurch and at the fire research laboratory of Building Technology Limited, Wellington.

This project would not have been possible without the financial assistance of the New Zealand Fire Service and the numerous products donated by Hunter Timber Laminates of Nelson, Wormalds, Nuplex Industries and Adhesive Technologies Ltd.

I would like to thank my supervisor Dr. Andrew Buchanan for all his time, guidance and enthusiasm over the duration of this project. I would also like to thank him for sending me to various conferences throughout the country, where I learnt a great deal of valuable information. Thanks must also go to Dr. Jonathan Barnett and Assistant Commander Wayne Bedford for their knowledge, enthusiasm and ability to always pay for the first round of beers.

I would also like to thank Mark Stuart-Jones for his time and input during the testing (and also letting me listen to RDU in the lab!). Thanks also go to Ray, Norrie, Frank and to Geoff Hill for his overall assistance.

Of course a big thanks goes to all my friends and flatmates for putting up with me, to Scott and Steve for answering my phone and to William for helping with the spreadsheet approach. Finally thanks must go to Kate for keeping me out of trouble.

TABLE OF CONTENTS

List of Tables and Figures.

Tables

Figures

Chapter 1

Chapter 2

Chapter 3

Chapter 4

Chapter 5

Chapter 6

Chapter 7

Notation Used

A	=	Cross sectional area (m^2)
A_c	=	Core thread area (mm^2)
c	=	Specific heat (J/kg °K)
c_c	=	Specific heat of char (J/kg °K)
c_w	=	Specific heat of wood (J/kg °K)
D	=	Dead load (kN)
D_b	=	Basic density (kg/m^3)
$D_{n,12}$	=	Density at 12% moisture content (kg/m^3)
d	=	Bar diameter (mm)
d	=	Depth of timber section (mm)
F	=	Pull out strength (kN)
f_b	=	Characteristic stress of timber in bending (MPa)
f_c	=	Char contraction factor
f_u	=	Stress capacity of a timber member (MPa)
f_y	=	Yield strength (MPa)
H	=	Quantity of heat transferred (W)
H_f	=	Calorific value of wood at a particular moisture content (MJ/kg)
H_u	=	Calorific value of dry wood (MJ/kg)
k	=	Thermal conductivity (W/m°K)
k_a	=	Bar type factor
k_b	=	Epoxy type factor
k_c	=	Moisture content factor
k_1	=	Load duration factor
k_4	=	Parallel support factor
k_8	=	Stability factor
k_9	=	Glulam size factor
L	=	Live load (kN)
L	=	Length (m)
l	=	Embedment length (mm)
m	=	Moisture content (%)
r	=	Radial distance from centre line of bar to fire exposed edge (mm)

r	=	Corner radius (mm)
r_h	=	Ratio of hole diameter to bar diameter
r_e	=	Ratio of edge distance from bar centreline to bar diameter
S_o	=	Specific gravity
t	=	time (seconds)
T	=	Temperature (°C or °K)
T	=	Tension load (kN)
ΔT	=	Difference in temperature (°C)
T_g	=	Glass transition temperature (°C)
X_c	=	Thickness of charred sample (mm)
X_o	=	Original thickness of sample (mm)
$X_{w,res}$	=	Thickness of residue once char removed (mm)
Y_c	=	Mass fraction of char
α	=	Thermal diffusivity (m^2/s)
β	=	Charring rate (mm/min)
ρ	=	Density (kg/m^3)
ρ_c	=	Char density (kg/m^3)
ρ_o	=	Oven dry density (kg/m^3)
ϕ	=	Capacity reduction factor

CHAPTER 1

INTRODUCTION

1.1 Timber Connections.

Traditional methods of providing moment resisting connections in glue-laminated timber (glulam) has been to use metal or timber plates, nailed or screwed to the exterior. Bolts can also be used. Curved members can eliminate the need for moment resisting connections (Charleson & Patience, 1993). A method developed and used in Denmark is to place threaded steel rods (dowels) into pre-drilled holes in glulam beams and bond these with epoxy.

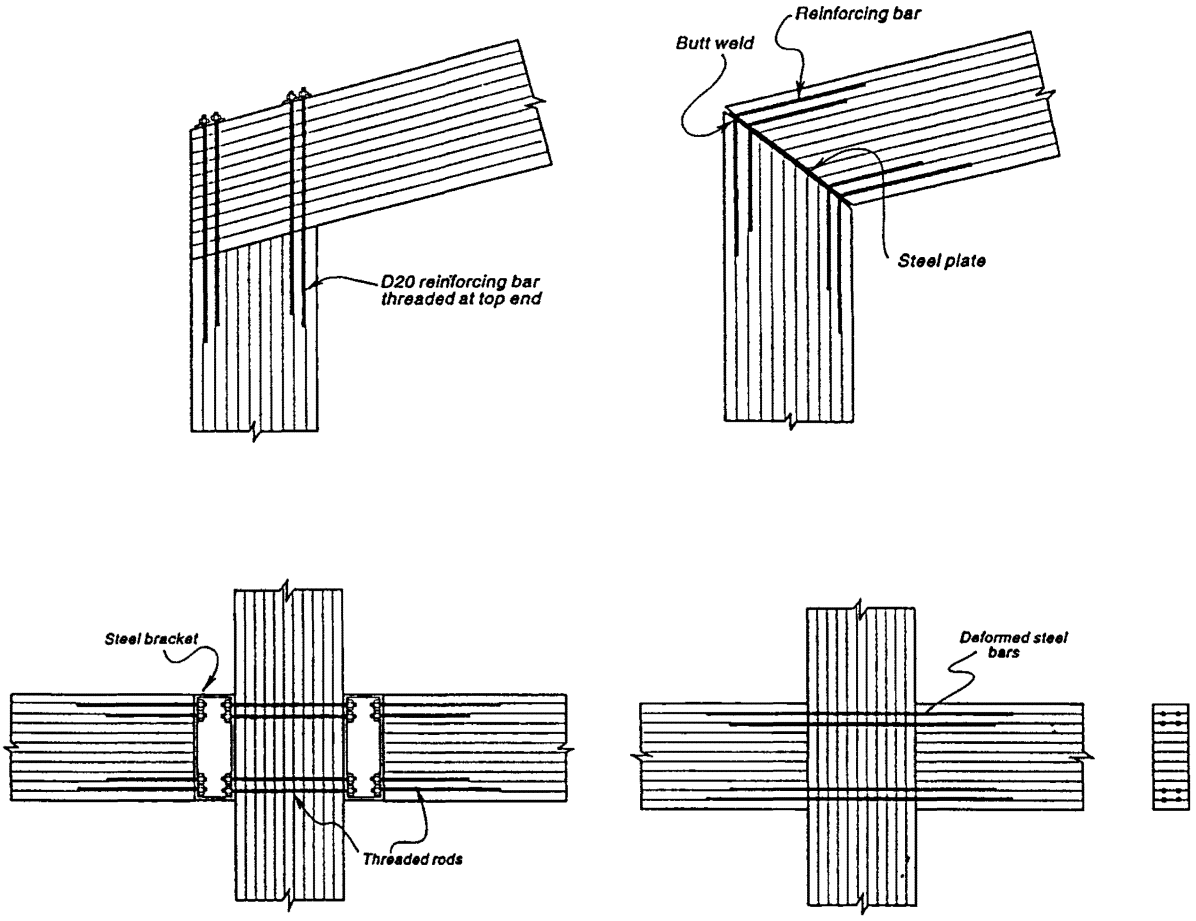

Figure 1.1. Examples of Epoxy Rod Connections in Glulam Joints, (Buchanan & Fairweather, 1994)

Research into applying this method in New Zealand conditions has been carried out at the University of Canterbury by Townsend (1990), Fairweather (1992) and Deng (1993). Experimental work has all been carried out using radiata pine. These connections have been used in a small number of major glulam structures (Buchanan and Fletcher, 1989; McIntosh, 1989). The advantages of using the epoxy rod connections are,

a, the hidden fastener provides an aesthetic connection,
b, connections can be fabricated off the building site,
c, steel components are protected from corrosion by the timber,
d, steel dowels are not as susceptible to fire, as are exterior metal or timber plates.
e, the epoxy provides a bond stronger than the wood.

It is hoped that once current research is completed into epoxy rod connections, their use will become more prevalent in the timber construction industry.

1.2 Aim of Research.

This research investigates how the epoxy rod connection reacts in fire conditions. The epoxy dowel connection has been assumed to have good fire resistance due to timber possessing a very low conductivity of heat. To investigate how the full-size connection would react at elevated temperatures, computer modelling was used to analyse heat transfer through the charring wood and was validated by two series of tests. The first set of tests was to investigate the tension strength of the connection at elevated temperatures by using an oven to heat the epoxy rod connection. Temperatures in the range of 40 to 90°C were chosen for the testing program. The second set of tests were full-size tension members exposed to standard fire conditions in a furnace. These tests were to validate the computer modelling and to compare the oven tests with results from a full-size fire test, following a standard time temperature curve.

1.3 Connection Resistance to Load.

The epoxy rod connection resists forces by transferring loads from the steel into the epoxy and then to the wood fibres. The general term to describe this process is bond stress, which describes the shear transfer process. Bond strength between epoxy and wood provides the connection with the means to resist the applied loads. Epoxy-wood bond strength is due to adhesion and microscopic penetration of the epoxy into the wood. Bond between the steel and epoxy cannot be relied on, unless the steel is sandblasted and cleaned thoroughly. Thus the main component of resistance between the threaded rod and the epoxy is the mechanical bearing of the threads. This is shown in figure 1.2. Failure of the connection can occur in five ways,

a, failure by shear within the epoxy, along a plane at thread top height

b, failure by bond at the wood/epoxy surface

c, wood failure in splitting, due to lack of confinement

d, wood failure in tension

e, yielding of steel bar in tension.

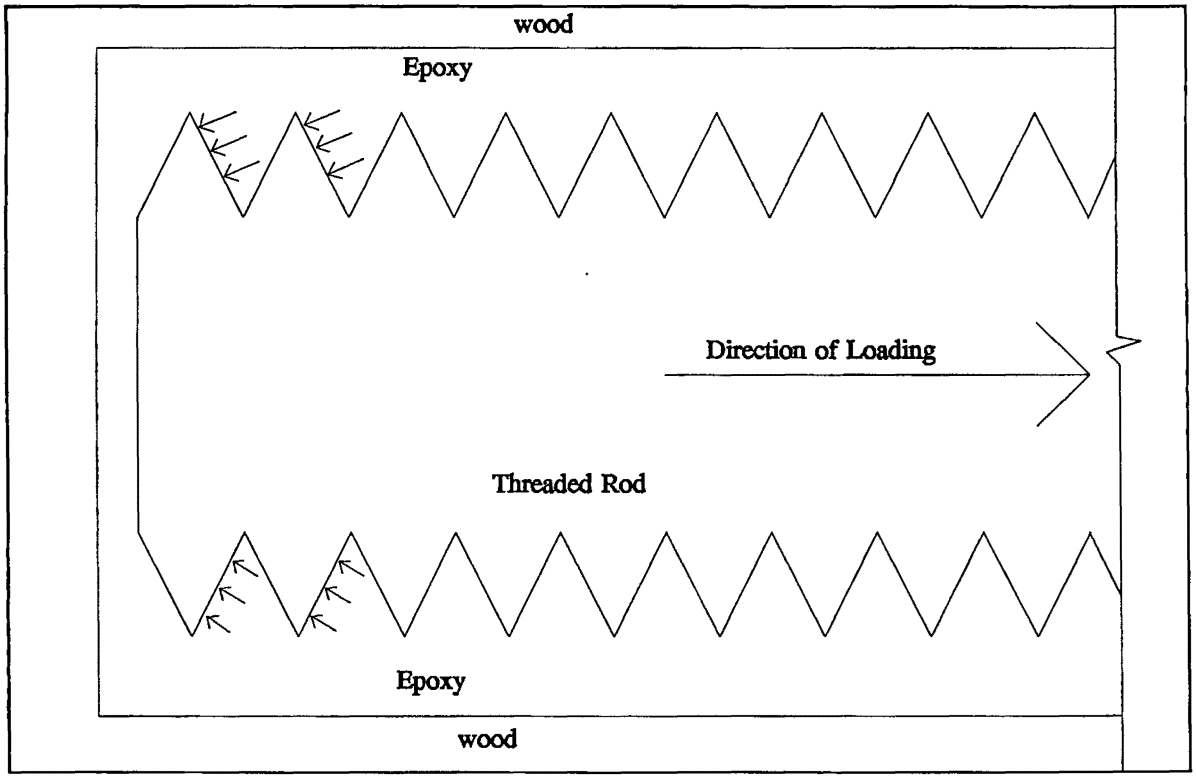

Figure 1.2. Schematic Diagram of Mechanical Resistance to Applied Load at the Epoxy - Threaded Rod Interface (not to scale).

1.4 Fire Resistance Rating.

A fire resistance rating (FRR) for a material or a construction is the length of time that it will carry its design load and fulfil its design function when subject to a standard fire in a carefully controlled test. The accepted approach to achieve a FRR is to expose the member to a standard fire test (figure 1.3) for a specific time under a design load. The prime requirement tested for is that a structural element must not collapse under load. Additional requirements for containing elements such as floors and walls are that they must retain insulation and flames must not pass through.

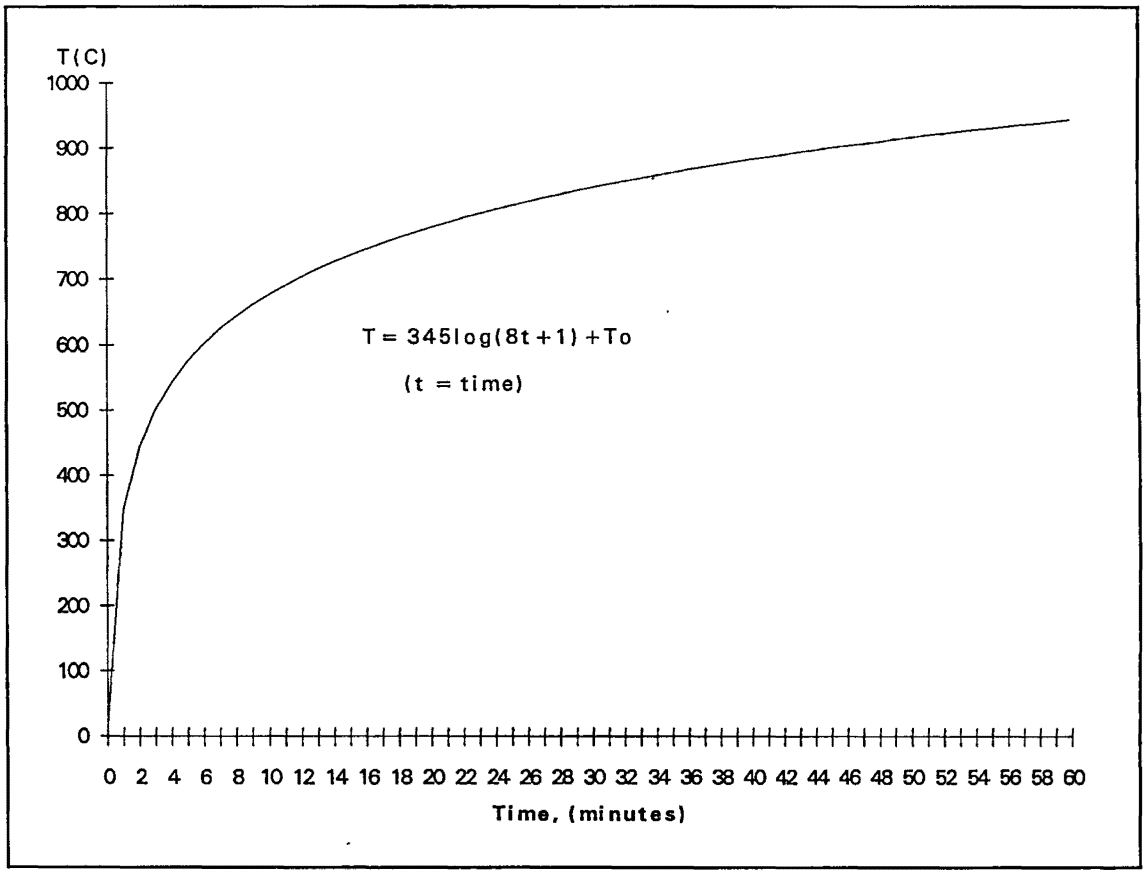

Figure 1.3. ISO 834 Standard Fire.

FRR values required for a structure vary due to building requirements and type of hazard involved. Usual requirements for structural elements are 30, 60 or 90 minute FRR. A minimum of 30 minutes FRR must be attainable to allow fire service access. From the structural point of view the requirements in a fire are for the elements to contain the fire in compartments and ensure that the structure remain intact and carry load throughout the fire and subsequent salvage operations. Life safety is of prime consideration (FEDG, 1993).

1.5 The Standard Fire.

To compare fire tests throughout the world, a standard furnace time-temperature curve is used. The ISO834 fire curve is designed not to predict actual fire conditions but to prescribe a standard fire for comparing the performance of various materials (figure 1.3). Because fire is so complex, efforts to mimic real fire with bench-scale testing are almost futile. Instead, the predominant philosophy of fire testing is to use a standard test with full size specimens.

CHAPTER 2

STRENGTH OF WOOD IN FIRE

2.1 Pyrolysis of Timber.

Timber as a structural material differs from most other common building materials as it is combustible. When heat is applied to wood a process of thermal degradation or pyrolysis occurs, leading to production of flammable vapours, accompanied by a loss in weight. Wood weight decreases initially above 100°C due to loss of moisture and at temperatures greater than 200°C complete carbonization will start to occur. When a surface has been ignited, the combustion continues at a certain rate of penetration. A surface charcoal layer is then formed, which because of its low thermal conductivity becomes good protection against heat for the interior timber. The charcoal layer also obstructs the oxygen access from the outside to the interior combustion zone. The penetration of heat into the pyrolysis zone can be markedly increased by cracks or other deformities in the timber.

2.1.1 Rate of Pyrolysis.

The rate of pyrolysis can be defined as the rate of weight loss measured during a fire, thus the rate of charring is proportional to the timber weight loss. When heat is applied to wood a process of thermal degradation or pyrolysis occurs, leading to the production of combustible and non-combustible gases, inflammable tars, charcoal and accompanied by a loss in weight. In the presence of oxygen the pyrolysis gas leaving the surface may be ignited and flaming combustion may be self-sustaining if enough of the heat is retained by the wood. The pyrolysis process is impeded by the build up of a layer of thermally insulating char. Thus the burning rate describes the rate at which a given material is consumed by fire and can be described in terms of heat release rate, mass loss rate or charring rate.

2.1.2 Heat Transfer Through Wood.

Wood is unique in the fact that whilst burning occurs it insulates itself with a layer of charcoal. Just after ignition the rate of heat release is high because volatiles diffuse easily

through the surface layer. But later the growing char layer acts as an insulator for the uncharred wood within, due to the thermal conductivity of charcoal being one half to a third that of unburnt timber (Mikkola, 1990). This means that the heat exposure for the protected uncharred wood is lower than for unprotected wood. As a consequence the rate of heat release decreases from its maximum, and after some time reaches a nearly constant value when the thickness of the char layer remains practically constant. The amount of heat transferred by surface flaming to the unburnt portion of wood decreases as the layer of char on the surface increases, resulting in a decrease in the rate of pyrolysis. Eventually flaming will stop unless there is sufficient external heat impinging on the surface. The penetration at the edges of the cross-section is also more rapid, giving a more rounded shape to the edges of the section. As wood burns, changes gradually take place (Tsoumis, 1991);

1. Evaporation of moisture (up to 100°C)

2. Evaporation of volatile substances (95 - 150°C)

3. Superficial carbonization and slow exit of flammable gases (150 - 200°C)

4. Faster exit of flammable gases, followed by ignition and glow (200 - 370°C)

5. Fast ignition of flammable gases and formation of glowing charcoal (370 - 500°C)

The calorific value (heat of combustion) of dry wood varies from 17MJ/kg to 22.5MJ/kg. Average values quoted are 18.6 to 19.75 MJ/kg (TRADA, 1971). Of this about one half to two thirds is liberated by flaming and the rest by glowing once the wood burns. The value is lower in wet wood as the heat must warm the water first before burning can occur. To convert a dry wood calorific value, H_u (MJ/kg), to that at a particular moisture content, the following equation can be used (CIB, 1986),

$$H_f = H_u(1-0.01m) - 0.025m \quad MJ/kg \qquad 2.1$$

where m = moisture content in %, by weight

2.2 Modelling Pyrolysis of Wood.

A theoretical study of the pyrolysis of a wood slab has been carried out by Kung (1972), based on a section of wood with one side heated and the other side insulated and impervious. Assumptions of the model include, the fuel volatiles are regarded as flowing out of the solid immediately after generation, inward moisture migration is ignored and secondary chemical reactions between the char and volatiles are ignored. The model does include heat convected by outward flow of volatiles. A partially pyrolysed element of wood is regarded as being partly residual char and partly as yet unpyrolysed active material. As the element pyrolyses the active material is continuously converted into fuel volatiles and residual char. Thus differential equations are set up and solved using linear interpolation between wood properties and char.

Parker (1988) has developed a model to predict the heat release rate of wood during flaming combustion. The model is based on the thermochemical properties of Douglas fir and will calculate the time to ignition, heat release rate and heat of combustion. The model takes into account char contraction, mass retention fraction of char, absorbed moisture and the variation in thermochemical and thermo-physical properties with temperature. The model was validated using slabs of Douglas fir at specific external flux's and had reasonable agreement.

2.2.1 Modelling Fire Resistance and Strength of Glulam Timber Members.

An early model for predicting fire resistance of timber members was formulated by Lie, based on theoretical and experimental work by other researchers (Lie, 1977). Using the semi-empirical formulas of Imaizumi (1963), Lie developed some simple formulations for columns and beams exposed to fires. The formulations were validated by using the data of fire tests on glulam beams other researchers had completed. Lie has assumed that the load conditions during a fire should not include wind or earthquake, due to the low probability that all these conditions will occur at once. But he has assumed that there may be snow load present, and has accounted for this with an applied design snow load of 50%. To check the theoretical formula he compared it with collected experimental beam fire tests of Fackler, Malhotro and Rogowski and derived approximate formulas for the fire resistance of beams.

Majamaa (1991) formulated a time-to-failure model for timber beams under standard fire exposure. The model is based on linear theory of elasticity and takes into account temperature and moisture affects on strength and stiffness. Majamaa's model predicts the time to failure for a wooden beam by calculating analytically the effect of a transition zone between charred and uncharred wood, by splitting this transition zone into layers. Each layer is assumed to have constant thermal properties, modulus of elasticity and bending stress. The bending moment capacity of a fire exposed wooden beam cross-section is restricted by the natural defects of wood as well as by finger joints. This work assumes failure in the tensile edge of a beam before any plastic deformation at the compressive edge can occur. In wooden beams defects such as knots and sloping grain can cause a reduction in the tensile strength, thus normally the beam will fail in tension. With burning around three edges normally exposing the tension edge, the assumption of failure on the tension side is reasonable for simply supported beams. The model results in a set of equations for the reduced bending stress due to the number of transition areas and reduced moment of inertia. The calculated values compare well with fire test results and are able to predict specific code failure times within 10%, and on the safe side.

A reliability-based model has been developed to predict the strength of glulam beams and the time to failure, under fire conditions (Bender et. al, 1985). The model is based on beams in bending and the assumption the failure is in the tension zone and that the section acts in an elastic manner. Based on the strength equations of Imaizumi (1963) and using a Monte Carlo simulation for the values of modulus of elasticity, tensile strength, end joint tensile strength and timber length a model was derived to predict the strength of the beam in cold conditions. Once the model had been validated with failure tests, all at room temperature, the model was extended to predict fire conditions. The model was able to predict accurately fire tests on Douglas fir glulam beams, though further fire tests on a more extensive size and species range will be needed.

2.3 Timber Strength.

Glulam strength is classically based on testing small clear specimens and reducing this strength by appropriate factors for size, knots and imperfections. Latest methods include finite element calculations, Monte-Carlo simulations and full-scale testing of ordinary specimens.

Most timbers have good tensile strength in relation to compressive strength, and because of their high tensile and compressive strengths along the grain, they can withstand substantial bending loads. Strength properties are roughly related to wood density, with denser timbers tending to be stronger than lighter ones.

In New Zealand the design load under fire conditions is less than for normal design because of the low probability of coincidence of maximum live load and fire (SNZ, 1993). Although wood is a combustible material its load bearing capacity is good as long as the residual cross-section is large enough. This is due to the uncharred wood in a large cross section staying at moderate temperatures, even in a long duration fire.

2.3.1 Strength Reduction in Fire Conditions.

Usual fire performance prediction method assumes a constant char rate and simply calculates the amount of wood consumed during some interval. The strength of the uncharred beam cross section is then calculated using classical beam bending theory. When a specific time for fire endurance is stipulated, the calculated residual section is expected to support its design loads.

Imaizumi (1963) has used this basic method to calculate the residual strength in a section exposed to fire. A strength reduction factor is applied to account for the temperature affects on modulus of elasticity and other strength properties. The Imaizumi equations are simple to use and provide a quick method for checking fire resistance.

The strength of wood parallel to the grain is in general decreased by a rise in the temperature and the duration of the application of load (Schaffer, 1977). Strength losses become significant once the temperature range of 150 to 200°C is reached within the wood. Prolonged high temperature may considerably reduce the strength of exposed wood, but if the wood is exposed to high temperatures for a relatively short period there may only be a small reduction in its strength properties (TRADA, 1971). Under fire exposure a heavy member will show a slow predictable reduction in cross-section and reduction in strength, due to the charring action. Loss of load carrying ability is caused by the loss in cross section and also by the decrease in strength properties due to the timber being heated. Also the change in moisture

content affects the strength of the timber, as strength will decrease rapidly at first due to the increased moisture content, but this affect is for a relatively short period.

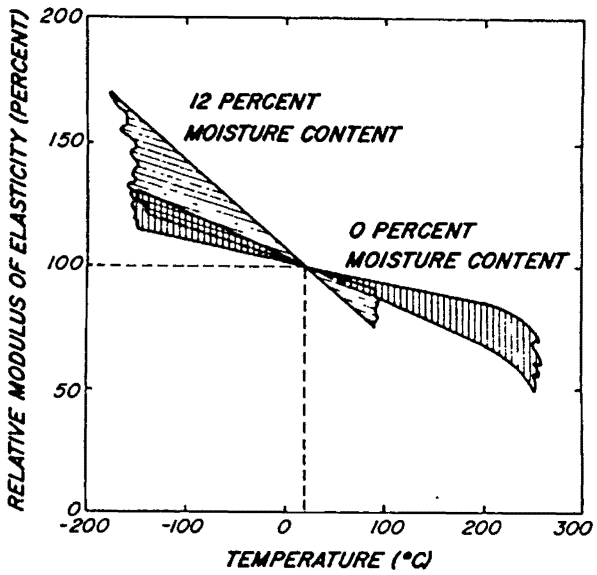

Figure 2.1. Immediate Effect of Temperature on the Modulus of Elasticity, Parallel to the Grain, Relative to the Value at 20°C. Plot is a Composite of Results From Several Studies. Variability Illustrated by the Width of the Bands (Wood Handbook, 1987).

As the heat continues to enter the timber and the temperature rises, strength properties are reduced. Beam failure will occur when its cross section has reduced to such an extent that it can no longer support the applied load. Failure of columns is dependent on the slenderness ratio, so when a column chars the effective area is reduced and the slenderness ratio increases and thus the chance of buckling will increase.

Strength properties are decreased by heat in the following sensitivity, (most sensitive to least sensitive) (Knudson & Schniewind, 1975),

1. Toughness and impact bending
2. Compression strength parallel to grain
3. Modulus of rupture
4. Modulus of elasticity.

Work by Tenning and Odeen in Sweden in 1959 were some of the first fire tests on full-size glulam beams (Tenning, 1967 & Odeen, 1967). Strength, temperature distributions and charring rates were all recorded during testing using the ISO834 standard fire, on cross-sections of 420x143mm. The results showed that the ultimate bending stress decreases linearly from 60.8MPa at 20°C to 30.4MPa at 100°C within the unburnt section. This reduction in strength due to heating of the interior wood reveals how conducted heat decreases the load carrying ability of timber sections. What must be considered though is that the temperature of 100°C in the beam of 140mm width, was not reached until 60 minutes into the standard fire. Thus strength is reduced, but only after long exposure. The testing also found that Youngs modulus may fall by 70-80% after exposure to fire conditions.

2.4 Thermal Properties of Wood.

The ability of wood to limit the flow of heat and be ignited is controlled by the properties of thermal conductivity (k), specific heat (c) and density (ρ). These terms are often grouped as kρc and called the thermal inertia of a material. These terms are defined and elaborated on below.

2.4.1 Thermal Conductivity.

The steady-state flow of heat is described by Fourier's law, which is analogous to Darcy's Law for the transport of fluids. The thermal conductivity of a material is equal to the flux divided by the temperature gradient and mathematically it may be stated as (Siau, 1971),

$$k = \frac{H/tA}{\Delta T/L} = \frac{HL}{tA\Delta T} \qquad 2.2$$

or as

$$H = \frac{ktA\Delta T}{L} \qquad 2.3$$

where k = thermal conductivity (W/mK)

H = quantity of heat transferred (W)

t = time interval (s)

A = cross-sectional area perpendicular to heat flow (m^2)

L = length of flow path in the transfer medium (m)

ΔT = Temperature difference between surfaces, separated by L (°C)

The meaning of thermal conductivity, k is the opposite of the thermal insulation capacity of the wood (Tsoumis, 1991). Thermal conductivity is specifically defined as a measure of the quantity of heat in calories which will flow during a unit of time (seconds), through a body 1cm thick with a surface area of $1cm^2$, when a difference of 1°C is maintained between the surfaces.

The thermal conductivity of wood is affected by density, moisture content, grain direction and structural irregularities such as knots. It is nearly the same in the radial and tangential directions, though radially thermal conductivity is a little higher due to wood rays. These directions are both perpendicular to the fibre axis where there is high resistance to flow due to the interruption of the path by the poorly conducting air-filled lumens (Parker, 1988). The thermal conductivity along the grain is considered to be between 2.2 and 2.8 times greater than it is across the grain. A typical ratio is 2.5. This higher thermal conductivity is mainly due to the fibrous morphology and the axial placement of most wood cells.

The insulating properties of wood have numerous advantages and contribute greatly to the fire-resistant properties of wood compared with highly conducting metals, which soften at high temperatures. The low conductivity of wood also accounts for the considerable time interval required to bring a large dimensioned timber specimen to a uniform temperature when heat is applied to its external surfaces.

2.4.2 Thermal Conductivity Determination.

The TRADA (1971) literature survey gives a good historical record of the experimental work carried out since 1912 that has attempted to accurately model thermal conductivity over a range of temperatures.

Parker formulated a heat release rate model for Douglas fir during flaming combustion and used the following formula for conductivity, based on work by Maclean (Parker, 1988),

$$k = [0.237 + 2.00S_o(1 + 0.02m)]x10^{-4} \quad kW/m°K \qquad 2.4$$

where S_o = Specific Gravity (oven dry)

m = Moisture Content (%)

This holds for specific gravities of 0.3 to 0.8 and a moisture content of 0 to 40%. It also holds for charred wood up to a mass loss of 37%. Siau (1971) has also referenced Maclean's work. Maclean measured the thermal conductivities of many samples of wood with a large range of moisture contents and specific gravities. An empirical equation was developed to best fit the data for moisture contents less than 40%,

$$k = [S_o(4.80 + 0.090m) + 0.57]x10^{-4} \quad cal/cm°C\ s \qquad 2.5$$

where S_o = specific gravity

m = moisture content (%)

and 1 cal/(cm °C s) = 418 W/m°K = 2903 BTU in/(ft^{2}h °F).

2.4.3 Specific Heat.

Specific heat of a body is the quantity of heat (kJ) needed to increase the temperature of its unit mass (kg) by 1°C (°K) and is measured in kJ/kg°K .The specific heat of wood is comparably higher than that of other materials such as steel, as wood contains water. Thus its ability to be heated is closely related to the heating properties of water. The substantially low temperatures in the centre of a beam in a fire test are due to the high energy input required for the latent heat of steam. This means greater quantities of heat are required to raise the temperature of the wood. Specific heat does not vary much between species and with density, but does with moisture content and temperature.

2.4.4 Specific Heat Determination.

The specific heat of wood is defined as the number of calories (heat) required to raise 1 gram 1°C in temperature. To record this the initial temperature is usually 15°C as the heat capacity of water at 15°C is 1 calorie per gram per degree C (Parker, 1988). Specific heat is usually measured in kJ/kg °K, where 1 kJ/kg °K = 0.2388 cal/g°C. The specific heat of wood is

fairly constant up to 100°C.

Work to determine specific heat over a range of temperatures was first carried out by Dunlap in 1912, for twenty different species, producing the following equation,

$$c_w = 1.11 + 0.00486T \quad kJ/kg°K \qquad 2.6$$

where T is the temperature in °C.

Koch (1969) found the specific heat for spruce pine evaluating 72 samples with a scanning calorimeter making 6696 observations. A temperature range of 60 to 140°C was observed and an empirical equation was produced with a 95% confidence level,

$$c_w = 1.11 + 0.0042T \quad kJ/kg°K \qquad 2.7$$

where T is the temperature in °C.

Koch's work confirmed Dunlap's work to 140°C and since relatively little chemical change would be expected up to the point where rapid thermal decomposition begins (charring), it is appropriate to use equation 2.7 up to 200°C.

The specific heat of charcoal is approximately 0.67 kJ/kg°K, as reported by Dunlap (Koch 1969). For the purpose of calculating the specific heat of partially charred wood, it is assumed to be a mixture of virgin wood and charcoal. Parker (1988) incorporated the specific heat of charcoal and derived an equation for the specific heat over the range of temperatures 0 to 500°C as,

$$c_w = 1.11 + 0.0037T \quad kJ/kg°K \qquad 2.8$$

where T is the temperature in °C.

Knudson used the above relationships to produce an overall relationship for the various changes in specific heat over a broad range of temperatures (Knudson & Schniewind, 1975). This relationship can be seen in figure 2.2. Using Dunlaps formula to 200°C, but assuming 10% moisture content, line A was constructed. The sharp peak between 99.5 and 104.4°C represents the latent heat of vaporization of the bound water and line C was constructed assuming oven-dry wood and Dunlaps formula. From 350°C a constant value for charcoal was used. As there is little information on decomposing wood between 200 and 350°C a straight line was used to connect lines C and E.

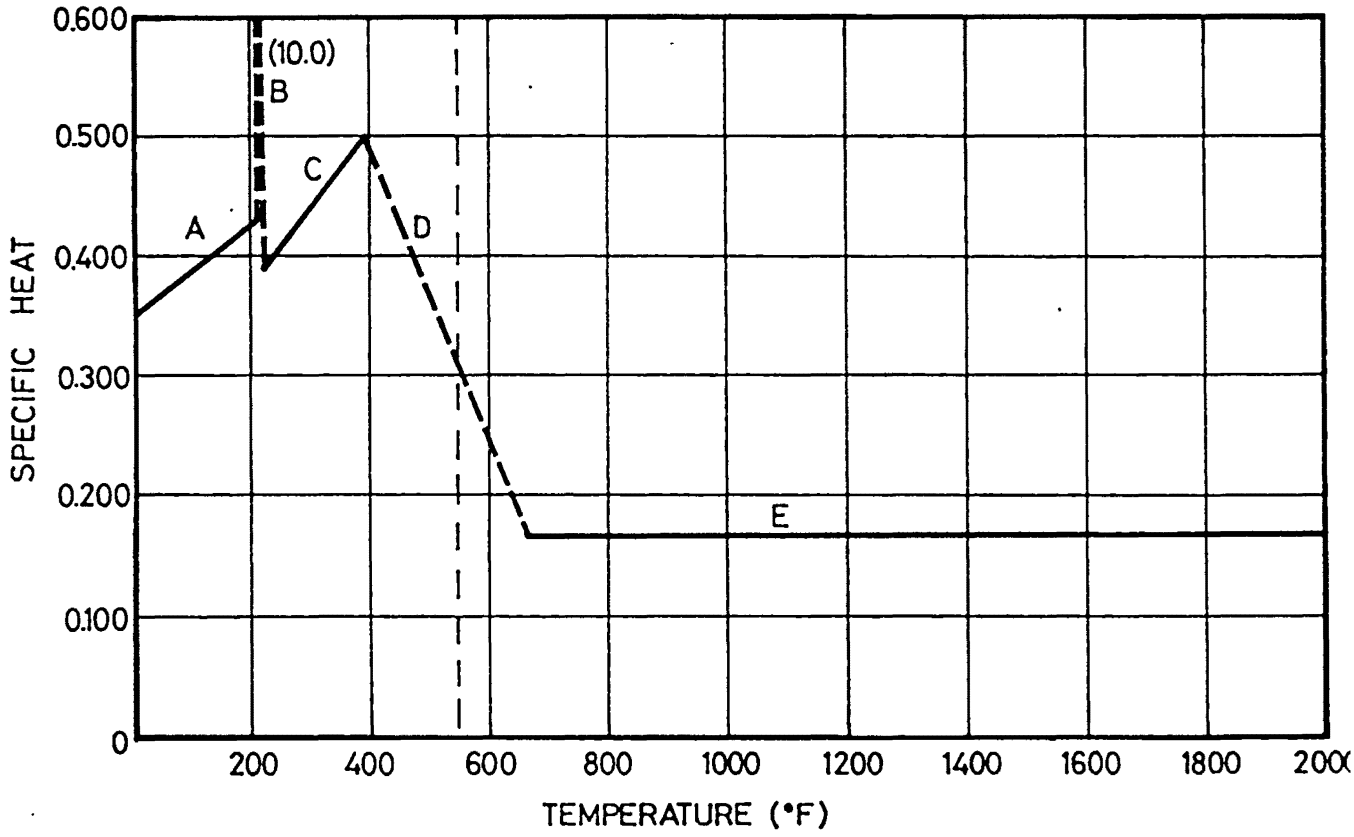

Figure 2.2. Variability of Specific Heat with Temperature. Regions of unknown relationships are shown with dashed lines, (Knudson and Schniewind, 1975).

2.4.5 Density.

Density is closely related to the strength and other properties of wood and varies radially as well as transversely. Density tends to increase with increasing distance from the pith, the

centre of the tree (see figure 2.3). The main influences that affect density within a given species are temperature, latitude and altitude (Collins, 1983).

Other definitions of density associated with different moisture content conditions and shrinkage are used in particular situations. Some are listed here,

Basic density = oven dry weight / green volume (M.C. > 30%)

Nominal density at 12% moisture content = oven dry weight / volume at 12% moisture content.

Green density = green weight / green volume when freshly cut

Oven dry density = oven dry weight / oven dry volume

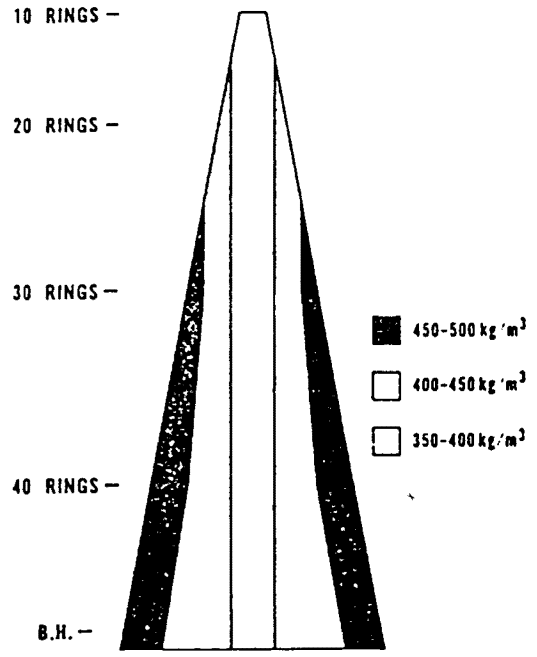

Figure 2.3. Typical Pattern of Wood Density Variation in Old Crop Radiata Pine, (Cown & McConchie, 1983).

To convert the Basic density (D_b) to a Nominal density at 12% ($D_{n,12}$), the following equation can be used (Collins, 1983),

$$D_{n,12} = \frac{3000D_b}{3000-(30-m)(0.017D_b+4.7)} \qquad 2.9$$

where m = moisture content (%)

Other conversion formulas are listed by Collins (1983).

2.4.6 Density of Charred Wood.

As wood burns and chars, mass is lost due to pyrolysis and thus the density of the wood is reduced. Tests by Cutter and McGinnes on the density change in seven species show a marked drop in density between 300 and 350°C. This decrease continues to 600°C (see figure 2.4).

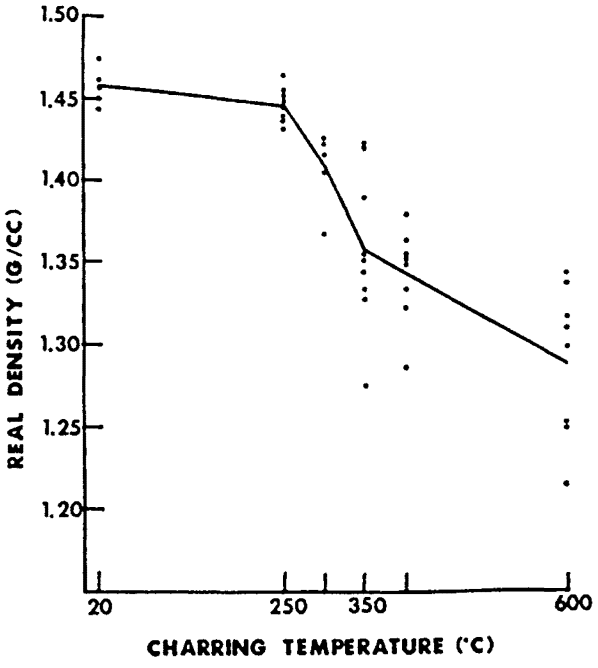

Figure 2.4. Change in Real Density of Wood and Char Substances for Seven Species. Solid Line Illustrates the Overall Trend, (Cutter & McGinnes, 1981).

2.4.7 Emissivity of Charred Wood.

Measurements of emissivity in pine by Parker (1988) show an increase from 0.6 to 0.93 as charring occurs in the burning timber. As burning continues the emissivity remains constant. Tran and White (1992) used a value of 0.88 for their measurements.

2.4.8 Thermal Diffusivity.

Thermal diffusivity is a measure of the rate of change of temperature of a material, when the temperature of its surroundings changes. Thermal diffusivity is equal to the thermal conductivity divided by the density and the specific heat. Wood has a much lower diffusivity than steel, that is why it feels warm to touch. Thermal diffusivity α is given by,

$$\alpha = \frac{k}{\rho c} \qquad 2.10$$

where k = thermal conductivity (W/m°K)

ρ = density (kg/m^3)

c = specific heat (J/kg °K)

2.4.9 Moisture Content.

When wood is heated, the temperature gradient causes moisture to retreat into the wood, resulting in a slightly increased moisture content below the char layer (White & Schaffer, 1981). However after a length of time the heating is so significant that all moisture will be evaporated and the temperature will rise rapidly. Moisture content significantly affects burning rate. A difference in moisture content of 10% results in a change of 20 - 30% in burning rate (Tran & White, 1992). The change in moisture content also affects the strength properties in the unburnt interior of the wood, reducing these with the small increase in moisture content.

2.4.10 Shrinkage and Expansion.

Shrinkage is an important wood property as the extent of shrinkage is often used as a guide to the anticipated stability in service (Cown & McConchie, 1983). Because wood is anisotropic, it normally shrinks about twice as much tangentially as radially. This shrinkage occurs during heating of timber as the moisture is evaporated and causes cracks to open up,

which will increase the rate of charring once ignition occurs. Timber has a very low coefficient of linear thermal expansion of around 0.000005 per°C longitudinally and this is positive, i.e. it expands when heated (Swedish Finnish Timber Council, 1981). Even this very small thermal movement is in fact counteracted, since heating timber reduces its moisture content making it shrink slightly. The nett effect is that in fire the longitudinal dimension is virtually unchanged.

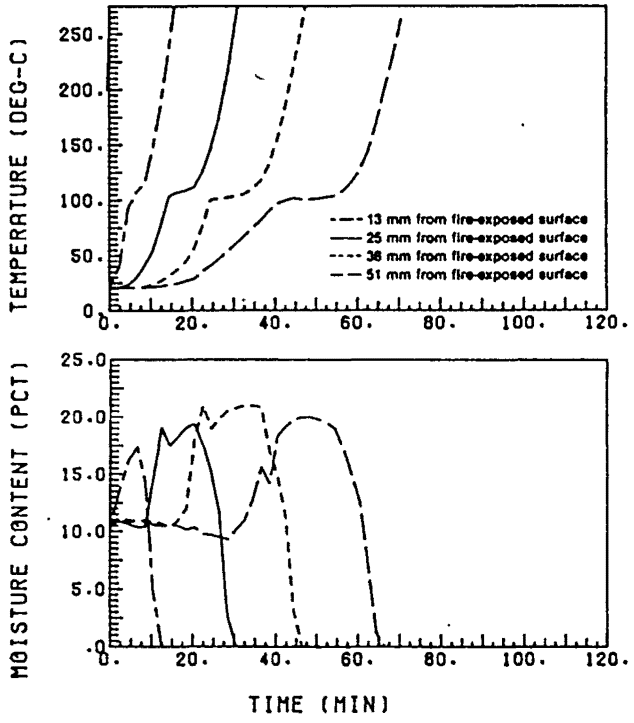

Figure 2.5. Change in Moisture Content With Increasing Temperature in Southern Pine Wood Slab, Exposed to E119 Fire Test, (White & Schaffer, 1981).

2.5 Charring of Timber.

2.5.1 Charring.

Unless subjected to radiation of such intensity that the ignition temperature is reached in a fraction of a second, wood does not burn directly. It first undergoes a thermal breakdown or pyrolysis and the process of charring occurs. In the presence of air the released products of combusted gases may be ignited. If enough of the heat of combustion is retained by the wood the pyrolysis may be self sustaining, producing further gases and subsequent combustion. Time to ignition is thus related to the temperature of the surface of the timber and the ability of the wood to transfer heat.

2.5.2 Fire Tests.

To evaluate the charring rate of timber and define the char front, full scale fire tests using the standard time temperature curve, i.e. ISO834 fire curve, have been carried out on sections of timber. Internally situated thermocouples record temperatures in the section, thus providing an overall picture of how the section is responding to the fire.

2.5.3 Char Rate.

Rate of char is affected by the external heat flux, oxygen concentration of the surrounding air and the thermal properties of the wood, (including density, moisture content, annual ring orientation, and combustible volatile content). The temperature directly below the char line may be relatively low, approximately 180 to 190°C (TRADA, 1971). Charring rates vary from 0.85mm/min to 0.50mm/min, with 0.6mm/min normally quoted. Work by Collier (1992) has determined a value of 0.65mm/min for radiata pine in New Zealand. Laminated beams generally char at the same rate as solid timber. British Standard BS5268 (1978) states a charring rate of 40mm in 60 minutes (0.667 mm/min) for softwoods. There are also differences in charring parallel or perpendicular to laminations. The type of loading on a beam or column has no affect on charring type or rate (Rogowski, 1967).

2.5.4 Measuring and Predicting Char Rate.

An empirical method to predict the charring rate of timber exposed to the E119 standard fire has been developed by White and Nordheim (1992), based on the fundamental thermal properties of the timber. Eight species were tested for thermal properties and charring rates. Differing empirical relationships were developed using species specific coefficients and coefficients differentiating between hardwood and softwoods. The final empirical relation is dependent on moisture content, density and char contraction factor. For southern pine, the relationship for charring rate (β) is,

$$\beta = 0.1526 + 0.508\rho + 0.1475 f_c + 0.005m \quad mm/\text{min} \qquad 2.11$$

where ρ = density g/cm^3

f_c = char contraction factor

m = moisture content (%).

The charring rate decreases with increasing density of the wood and increasing moisture content. During the first minutes from ignition of the timber a char rate greater than 1mm/min can be measured due to only a thin layer of insulating char being present. After 5 to 10 minutes from ignition, char will have built up on the wood, thus stabilising the char rate at 0.6 to 0.8 mm/min (Majamaa, 1991).

Extensive fire tests were carried out at the Swedish National Testing Institute in October of 1959 (Tenning, 1967). Tenning and Odeen tested 143 x 420mm Douglas fir glulam beams and the depth of char was measured by sawing beams in half once the fire tests had been completed. Charring was rapid during the first half hour (23mm) then diminishes in the next half hour (35mm total). After the first hour of burning the charring rate increased as the moisture content significantly lowered throughout. These char depths correspond to an initial char rate of 0.77mm/min in the first half hour. The average over one hour was 0.58mm/min. The rate increased as failure of the beams was neared.

Full-scale fire tests in Australia by Gardner and Syme (1991) using glue-laminated beams of dimensions 4800x270x150mm, with resorcinol adhesives, had an assumed char front location temperature of 288°C. This was based on Schaffers work on determining a definitive char front location value, (Schaffer 1984). Resulting char rates of 0.93mm/min and 0.80mm/min were found for radiata pine of density 526 kg/m^3 and moisture content of 9.2%, in two different furnace tests. When sections were tested with a gypsum plasterboard protective cladding, the charring rate was reduced to 0.44mm/min.

2.5.5 Char Front Location.

Under fire conditions the char will be at 300 to 400°C but the temperature in the interior char edge will be approximately 100°C, due to the moisture content held in the wood. The temperature that determines the location of the char front has been quoted as 290°C by Schaffer (1977) and determined precisely as 288°C by Schaffer (1984). Other values range from 275 to 538°C.

2.5.6 Determination of the Char Front Location Temperature.

Schaffer's work in assessing the char front location temperature as 288°C is the most

referenced work and seems to have become the figure most values are compared against (Schaffer, 1984).

Tenning and Odeen (1967) fire tested 143 x 420mm Douglas fir beams and inspection of the thermocouples indicated that they were at just over 100°C when charring started. This conflicts with the 280-300°C char front location temperature determined by Schaffer.

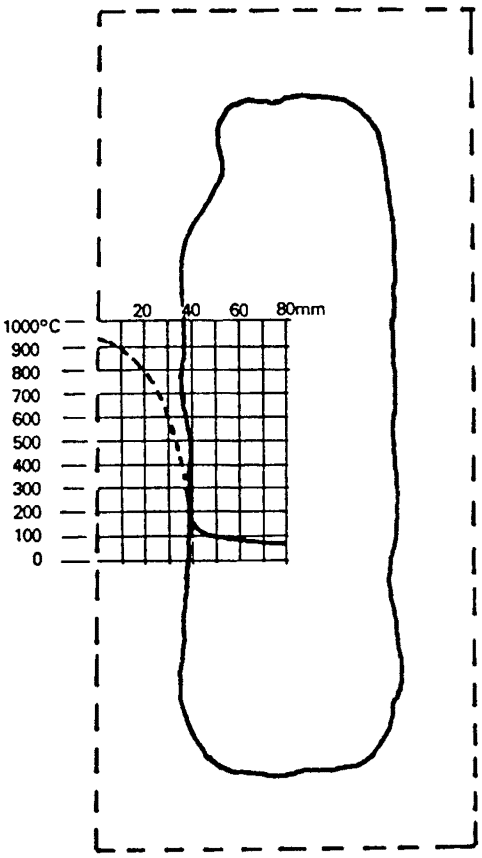

Figure 2.6. Typical Temperature Profile Through Burning Timber Beam, (Swedish Finnish Timber Council, 1981).

Using a heat release rate calorimeter Tran and White were able to correlate the char front with temperatures between 280°C and 350°C (Tran & White, 1992). Due to the temperature rising steeply in this range of temperatures the gradient of char across this range is also small. Thus a temperature of 300°C was decided on as indicating the arrival of the char front.

Work in New Zealand on char front location is very limited, but the best data is from work by Baber and Fowkes (1984). Tests were performed on 100 x 50mm radiata pine studs, using

an on-set of char method to determine the fire resistance of load bearing walls. Small scale tests of protected studs showed the char front to occur at 300°C.

Mikkola's cone calorimeter tests in Finland using spruce and pine used 360°C as the location of the char front (Mikkola, 1990). This is an estimate of the mean temperature of the pyrolysis of the wood as increasing temperature causes part of the water to penetrate more deeply into the solid wood and part of it to come out as vapour. Thus there is still some strength left in the timber until this temperature is reached. Majamaa (1991) used this temperature for his model of beams in fire conditions though did not confirm the temperature with experiments.

2.5.7 Differential Charing Rate.

A differential in the charring rates between sides and base of approximately 10%-20% has been found to occur in glulam sections. This has been observed by Rogowski (1967) and Schaffer (1977). Also Gardner and Syme (1991) observed evidence of this. Rogowski evaluated the data from the fire tests of Tenning and Odeen and found the charring perpendicular to the laminations was approximately 20% greater than that parallel to the laminations. This was due to delamination and thus the subsequent loss of the protective charcoal layer. This differential in charring is also suspected to be caused by differences in density in moisture content between sides and base. Gardener and Syme found that the difference in char to be more random and the difference below 10%. The affect may have been due to experimental problems with the furnace.

2.6 Char Contraction.

As the pyrolysis proceeds the char that is formed contracts and ultimately approaches a graphite structure. This process is called char contraction and is defined as the linear volume fraction of the pyrolysed wood that is converted to char. This volumetric change alters the amount of heat being transferred through the char at the surface. This is dependent on the moisture content and contraction is smallest along the grain and greatest in the tangential direction (Parker, 1988).

2.6.1 Char Contraction Determination.

Data on char contraction is not readily available as most researchers do not seem to record this value. The best and most recent data is by Tran and White (1992) who evaluated the contraction factor for four differing species. Southern pine with an oven dry density of 508kg/m^3 was found to have an average char contraction (f_c) of 0.589 and char yield (Y_c) of 0.24 (char yield is defined as the char to wood ratio).

2.6.2 Corner Affects.

The corners and edges of a beam or column are affected adversely in a fire due to heat conduction through two adjacent faces. This results in rounded corners in burnt sections. Corner rounding can affect the bending strength of a section but this is usually dependent on the depth-width ratio (TRADA, 1971). Differing methods have been put forward to estimate the amount of timber lost due to corner rounding. The corner radius can be calculated as $r = 0.8\beta t$ where β represents char rate (Majamaa, 1991) or as $r = \beta t$ (MP9, 1987).

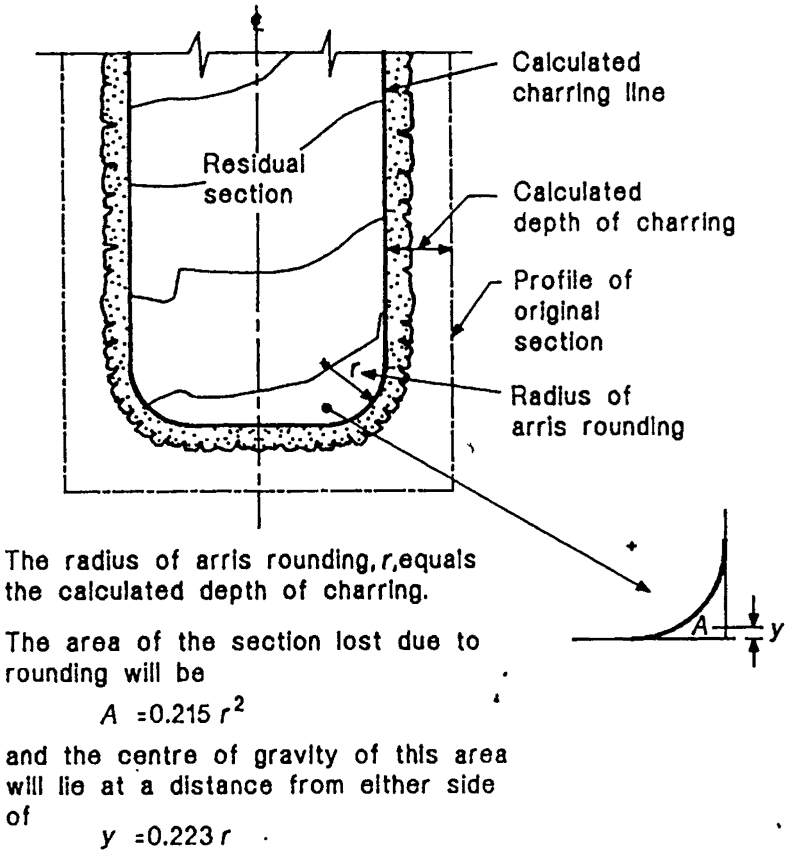

Figure 2.7. Corner Rounding in a Beam Exposed to Fire, (SNZ, 1993).

2.6.3 Char Fissures.

The pattern of fissuring produced by burning can indicate how intensely a timber section may have burned and can indicate fire development. Char fissures govern both volatile release and heat transfer and thus affect the rate of degradation of the wood to char. Drysdale (1985) states that the char fissures will widen as the depth of char increases. Australian data indicate that fissure width is more likely a function of heating conditions than char depth (Gardner & Syme, 1991).

2.7 Standard Fire Test Versus Cone Calorimeter.

In cone calorimeter tests the oxygen concentration of the surrounding air is the normal concentration, 21%. This means that the charring rate is higher than in a standard ISO834 fire test, in which oxygen concentration is considerably lower, usually in the range of 4-10%. Mass loss rate results can be used to determine the oxygen effect. In the standard fire test after the wood samples have ignited, the oxygen concentration decreases. Tests by Ohlemiller et. al. show a 20% decrease in mass loss rate between 21% and 10% O_2 (Mikkola, 1990). Hence it is reasonable that charring rates measured in the ISO834 standard fire test will be approximately 20% lower than in the "oxygen rich" cone calorimeter test when the average external heat flux is identical. For comparisons between cone calorimeter results and standard fire results the heat flux in the standard fire test must be averaged over the test period.

Comparisons between real fires and standard fires can be made as a real fire is like a standard fire, if the ventilation is controlled. Thus fire tests using a standard fire will closely predict actual burning that occurs in a real fire.

2.8 Finger Joints.

Fire tests on full size glulam beams have shown that the strength of finger joints in the tension side laminates might have an affect on the load carrying capacity of the glulam (Nielsen & Olesen, 1982). Finger joints may lose strength because of the heat. Test results showed finger jointed specimens had a marked drop in strength from 20 to 90°C whereas the significant drop for the unjointed boards was between 90 and 160°C.

2.8.1 Failure Mode.

For beams and columns under stress it is commonly thought that finger joints should be avoided at the extreme fibre, due to them being susceptible in fire conditions. At higher temperatures like those in all fires research shows that they may not be a weakness. Shear strength is assumed to govern the failures in the finger jointed specimens at lower temperatures but the failure mode at the higher temperatures is governed by tension strength. This is due to shear strength being less dependent on temperature than tension strength. Thus wood strength is more sensitive to an increase in temperature than is the glueline. This is supported by the observation that all finger jointed specimens (resorcinol glue) tested at 230°C by Nielsen and Olesen (1982) had 100% failures in the wood.

2.9 Retardants.

Fire retardant treatments come in two types, pressure impregnation and surface coating. Both involve the mixing of chemicals which are designed to either control ignition and flaming or control after-glow in the charcoal. The retardants reduce the rate of flame spread by raising the exothermic point (ignition temperature) by producing non-combustible gases or a physical barrier. Unfortunately a fire retardant material cannot render a timber section fire resistant, in the sense of protecting it from damage. Early fire tests on retardants have shown that they have little affect on the fire resistance of the timber member (Wardle, 1966).

2.9.1 Fire Tests on Retardants.

Fire retardant paint tested by Odeen (1967) showed that the time to ignition was slowed, but after ignition, penetration rate of the flames was the same as untreated timber. Malhotra and Rogowski's work (Schaffer, 1977) has shown that retardants have a variable affect on the fire resistance of columns. A timber specimen pressure treated to 53kg/m^3 improved endurance by 11 minutes whilst one pressure treated to 40kg/m^3 reduced time insignificantly. Intumescent paints were found not to alter fire endurance significantly.

Fire protection by using gypsum plasterboard is a relatively easy method of increasing the fire resistance rating. By encasing a column with 13mm asbestos insulation board the fire resistance of a tested section was found to increase by approximately 20mins (TRADA, 1971). Australian fire tests (Gardner & Syme, 1991) have showed that gypsum plasterboard

can reduce char depth formation in radiata pine by approximately 41%. This protection is due to the insulation caused by plasterboard dehydrating and its continued heat protection.

2.9.2 Increasing Fire Resistance Rating With Retardants.

Protecting timber members from fire with retardants only increases fire resistance by a small amount, but this small time increase in a members ability to withstand heat may be important in achieving the desired fire rating, as for the epoxy dowel connection. Using gypsum plasterboard as fire protection is questionable though. Spending money on fire protection by this method cannot be justified, when an increase in the size of the member will have approximately the same affect and may be more cost-effective.

CHAPTER 3

WOOD ADHESIVES

3.1 Glulam Adhesives.

3.1.1 Charring of Adhesives.

For a glulam section to perform well in fire conditions, the glue used to laminate the timber must maintain its integrity. Adhesives must be capable of maintaining a sound glue line during a fire by resisting the heat and charring at a lesser rate than the timber and retaining their bond, as the timber is pyrolysing. A charred laminated member will sometimes exhibit longitudinal separation of the char at the glue lines. This is of no significance if the separation occurs in the destroyed wood of the charred zone, but has serious implications if it occurs in the uncharred timber. The integrity of the glue line can normally be ensured by the use of thermosetting adhesives such as,

Urea formaldehyde
Resorcinol formaldehyde
Casein formaldehyde
Phenol formaldehyde
Melamine formaldehyde

During curing, thermosetting occurs creating strong cross-links between the molecules. Cured resins are non-combustible and are destroyed in fire by charring, not by flaming combustion. Charring of these adhesives occurs at approximately the same rate as the timber but there is some glue line porosity due to entrapped air bubbles or minor delamination. These imperfections can accelerate the penetration of fire into the member.

Thermoplastic adhesives are unsuitable for use in fire-resistant construction as they lose their strength quickly in fire conditions and ignition may occur (Kenna, 1973). Most thermoplastic adhesives are also subject to creep when under load and should not be used in structural

laminations.

3.1.2 Char Rate of Adhesives in Fire Tests.

The results of fire tests show that adhesives char at approximately the same rate as that of the timber. The char process may be quicker in some instances due to the higher conduction of heat through the adhesive (TRADA, 1971). Failure in the lamination occurs by glues charring quicker than the surrounding timber or losing their bond under extreme heat. These failures cause opening of the laminations and thus greater penetration of the heat. Thus the penetration rate at the glue line may be slightly greater than in timber. Tests on casein glue have shown faster penetration than the surrounding timber. Phenolic, resorcinol and melamine glues have been shown to perform similarly to that of the timber (TRADA, 1971).

3.1.3 Fire Testing Glulam Adhesives.

Some of the first work to find how the glulam adhesives worked in fire conditions was carried out by Tenning and Odeen (Tenning, 1967). No adverse effect could be found in the glued joints between the laminations after the full-scale fire testing. Both casein and cascosinol glues were used. Work by Rogowski (Rogowski, 1967; Kenna, 1973) revealed that the effect of glue on the charring rate is small and the only affect is slightly more delamination along the char line. Phenolic and resorcinol glues were found to be 20% superior than urea and casein glues (see figure 3.1).

Schaffer's work on burning 1 inch Douglas fir and southern pine glulam specimens was the first successful attempt to record how differing adhesives reacted in fire (Schaffer, 1968). Test specimens were fire tested with a frame and bunsen burner arrangement. Once charred, specimens were fractured and examined for delamination and depth of separation of the wood (see figure 3.2).

A degradation index was formulated based on depth of separation and wood failure with a higher index corresponding to a poorer behaviour of the adhesive under charring. The testing on southern pine showed melamine and phenol-resorcinol having the best adhesion with no delamination in the pyrolysed zone or the unaffected wood. Commonly used urea and casein only maintained bond throughout the normal wood and not in the pyrolysed region. Polyvinyl

adhesive was found to have bond separation occurring in the normal wood. Phenolic adhesives have established reliability under fire exposure because of their thermal and moisture stability and thus do not influence timber charring rate. Casein glued laminations appear to have charring rates comparable to phenolic and resorcinol-bonded wood if outer laminates are thick enough to meet desired fire endurance time. Urea adhesive presently allows both increased charring rate and separation as a heated zone develops in the timber.

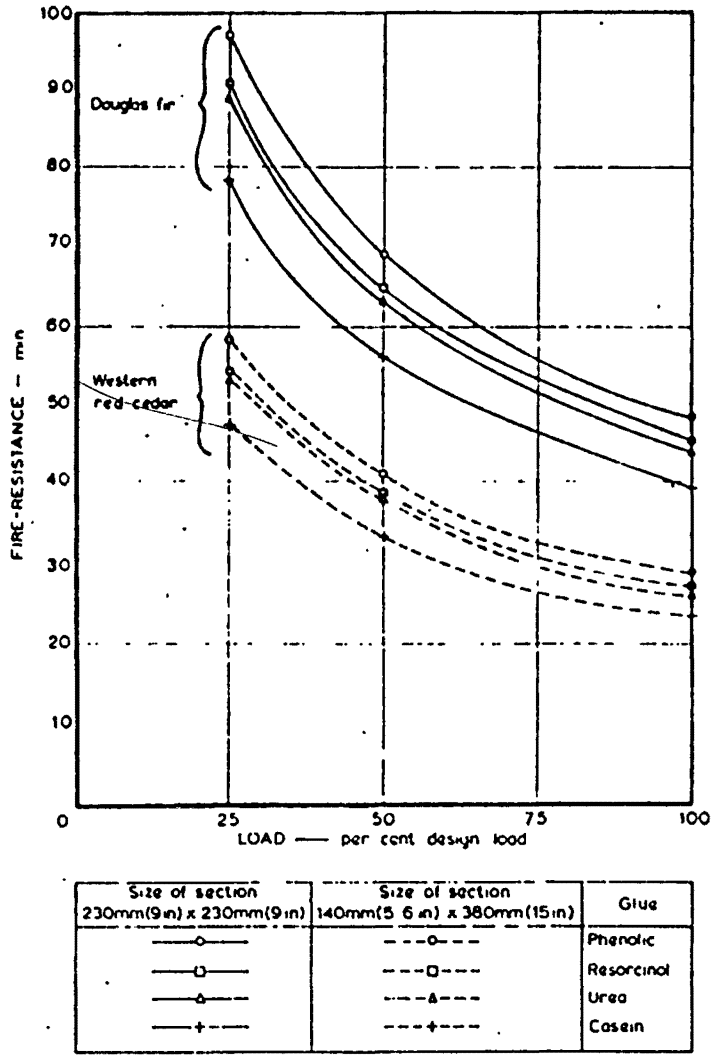

Figure 3.1. Effect of Differing Adhesives on the Fire Resistance of Glulam Columns, (Kenna, 1973).

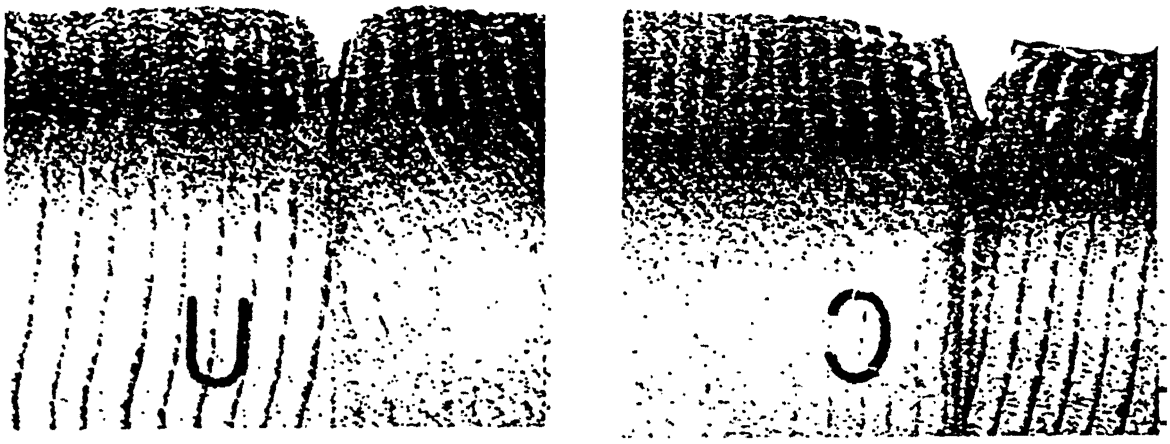

Figure 3.2. Charred Wood Samples Showing Delamination, (Schaffer 1968).

3.2 Epoxy

Epoxy has widespread use in the construction industry due to its ability to bond most construction materials and ease of use. It has the ability to convert from a liquid to a solid with little change in volume and no harmful by-products.

An epoxy is normally a combination of two liquids that undergo a chemical reaction to form a solid. Epoxies can be used as protective coatings, laminates and adhesives. The epoxy resin is based on three-member heterocyclic molecular chains that contain epoxide groups; oxygen and carbon atoms capable of chemical reactions with groupings of other compounds in the curing compound, resulting in chains and connecting links between resin molecules. Epoxies are thermosetting resins and thus the curing process is irreversible, i.e. they may soften once heated but will not re-liquify. Thermosets are classed as polymers which harden irreversibly on the application of heat to give, on a molecular scale, highly cross-linked three-dimensional networks. The resin and hardener combination that will form the epoxy have an exothermic reaction on mixing and this generally provides the heat for curing.

3.2.1 Curing of Epoxies.

All epoxies have a working time termed pot-life, or gel time. This is the time from blending of the resin and hardener to the point where it first starts to become jelly-like, or unusable. It is normally a matter of minutes and is dependent on the hardener used and the initial temperature.

Curing is the process of cross-linking the resin molecules through the epoxide ring. This mechanism causes hardening which can be slow (hours), or quickly (minutes), at room temperature. The curing time can be altered with a temperature change, as shown in table 3.1. For normal epoxies, a faster cure time can be achieved by having a room temperature of 35 to 45°C, whilst room temperatures of below 10°C will slow curing.

Temperature effects at the curing stage are two fold,

-Viscosity is a function of temperature and as temperature increases the liquid becomes more mobile and thus the ease of mixing increases.

-The rate of gelling and curing increase with a rise in temperature.

The change in temperature of the epoxy as it cures is described as the exotherm; the rise in temperature due to curing being an exothermic reaction. The rising temperature as the heat is evolved in the curing reaction, accelerates the rate of reaction, hence liberating more heat, thus it creates an irreversible cross-linking process.

Cure Temperature, °C	Pot-life (Gel time) (h)	Minimum Cure Time (h)
100	14	48
120	7	24
150	3	8
160	1.5	4
200	0.75	2

Table 3.1. Cure Time for a Long-Cure Epoxy, at Elevated Temperatures (Lee & Neville, 1957).

3.2.2 Epoxy Strength Properties.

The modulus of elasticity for resins is normally quoted at 25°C and ranges from 500 to 5000MPa (cf 30,000MPa for concrete, 9000MPa for glulam, (TUM, 1989)). The modulus of elasticity will increase at lower temperatures and will decrease at higher temperatures.

Epoxies also suffer from creep with both elastic and plastic deformations occurring. An elevation in temperature will thus increase both the creep and flexibility of an epoxy (Tabor, 1978). Compression strength is usually near 100MPa and tensile strength approximately 15% of the compressive strength (Townsend, 1990). West System epoxy has compressive strength of 79 MPa and tensile strength of 50MPa (West System, 1993). K80 epoxy has a compressive strength in the range 120-130MPa and tensile strength of 30-40MPa (Nuplex, 1993).

3.2.3 Shrinkage of the Epoxy.

Shrinkage of the epoxy during curing is small, normally 0-2% by volume. This small change in volume does affect the contact and mechanical bond strength in a connection such as those being tested. When shrinkage occurs in the epoxy, its contact bond strength with the timber walls will reduce due to the epoxy pulling away from the timber, due to its smaller volume. Also its mechanical strength to withstand tension pull-out may be reduced due to its smaller volume in the timber hole.

3.2.4 Epoxy Bond.

An adhesive will transfer load from one member to another by means of surface contact. The strength of the epoxy in its capacity as an adhesive comes from the three-dimensional cross-linking, which can be separated into two categories (Moss, 1982),

Mechanical - Well roughened surfaces with the epoxy filling the gaps and interlocking to form a mechanical bond.

Chemical - (i) Mechanical bonding on a microscopic scale, i.e. the ability of the epoxy to be absorbed into outer layers of a surface before it sets, rigidly interlocking these layers.

- (ii) Chemical bond adheres with surface due to interlocking of long-chain molecules.

Epoxies used in the dowel type of connection must be able to bond well with the timber, as there is only a relatively small amount of mechanical force resistance at the wood surface. The bond at the epoxy-wood interface must therefore rely on the microscopic mechanical

The bond at the epoxy-wood interface must therefore rely on the microscopic mechanical bond and the chemical adhesion obtained in curing. There is a good mechanical bond between the threaded rod and epoxy, as shown in figure 1.2.

Thus the type of bond and strength available from the wood-epoxy bond becomes of significant importance. The formation of a wood-resin bond needs about one half the energy required to form the equivalent resin-resin bond that will occur in the epoxy. The formation of a wood-glue bond could therefore involve two steps, first the formation of a resin-carbohydrate bond, then a resin-resin bond. The latter being the controlling step. Thus in order to form a strong bond, a higher energy level than that forming a resin-resin bond is necessary to complete the cure of resin in wood-glue connection. Thus heat applied to the connection will enhance the strength and formation time of the bond (Chow, 1969).

3.2.5 Moisture Content.

Moisture content of the wood must also be considered as green wood will shrink and cause stress on the bond and connection. Moisture in the wood may affect the ability of the epoxy to cure and manufacturers recommend that all surfaces should be dry. Also swelling due to increased moisture could also decrease the strength of the wood bond.

3.3 Epoxies at Elevated Temperatures.

As the temperature of the epoxy rises the repercussions are seen in the stability and strength of the epoxy. Epoxies undergo a change that resembles a change of state as temperatures rise. At room temperature the epoxy is rigid and glass like, but at a particular temperature a transition occurs and the epoxy becomes more rubbery and flexible. This transition is known as the glass transition temperature (T_g) and can be in the range of 40 to 100°C. (Timms, 1994; Crawford, 1987).

3.3.1 Heat Deflection Temperature.

As epoxy resins are thermosetting materials, when cured their molecular chains are permanently bound together and thus cannot slide past each other. There is flexibility in the chains and this causes softening. This softening is characterised by the HDT (Heat Deflection Temperature). This is the temperature when the first signs of deflection can be seen, under

the pressure of a standard probe. Each epoxy has its own characteristic HDT, dependent on the characteristics of the hardener and the type of fillers (additives) present. West System epoxy has a heat deflection temperature of 50.6°C (Timms, 1994).

3.3.2 Epoxy Strength Loss.

A substantial rise in the temperature of the epoxy will cause a drop in the mechanical strength due to softening. Strength will slowly reduce from 50 to 60 °C, but drop dramatically over the range of 70 to 110°C. Zero strength is normally reached by 200°C (Avent, 1984). At 200°C the kinetic energy of the molecules approaches that of the carbon-carbon bond energy, thus bond dissociation will occur. This process is the reverse of polymerisation and thus all strength of the cross-linking is lost. The strength reduction due to an elevating temperature can easily been seen in figure 3.3.

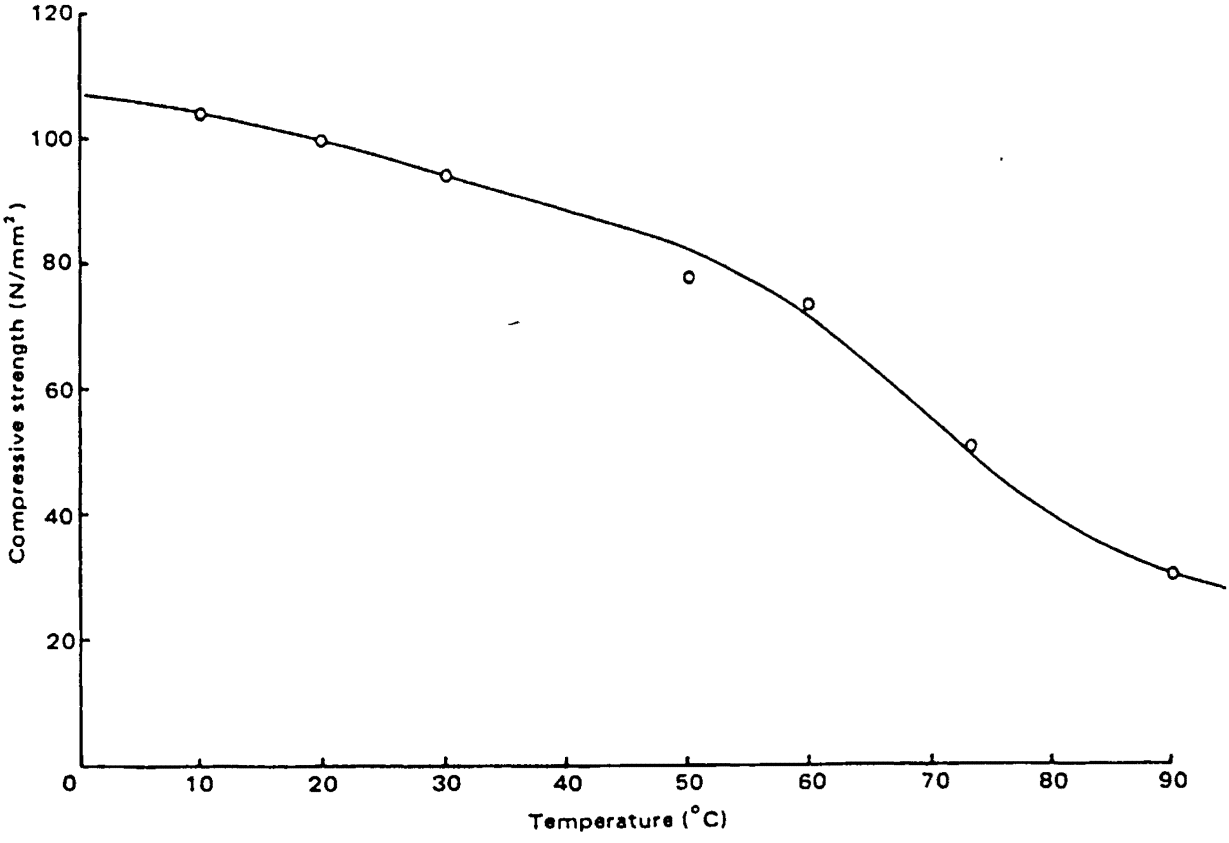

Figure 3.3. Effect of Heat on Compressive Strength of a Polyester Epoxy, (Tabor, 1978).

As an epoxy is heated without restraint, it expands at a relatively large rate, with a coefficient of expansion of 45-65x10^{-6} / °C (cf concrete 7-13x10^{-6} / °C). But as the temperature rises, the epoxy suffers a drop in its modulus of elasticity and thus becomes more flexible, causing the stresses due to expansion, to be reduced.

3.3.3 Tests on Epoxies at Elevated Temperatures.

Epoxies lose strength and soften at relatively low temperatures, which can be hazardous. Avent & Issa (1984) have completed various tests on epoxies at elevated temperatures and confirm that they will soften at temperatures of 82-110°C and the strength decreases rapidly until zero strength is reached at 204°C .

The best available data of full scale heat testing of epoxy is by Avent and Issa (1984). Two epoxies were tested in both shear and compression, one epoxy formulated for high temperature use and one for use in normal temperatures. Shear tests were carried out by using the ASTM D905-49 wooden shear blocks, tested at temperatures from 20 to 200°C. Both epoxies were tested, using the shear blocks. Also compressive tests were completed on cylinders of epoxy at temperatures also ranging from 20 to 200°C.

The shear block tests resulted in data conflicting with that of small scale compressive testing. The tests with actual stresses (lap tests) did not in practice translate to the strength shown in small scale compressive tests, as the high temperature epoxy performed well in the compression tests, but did not perform well at elevated temperatures in the lap shear tests. Thus it can be concluded that compression strength tests on a small scale may not be able to be scaled up to represent actual shear stress tests.

Other elevated temperature tests have been conducted with concrete epoxy-mortars. Epoxy-mortars contain aggregate filler with the epoxy, which is usually sand and silica based. Short term tests on the stress-strain relationship at temperatures ranging up to 80°C show a substantial reduction in stiffness in the 40 to 50°C range, in both tension and compression tests (see figure 3.4). The results showed that temperatures greater than 50°C affected the stiffness more than the strength of an epoxy-mortar as the stress-strain curves become more elongated as rigidity is lost (Johnson, 1970).

Ciba-Geigy (NZ) produce K80 adhesive and it is described as a low temperature adhesive, only retaining its full strength to approximately 40°C. The epoxy is manufactured to maintain up to 20% of its 25°C lap shear strength at 80°C (Caley, 1993). West System Z105/Z206 is expected to lose strength at approximately 50 to 60°C, though no exact strength reduction data is available.

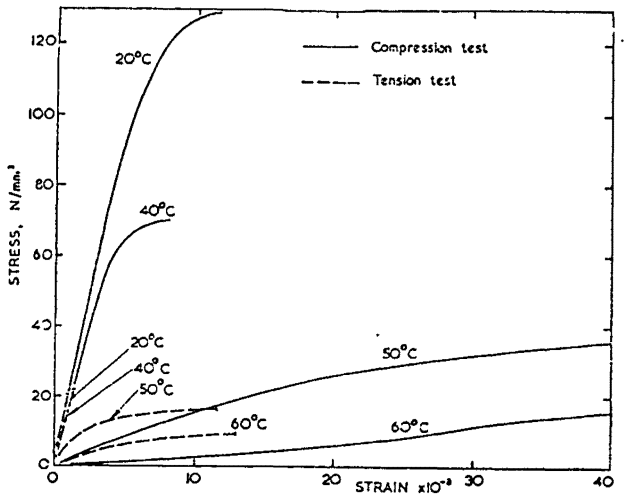

(a)

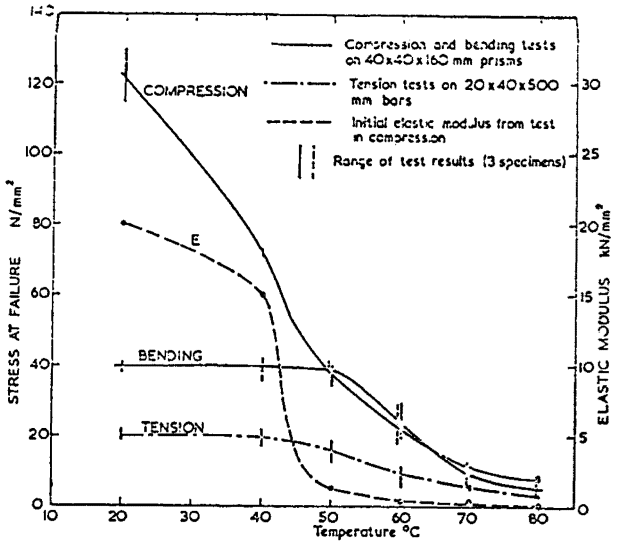

(b)

Figure 3.4. Properties of an Epoxy Mortar at Elevated Temperatures (a), Stress/strain Curves for Tension and Compression; (b), Ultimate Strengths and Elastic Modulus. (Johnson, 1970).

3.3.4 High Temperature Epoxies.

Epoxies that are designed to operate at elevated temperatures normally need long curing times (5-10 days) or high temperature curing (>100°C). Thus these types of epoxies are not suitable for use in building site construction. Phenolic epoxies are designed to operate at high temperatures, but these suffer from a lack of strength and are not easy to use (Timms, 1994).

Other types of high temperature epoxies have been developed. Halogenated resins are fire resistant due to a bromine atom. Gas is released under flame attack, thus extinguishing the flame. Though this type of epoxy still loses mechanical strength at approximately 50°C. Epoxy-phenolic blends have produced epoxies that hold their mechanical strength up to 100°C but these are expensive and difficult to work with.

3.4 Exotherms of K80 and WEST Epoxies.

The exotherm is the rise in temperature of the epoxy as it is cured and is method of identifying the type of epoxy mixture.

3.4.1 Measuring Epoxy Exotherm.

A sample of epoxy was mixed and poured into a round plastic container 42mm in height with a diameter of 62mm. A calibrated temperature sensor LM35DZ, (see section 4.3.5) was placed into the resin-hardener mixture so that it was completely submerged. As the epoxy cured the temperatures were recorded and are shown in figure 3.5.

Both exotherms show a steep increase in temperature to their respective maximums of 98°C for K80 and 145°C for West. Once this peak of temperature is reached, the resin and hardener have completed the thermosetting process and the chemical reaction stops. The epoxy then returns slowly to room temperature and long term curing continues.

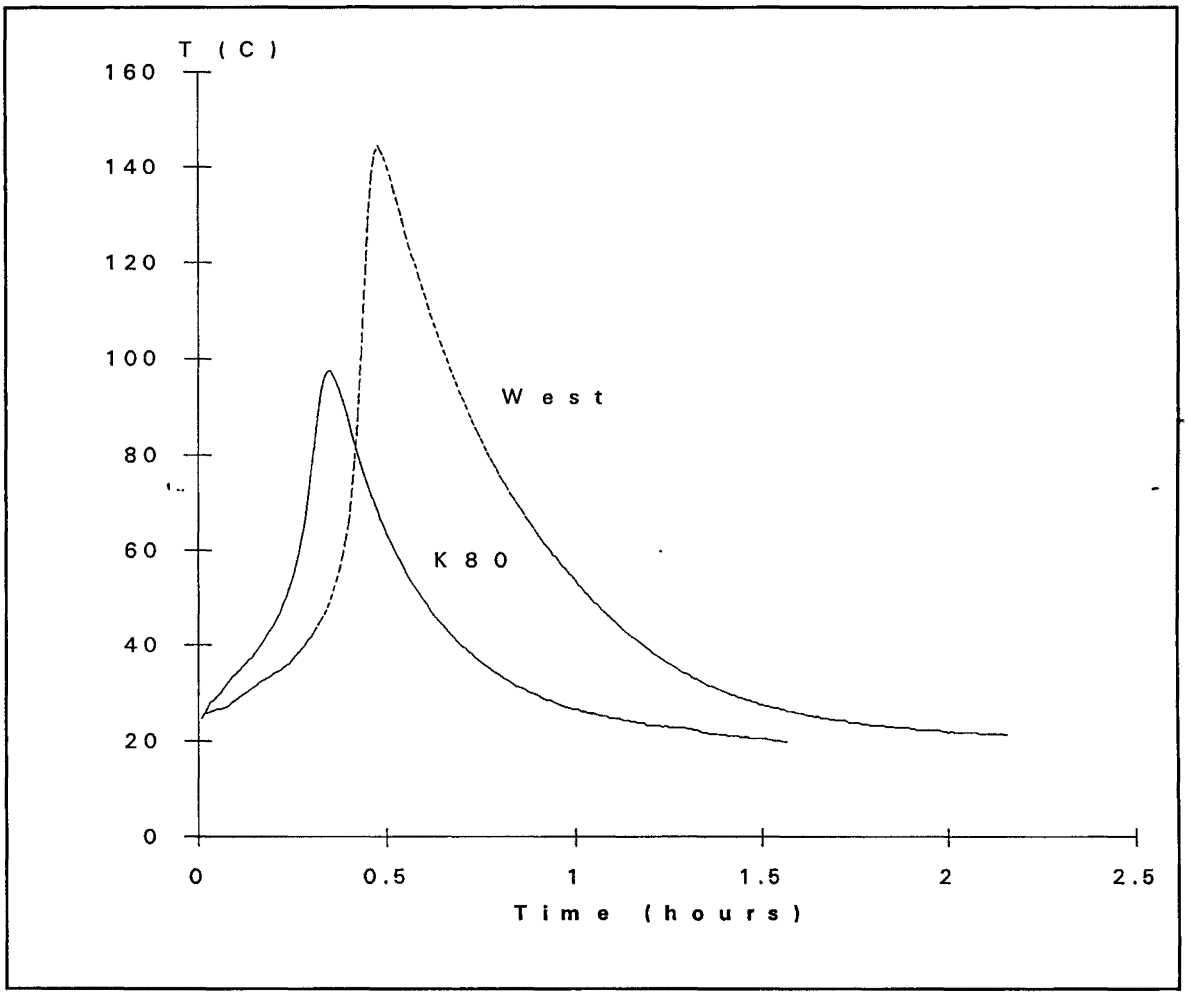

Figure 3.5. Measured Exotherms (Curing Temperature) of West System and Nuplex K80 Epoxies.

CHAPTER 4

OVEN TENSION TESTS

4.1 Introduction.

When the epoxy rod (dowel) connection is in a fire situation, the heat conducted through the timber will heat the epoxy. This heating of the interior of the connection can be simulated by heating a test connection specimen in an oven. The oven tests are to test the effect of elevated temperature of the epoxy on the connection performance, without considering charring or combustion of the wood. Knowledge of how this epoxy connection would react in a heated environment is very modest, so oven tests and tension loading of specimens over a range of temperatures were carried out to give some information on the behaviour in the fire environment.

A review of the literature shows that as the epoxy is heated, it softens and loses its strength in both compression and tension (see chapter 3). With this in mind it was expected that as the temperature was increased in the connection the strength would drop off and movement in the epoxy would occur. How this strength drop-off would occur in full size connections under a tension load was unknown.

4.2 Test Method.

To test connections at elevated temperatures, simulated connections were constructed by using radiata pine timber of 90x90x800mm with epoxied dowels in either end (figure 4.1). A tension load was then applied at each end by using an Instron Universal testing machine (250kN capacity), with constant extension.

4.2.1 Test Design.

An embedment length of 200mm was chosen due to its expected ultimate failure tension load at ambient temperatures being in the range 80-120kN. This range suited the equipment available for the testing. Deng had also found this short embedment length often caused confinement pull-out failures in the 90x90mm timber, not the wood tension failures that occur

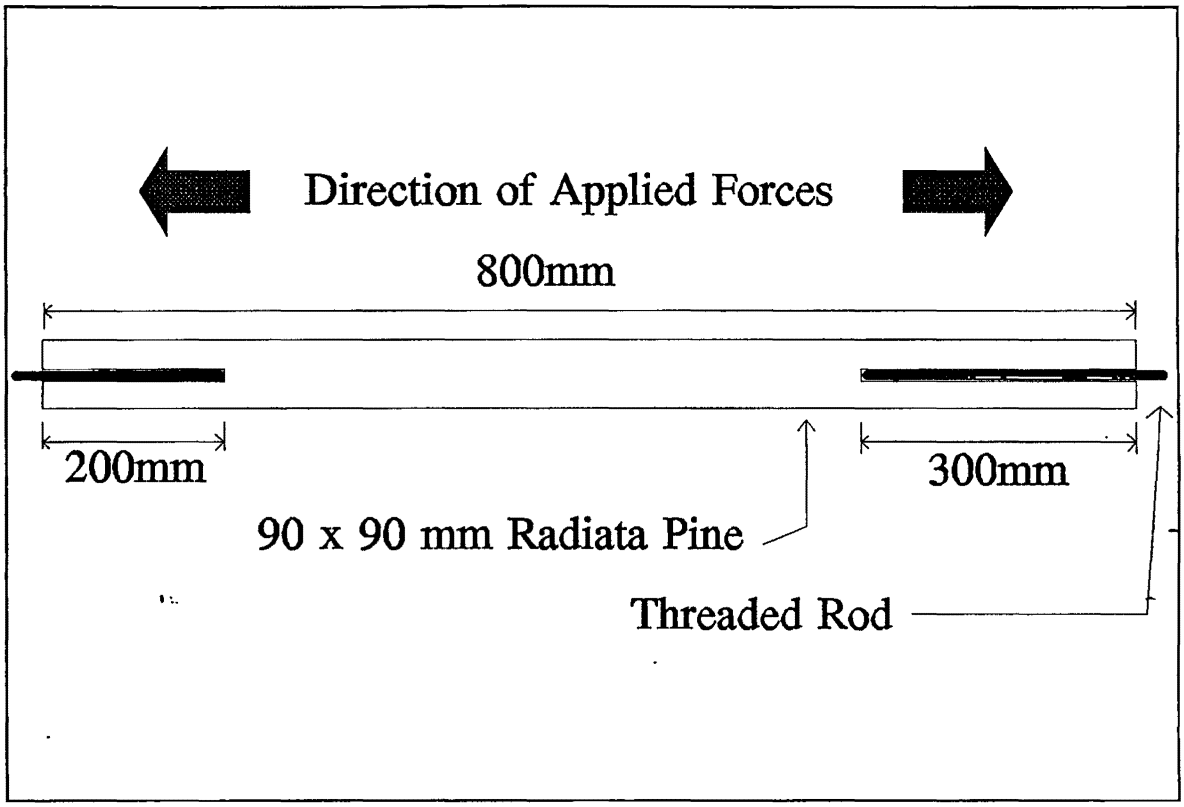

Figure 4.1. Tension Test Specimen With Epoxy Rod Connection at Each End.

when the embedment is longer. To ensure that a tension failure would occur at the testing end, the embedment length at the other end was increased to 300mm.

4.2.2 Predicting Strength

Deng (1993) has derived a pull-out equation for tension parallel to grain for differing bar types and epoxies,

$$F = 20.9\ k_a\ k_b\ k_c\ d\ l\ \sqrt{r_h\ r_e} \qquad 4.1$$

where F = pull out force (N)

d = bar diameter (mm)

l = embedment length (mm)

r_h = ratio of hole diameter to bar diameter - h/d

r_e = ratio of edge distance from bar centreline to bar diameter - e/d

k_a = bar type factor - threaded rod =1

- deformed rod = 0.793

k_b = epoxy type factor - K80 = 1

- West System = 0.846

k_c = moisture content factor (see table 4.1)

Moisture Content	Moisture Content Factor, k_c	
	West System	Nuplex K80
< 18 %	1	1
> 25 %	0.79	0.70

Table 4.1. Moisture Content Factor, k_c (Deng, 1993).

Applying this equation to the test specimens used,

d = 20mm	r_h = 26/20	k_a = 1.0
l = 200mm	r_e = 42.4/20	k_c = 1.0

thus the predicted pull-out strengths for the two epoxies with threaded rods are,

K80 - 138.8 kN

West - 117.4 kN

When longer embedment lengths are used the connection is stronger and able to resist higher applied loads. The increased embedment length results in more area for the bond stresses in the epoxy to distribute over, thus reducing the overall stress per length of bar. The reduced stresses within the epoxy connection thus lead to a lesser likelihood of failure. This theory is reflected in Deng's strength strength equation where ultimate tensile load is almost proportional to embedment length.

4.2.3 Timber Used.

To be consistent with all testing, including that by Deng, large cross-sectioned glulam beams were cut down to sizes of approximately 90x90x800mm. The glulam beams were salvaged from a damaged building in 1992. They were originally fabricated in 1984 at Nelson by

Hunter Timber Laminates Ltd, using radiata pine grown near Nelson. The beams were treated with CCA preservatives. All timber was selected so as to minimise the number of knots or pith present at the testing end.

Density measurements were carried out on the timber before heating and testing took place. The complete data is listed in table 4.2. Moisture content was also recorded before heating took place, using a Protimeter 'Timbermaster' Model D184T. These are also listed table 4.2.

4.2.4 Epoxy Used.

Two different epoxies were used to construct the test specimens for the testing program, Nuplex K80 and West System.

West System epoxy consists of Z105 resin and Z206 hardener, from Adhesive Technologies Ltd, Auckland. The epoxy is a specialist timber epoxy with a slow cure time of 5 to 7 days. The epoxy has a pot-life of approximately 40 minutes and is light amber in colour. It has a low viscosity with the consistency of light motor oil. West System epoxy does shrink slightly on curing (Timms, 1994).

Nuplex K80 Winter is an all-purpose epoxy that will bond concrete, steel wood and ceramics. The epoxy is grey in colour and has the consistency of heavy motor oil, with a cure time of 24 hours. K80 has no shrinkage on curing and low creep. K80 is manufactured by Nuplex Industries, Auckland (Caley, 1993).

To ensure epoxy would completely cover the threaded rod and bond well with the wood, 3mm of epoxy was placed around the entire rod, by drilling a 26mm hole in the wood specimen for a 20mm diameter bar (see figure 4.2). This hole diameter was also used by Deng (1993).

4.2.5 Steel Used.

The steel required for testing these connections must be of a high yield strength, such that failure occurs within the connection and not by the steel yielding. The threaded rods used for

the connections had a yield strength of 680Mpa. Deformed bars had a yield strength of 430Mpa. Both these stresses are 5th percentile strengths, as quoted by the manufacturers. All bars were of nominal 20mm diameter.

4.3 Construction of Test Connections.

4.3.1 Assembly of Connection.

Difficulties arise when constructing the epoxy dowel connection due to sloping grain in most timber causing the drilled hole to be slightly off-centre. Even in a short embedment length such as 300mm it is difficult to keep the long drill-bit parallel to the edges of the timber, as it deflects within the timber. Thus when these connections are being assembled in practice, care must be taken to ensure that long embedment lengths are drilled correctly. All holes once drilled were cleared of dust and wood-chips using compressed air. The threaded rods used in the connection were cleaned of visible oil and grit by rag and wire brush.

4.3.2 Epoxy Mixture and Insertion.

The epoxy was mixed as stated in the manufacturer's instructions using plastic containers for the preparation and mixed by hand using a wooden stirrer for 3-4 minutes, trying to ensure the minimum amount of air was being entrained. The mixture was then poured into prepared 328ml caulking tubes. Stated pot-life of the epoxies was about 30 minutes, though they became jelly like from about fifteen minutes. The epoxy was then injected into the pilot hole until it began to flow out of the air-hole (see figure 4.2). The epoxy level was continuously topped up as it slowly filled all the voids between the steel and the wood. Once the epoxy had begun to harden, more epoxy was injected in to ensure complete coverage, in case of shrinkage or leakage.

To assemble the connection, simple wire rings were placed on either end of the cut to length bar, so the epoxy could spread evenly around the bar on injection. A sealing putty was pushed into the end hole surrounding the bar, to stop the epoxy running out as it was injected in.

4.3.3 Epoxy Flow in Wood-Steel Cavity.

As the epoxy is poured into the cavity between the threaded rod and the wood it fills the visible minor orifices in the timber, but also moves into the wood due to the woods inherent

permeability. Thus a larger amount of epoxy must be poured into the cavity due to the woods permeability taking epoxy into the air cavities. West System epoxy has the consistency of thin oil and as such enters the wood more readily than does K80 epoxy, which has a thick oil consistency. Thus during the epoxy construction process more West epoxy will be needed as the wood readily soaks it up.

The cured epoxy that has entered the air-spaces in the wood should provide a better wood-epoxy bond, than that of an epoxy that has not permeated into the wood. Thus West system should have stronger bond strength, especially in shear resistance.

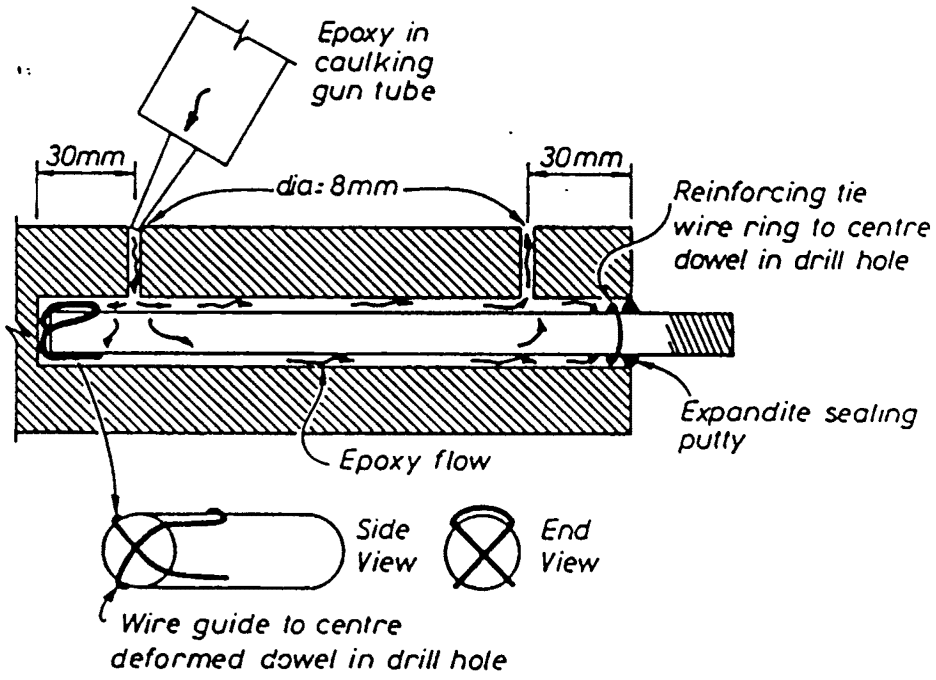

Figure 4.2. Schematic Diagram of the Epoxy Construction Method, (Townsend, 1990).

4.3.4 Temperature of Specimens.

To record the temperature in the epoxy, a temperature sensor was glued into each test specimen. This was positioned 2mm above the threaded rod (or deformed bar) in the epoxy cavity with the wires extending out an air-hole. The temperature sensor was placed in the 300mm embedment length control end to ensure that it did not affect the strength of the tested end. The sensor was placed 185mm from the base of the test specimen.

4.3.5 Calibration of Temperature Sensors.

The temperature sensors placed in the test specimens were small integrated circuits, designated LM35DZ. These small temperature probes are powered by voltages ranging from 5-30Volts and are accurate to ± 2°C over the temperature range of 0 to 100°C . These devices are also very linear so can be calibrated easily for complete accuracy. The LM35DZ have a linear scale of 10mV per °C and thus it is a simple procedure to connect a 10 volt power supply and volt meter to read the temperature directly.

To calibrate the sensors their actual output voltage (temperature) was checked using a Crison T-637 digital thermometer. Each sensor was calibrated at ambient, 40°C and 90°C to ascertain the error in temperature detection. From these readings linear interpolation could be used for intermediate temperatures. To ensure that the sensor wires could withstand the high temperatures in the oven and their resistance didn't alter, samples of wire were tested at various temperatures. The resistance altered little over a range of temperatures from 15°C to 160°C. The wire was rated at 70°C and breakages in the plastic coating were not evident until 150°C was reached. To ensure that temperatures were recorded during the testing procedure the sensors were connected to the data logger that was being used to record load and deflection.

4.4 Test Procedure

4.4.1 Heating the Test Specimens.

The first set of twelve tests with threaded rods were over a broad range of temperatures to see how the two epoxies, West system and K80, reacted to the heat (see table 4.2). Tests were also carried out on the two deformed bar specimens to see if there was any significant change in tension strength at elevated temperatures, compared with threaded rods. The next 14 tests were used to provide a more centralized guide to the strength reduction with the elevated temperatures.

Specimen Number	Epoxy Type	Oven-dry Density	Moisture Content (%)	Failure Load (kN)	Failure Temp. (°C)	Failure Mode
101	K80	398.4	11.5	88.2	41.5	a
102	K80	433.7	10.2	31.7	89	c,d
103	K80	419.5	8.9	148.5	41.7	a
104	K80	422.6	12.1	25.4	76	c,d
105	K80	364.9	9.3	51.1	55	a
106	K80	407.3	10.9	22	73	c,d
107	WEST	413.6	11.2	99.1	53.5	a
108	WEST	426.2	10.3	95.3	42.4	b
109	WEST	427.3	10.8	81.2	42	b
110	WEST	426.1	12.8	24.4	74.1	a,c,d
111	WEST	416.3	9.7	30.7	81.4	c,d
112	WEST	388.6	13.3	32.1	71	c,d
113	WEST	428.5	10.0	80.3	21	a
114	K80	399.2	9.9	93.1	21	b
115	K80	418.4	12.2	92.9	20.7	a
116	WEST	435.7	10.2	126.9	21	a
117	K80	411.3	11.5	79.9	63.5	a,c,d
118	K80	378.2	9.7	54.1	70	a,c,d
119	K80	412.8	10.9	78.3	46	a
120	K80	398.7	10.3	99.1	49.1	a
121	K80	364.7	13.1	59.7	60.1	a,c,d
122	WEST	418.9	13.6	54.5	59	a,c,d
123	WEST	411.6	10.3	108.9	48	a
124	WEST	429.4	11.4	93.9	46.4	a
125	WEST	417.8	9.7	52.8	62.3	a,c,d
126	WEST	427.9	13.1	41.8	66.6	a,c,d

Table 4.2. Oven Test Specimen Data, (Failure Modes - see section 4.5.3).

To be certain that the epoxy connection was at constant temperature throughout, the cured connection was placed in a pre-heated oven and left for 24 hours. Thus the wood, steel and epoxy were in equilibrium at the pre-set oven temperature and were then tested. The large oven for heating the specimens was electrically powered and used fans to circulate air over the hot elements placed in the bottom of the oven. Temperatures were recorded in the oven by using a Crison T-637 digital thermometer.

Density and moisture content measurements of test specimens yielded results of (see table 4.2),

Average density - 411.4 kg/m^3

average moisture content - 11.1%

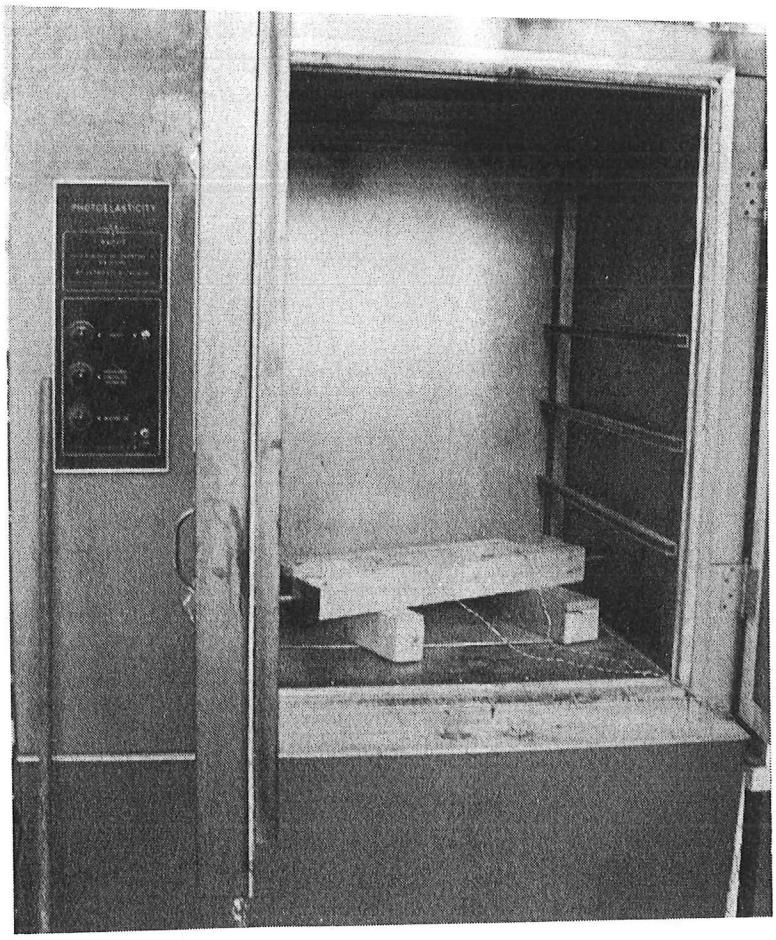

Figure 4.3. Test Specimens in Oven.

4.4.2 Testing Method.

To perform the tension tests the Instron testing machine was used. The test samples were loaded into the Instron machine (figure 4.4) directly from the nearby oven, i.e. still at the temperature of the oven. The installation of the specimen in the testing machine took about one minute to complete and thus the temperature in the test specimen dropped only 1-2°C by the time of failure.

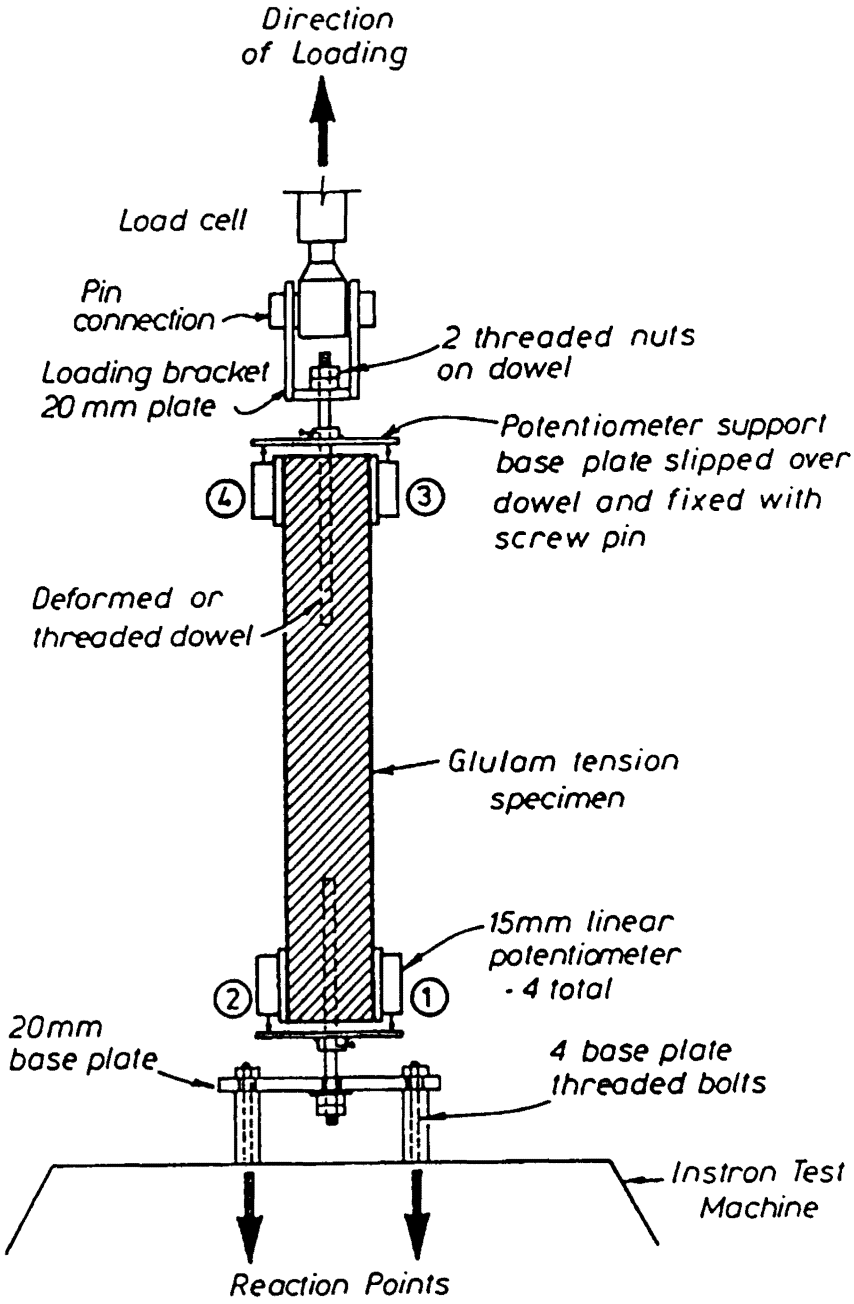

Figure 4.4. Schematic of Instron and Specimen, (Townsend, 1990)

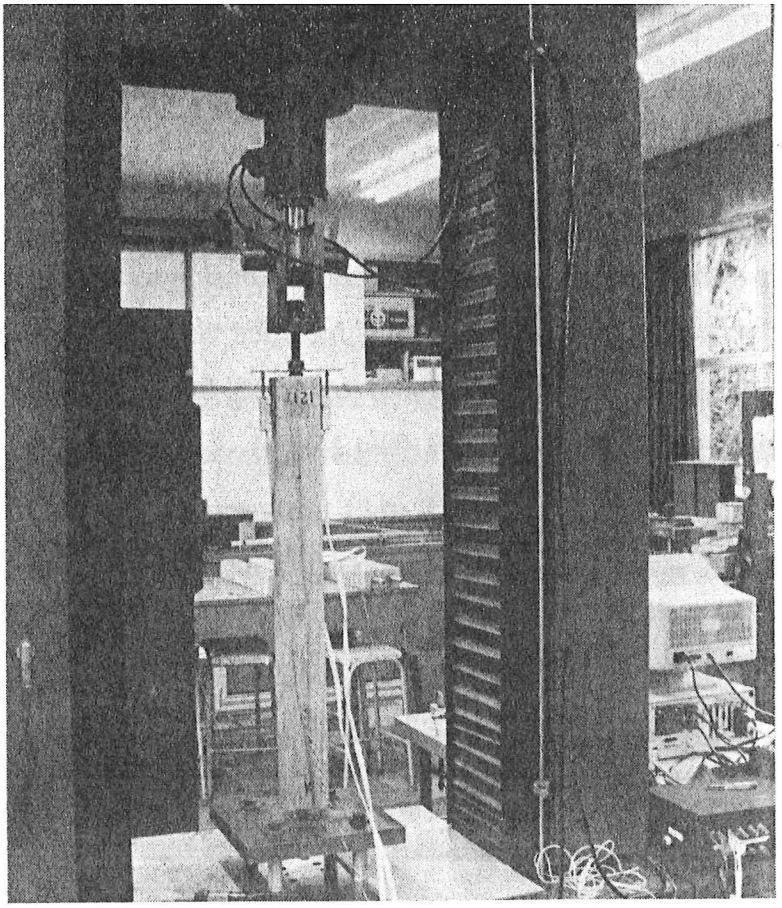

Figure 4.5. Specimen in Instron.

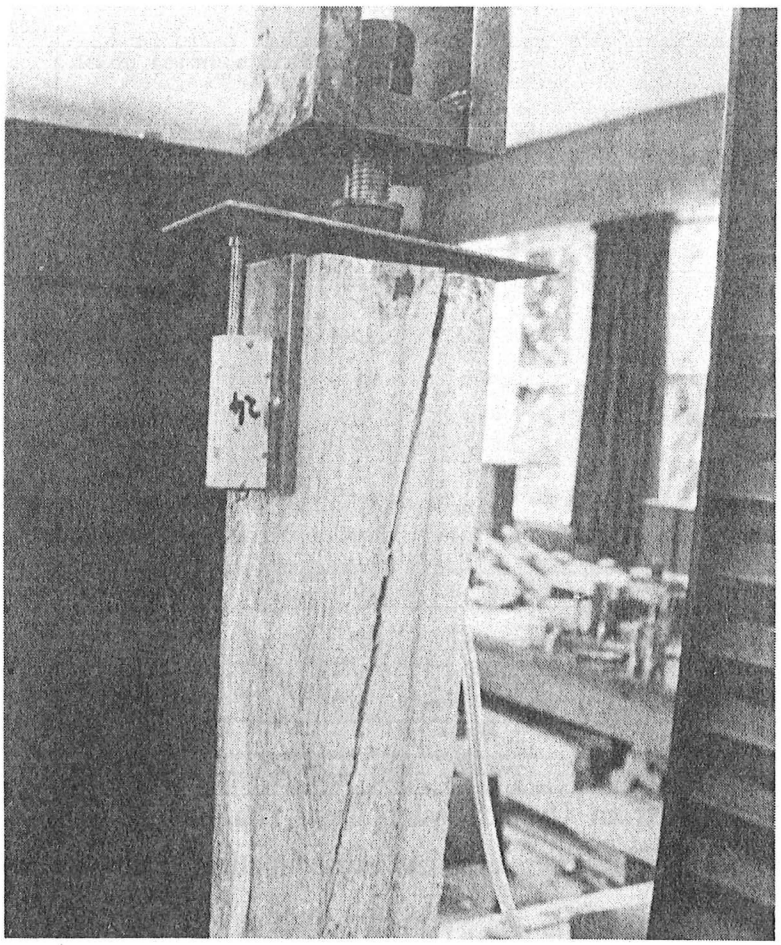

Figure 4.6. Failure of Specimen in Instron.

Each test specimen was loaded at a rate of 2cm/min, a faster rate than that used by Townsend (1990) and Deng (1993). This was to reduce the temperature drop during testing. Movement at the test end of the bar as it extended from the epoxy, was recorded via two deflectometers, which are averaged over their travel. The specimens were loaded until failure occurs, whether by timber failure or large pull-out deflection (greater than 15mm).

4.5 Test Results.

From the compiled results of the tests shown in table 4.1 and figure 4.7, it is easy to see how the tension strength of the connections was reduced by elevated temperatures. There is scatter in the results, as to be expected with such a small sample, but the trend of strength reduction at elevated temperatures is obvious.

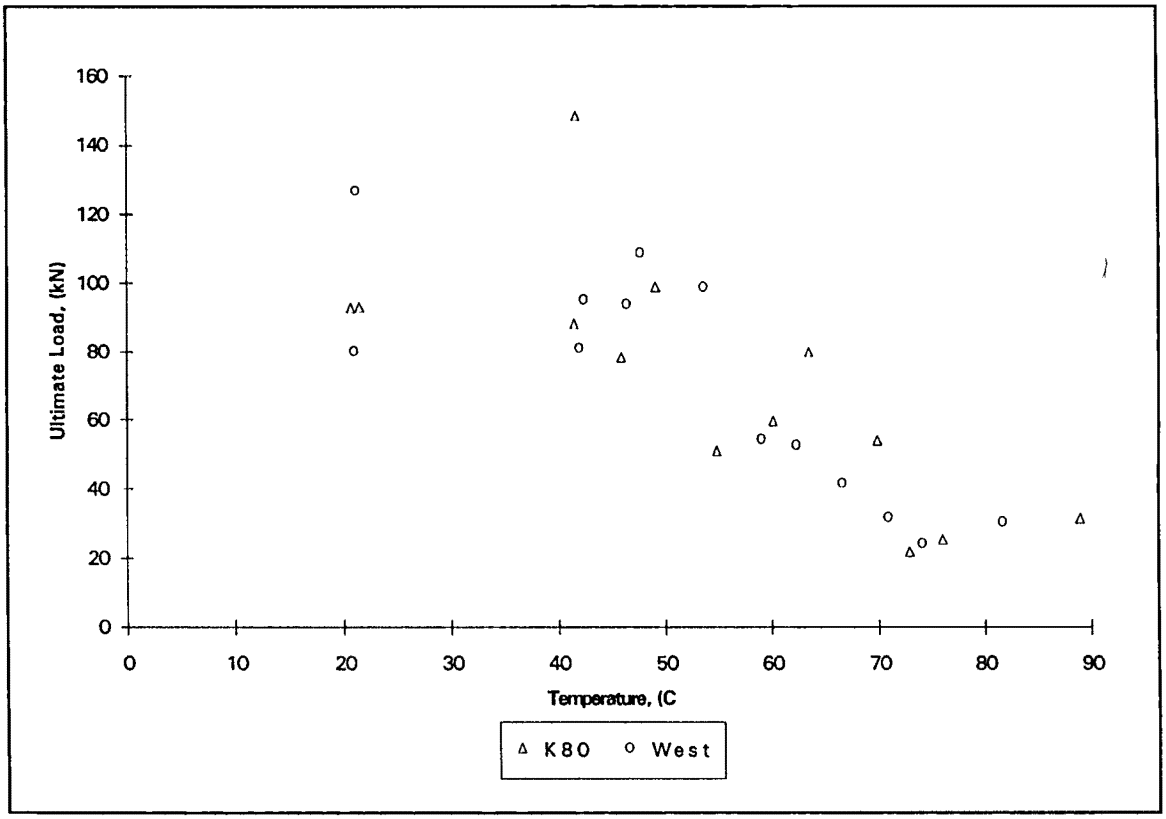

Figure 4.7. Complete Test Data from Oven Tension Tests. Failure Temperature Recorded is at the Point of Maximum Load.

The trend of strength reduction with elevating temperatures can be depicted by plotting three straight lines on the data, as shown in figure 4.8. These lines have been sketched by eye,

arranged so that there are about the same number of data points on each side. The failures can thus be segmented into three stages,

i, Full strength, unaffected by heat (temperatures below approximately 45°C)

ii, Critical temperature reached, with resulting reduction in strength as temperature increases (temperature 45 to 70°C).

iii, Residual strength in the connection (temperatures 70 to 90°C).

A complete description of how each specimen failed and load deflection curves are contained in Appendix 1. Other research shows zero strength in the epoxy will be reached at approximately 200°C (Tabor, 1978).

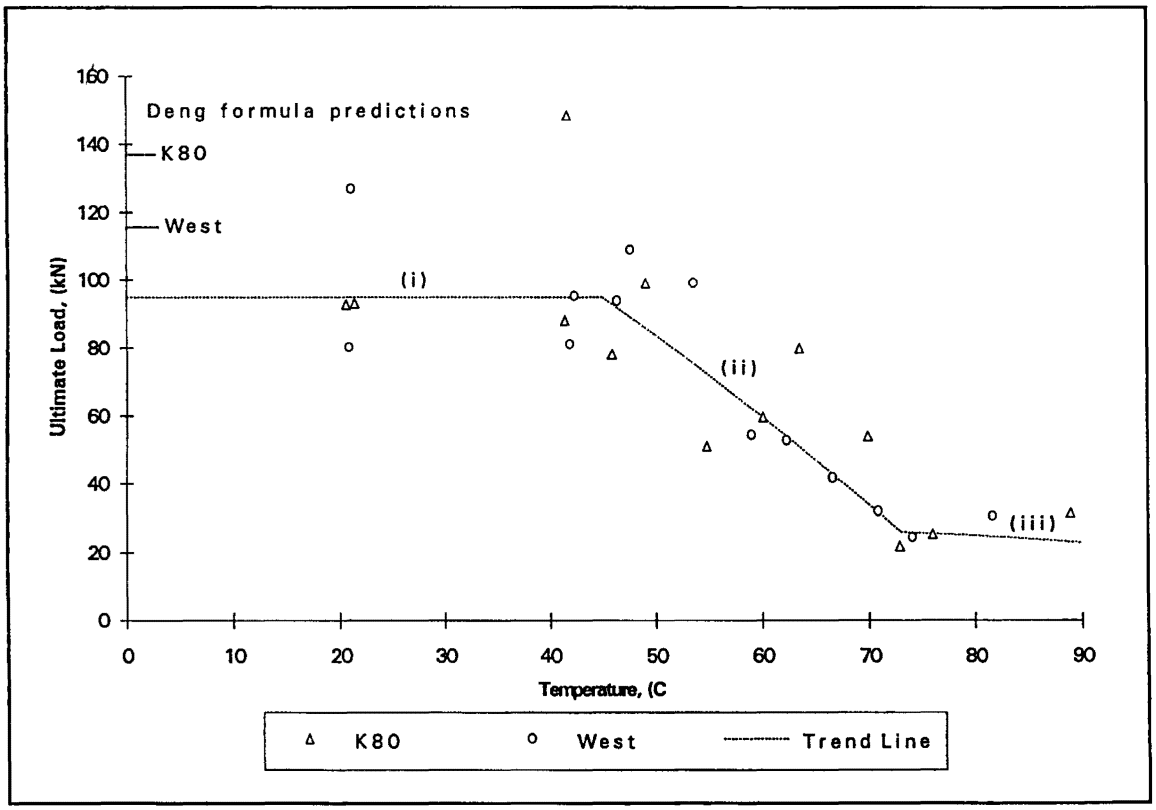

Figure 4.8. Oven Tension Test Data with Three Stages of Epoxy Strength Plotted.

The scatter in the results is less as test temperature increases, showing the importance of the epoxy in the high temperature failure modes. At elevated temperatures failures occur within the epoxy and not within the wood, thus the uncertainty and scatter in the results lessens as

the epoxy has only small variation in strength and stiffness properties, at a prescribed temperature.

4.5.1 Extension in the Connection.

Using bar extension (measured deflection) in the epoxy as it softens can be used as a guide to approximate critical temperature (see figure 4.9). Ambient temperature deflections at failure are of the order of 0.25 to 0.5mm. This extension within the connection started to become larger (1.5 to 2.5mm) when temperatures of approximately 40 to 50°C were reached (see figures 4.10 and 4.11). The extension is due to the loss of stiffness in the epoxy, thus causing the load-deflection curves to become more curved in shape. To display the extension, figure 4.9 is plotted showing the deflection per 100kN of applied load, at the various failure temperatures (tension specimens that had failure at the 300mm end are not included as the maximum deflection was not reached). The graph shows that the West System epoxy reaches a critical temperature at approximately 55°C. The K80 epoxy is more variable due to its more elastic-plastic progression through its critical temperature, at approximately 45-50°C.

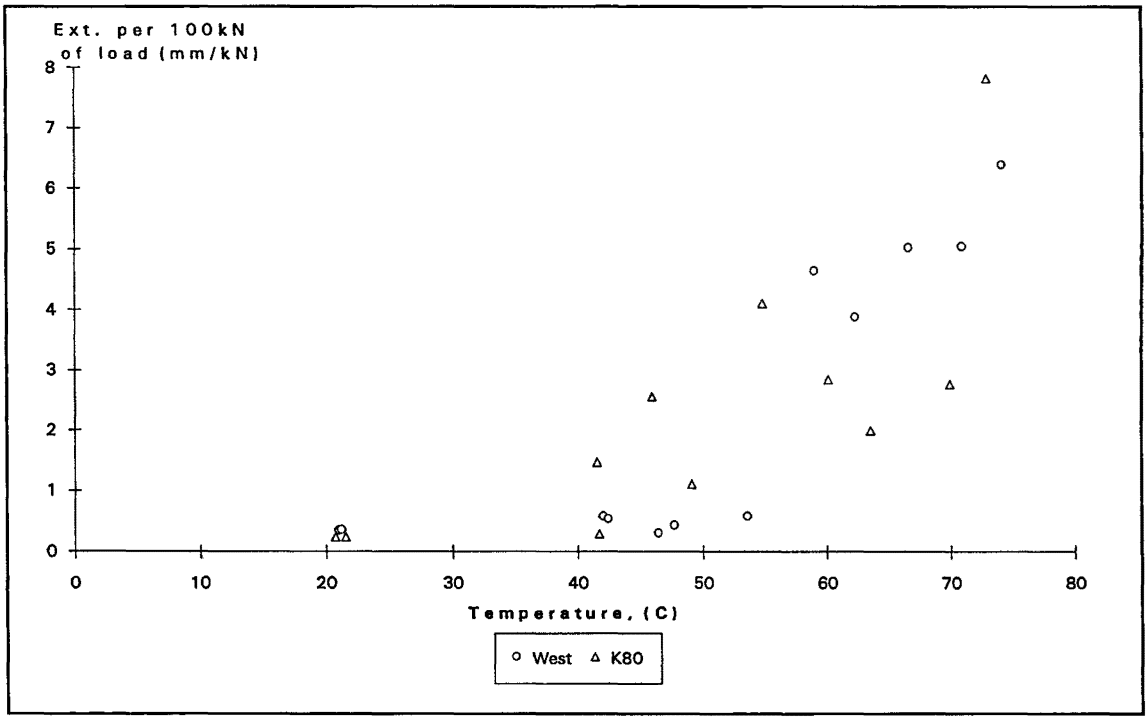

Figure 4.9. Extension of Threaded Rod per 100 kN of Load vs. Temperature at Failure.

4.5.2 Load Deflection Curves.

The load deflection curves at ambient temperatures are denoted by their very steep increase in load, then very fast, brittle failure as ultimate load is reached. Both K80 and West epoxies follow this pattern, though the transition into the more slower ductile failures is different.

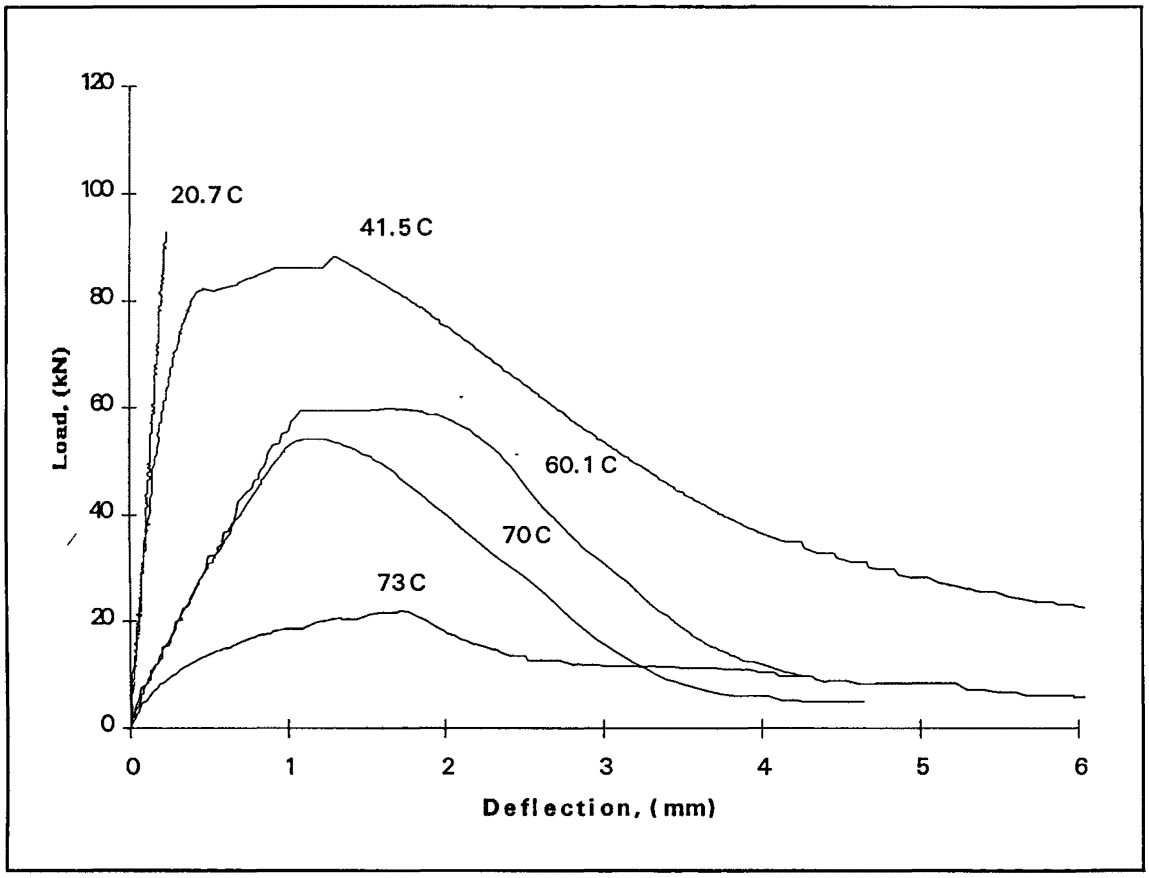

Figure 4.10. Typical Load Deflection Curves for Increasing Temperatures for K80 Epoxy.

The large deflection, slow pull-out failure that occurs when the epoxy loses its stiffness occurs at approximately 45°C for the K80 specimens. The West epoxy loses its stiffness at approximately 55°C. To show the loss of stiffness in the epoxy, load deflection curves for various temperatures have been plotted together. Typical curves are shown in figures 4.10 and 4.11. All load deflection curves are shown in Appendix 2.

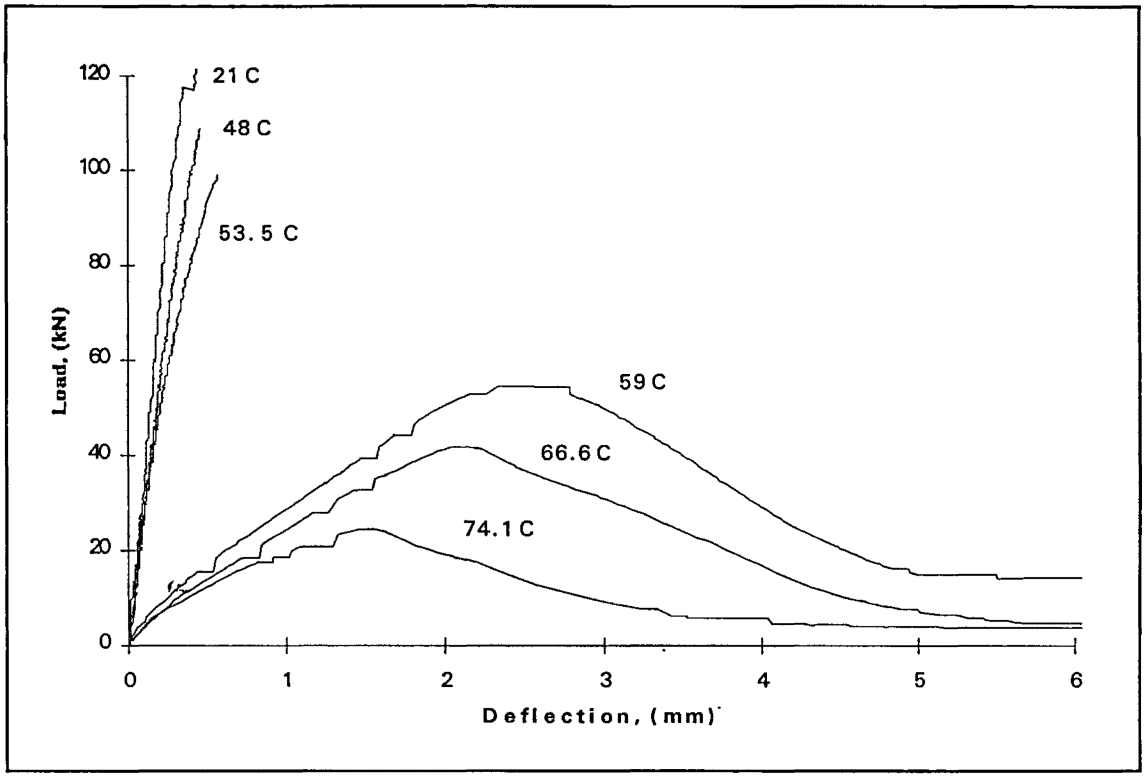

Figure 4.11. Typical Load Deflection Curves for Increasing Temperatures for West Epoxy.

4.5.3 Failure Modes.

The type of failures occurring are as follows,

a, Confinement failures due to the wood not being able to confine the movement of the steel and epoxy, due to the tension load. This is a fast brittle failure with large splits in the wood surrounding the connection and extending down the test specimen (figure 4.12).

b, Tension failures in the wood, at the end of the steel bar, or remote from it. The failure in the wood is due to its tensile strength only and the failure is brittle and fast. Failure is induced by weaknesses in the timber such as knots and the construction air-holes (figure 4.13).

c, Shear failure in the epoxy due to the elevated temperatures. This failure is slow and ductile and either occurs with slight splitting around the connection as some confinement is lost, or simply by a pure shear failure. The shear failure generally occurs in the epoxy at thread-top height (figure 4.14).

d, Bond failure between the wood and epoxy, causing a plug of epoxy to withdraw from the connection hole with the bar. A bond failure was usually accompanied with some form of shear failure in the epoxy (figure 4.15).

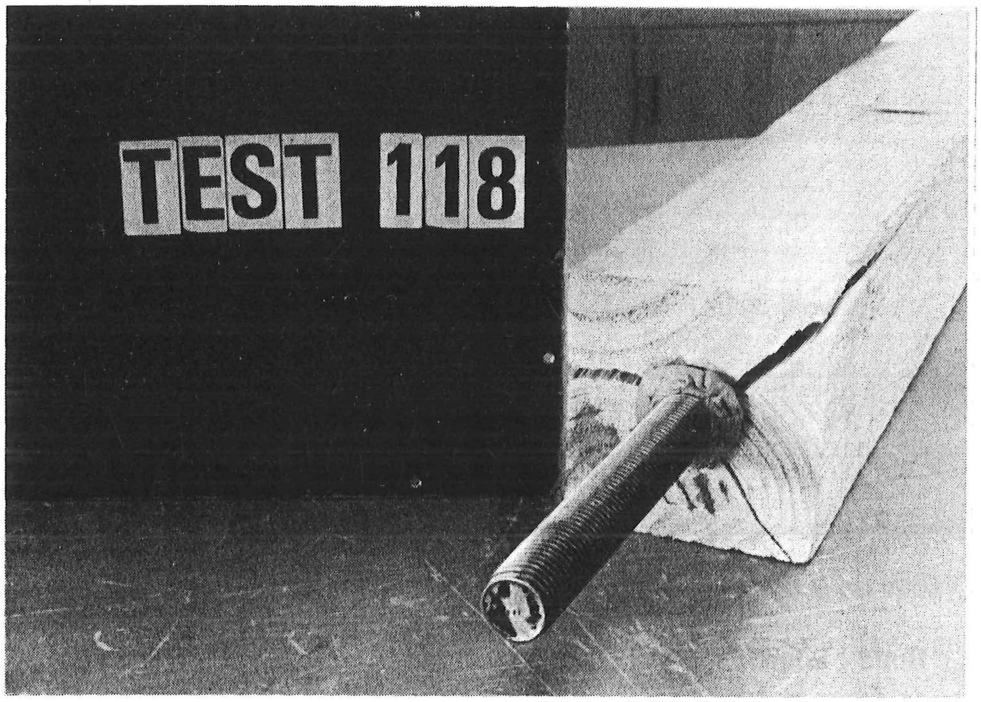

Figure 4.12. Confinement Failure in Wood.

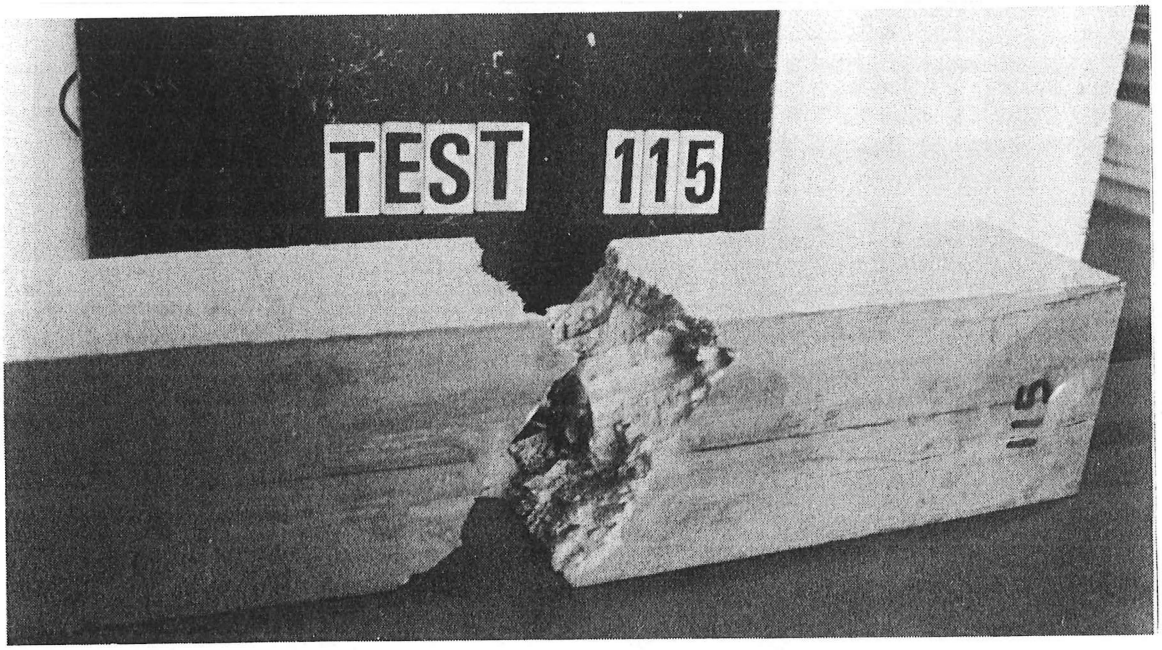

Figure 4.13. Tension Failure in Wood.

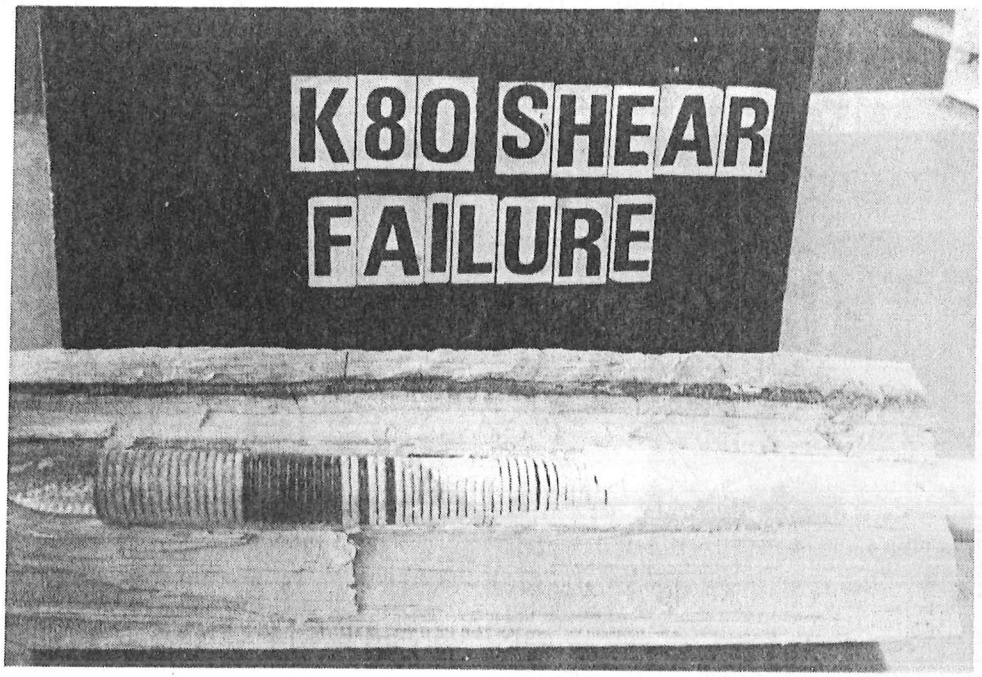

Figure 4.14. Shear Bond Failure in K80 Epoxy.

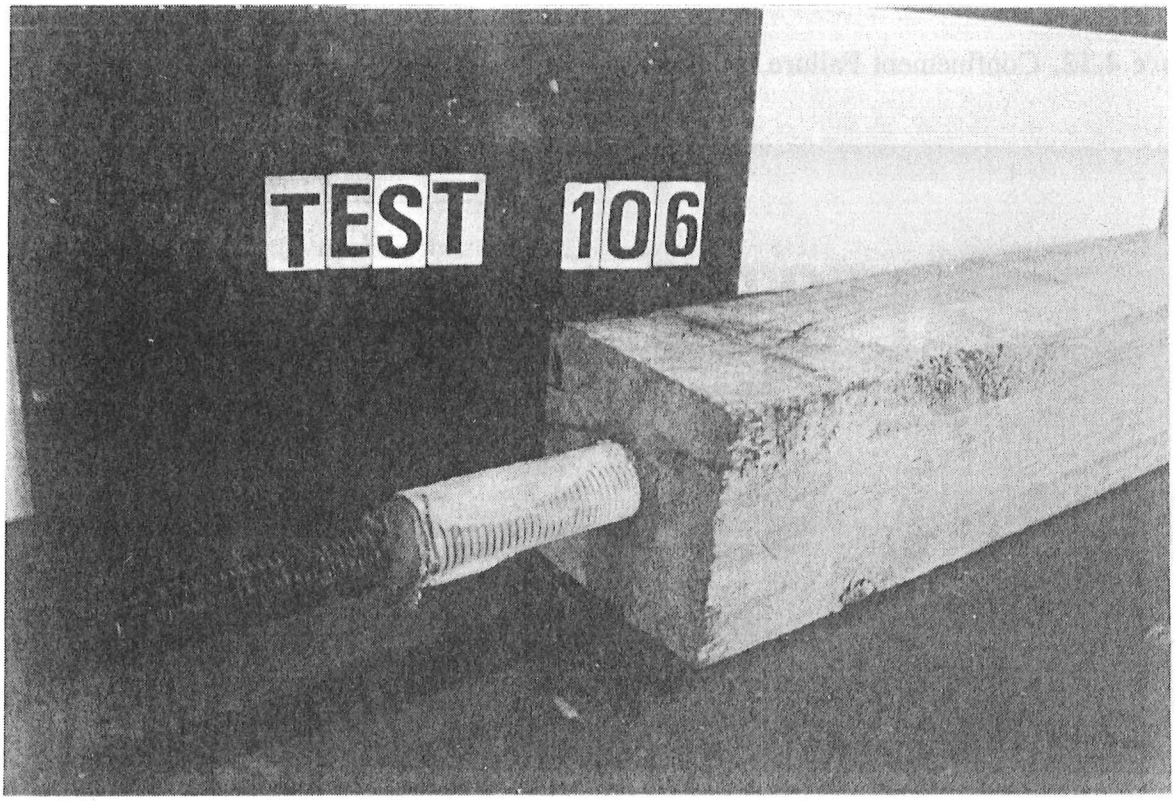

Figure 4.15. Bond Failure in K80 Specimen.

Failures a and b occurred at temperatures approximately less than 50°C, whilst failures c and d occurred at temperatures greater than 50°C. Failures a to d were observed in both K80 and West test specimens.

4.5.4 Shear Failure.

The shear failures occurring in the epoxies do differ in type and show how the epoxy stiffness reacts with heat. K80 shear failures occur by a sliding in a plane at the top of the threads (of the threaded bar). The epoxy movement is elasto-plastic with the threaded epoxy still holding its shape once the extension has stopped. Thus the K80 epoxy acts like a low viscosity fluid at the higher temperatures and retains some strength once back at ambient temperatures.

Shear failures in the West epoxy occur with the epoxy breaking and shattering due to the threaded rod, in a plane level with the top of the threads. At elevated temperatures the same failure would occur, but shattering of the epoxy was less widespread as the epoxy had a slight stiffness reduction. Thus there is still stiffness in the shattered West epoxy though it will have no residual strength once back at ambient temperatures, i.e. the epoxy is permanently shattered along the shear plane. Often there would be little no cracking evident in the timber as the shear failures occurred (figure 4.16).

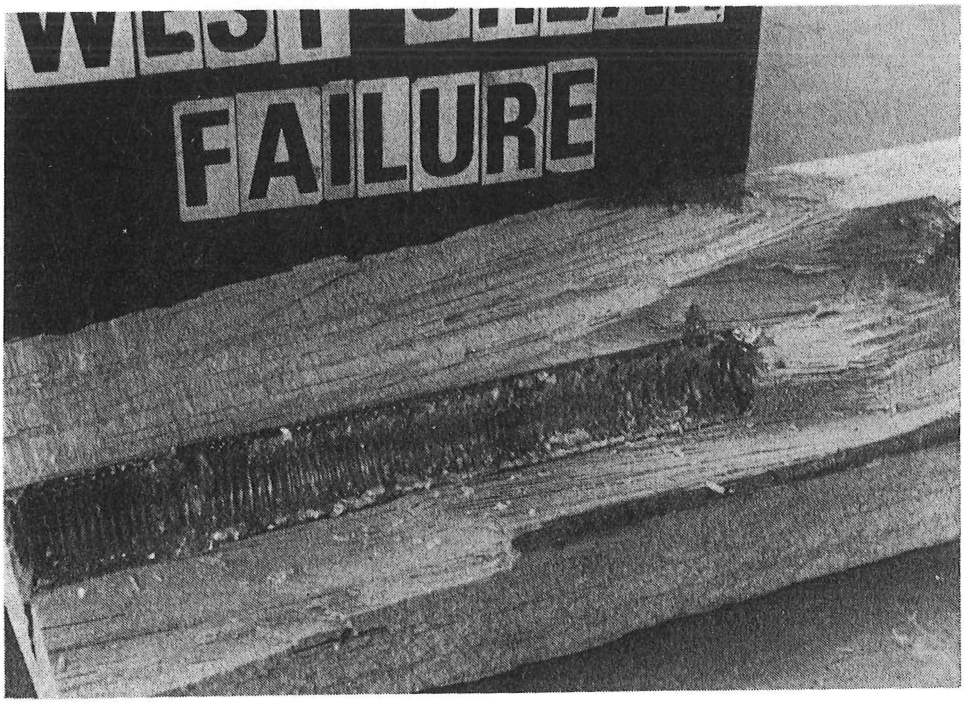

Figure 4.16. Shear Failure in West Specimen.

The elastic properties of the K80 epoxy were apparent at the end of most splitting or shear failure tests. Once the load was returned to zero and the specimen still in the testing machine, it would often re-load itself as the epoxy retracted back to its original pretest position. K80 obviously has good elasto-plastic properties as is shown by its attempt to regain its initial shape, even after 2-3mm of deflection.

4.5.5 Confinement Failure.

As confinement failures occurred at lower temperatures, splitting began around the connection and spread down the length of the timber. As the tension load increased the cracking and splitting continued, with large splits opening to 4-5mm in width and 300-400mm in length. Splitting and opening of the timber continued until failure by either slow opening of timber or fast and extensive splitting (figure 4.17).

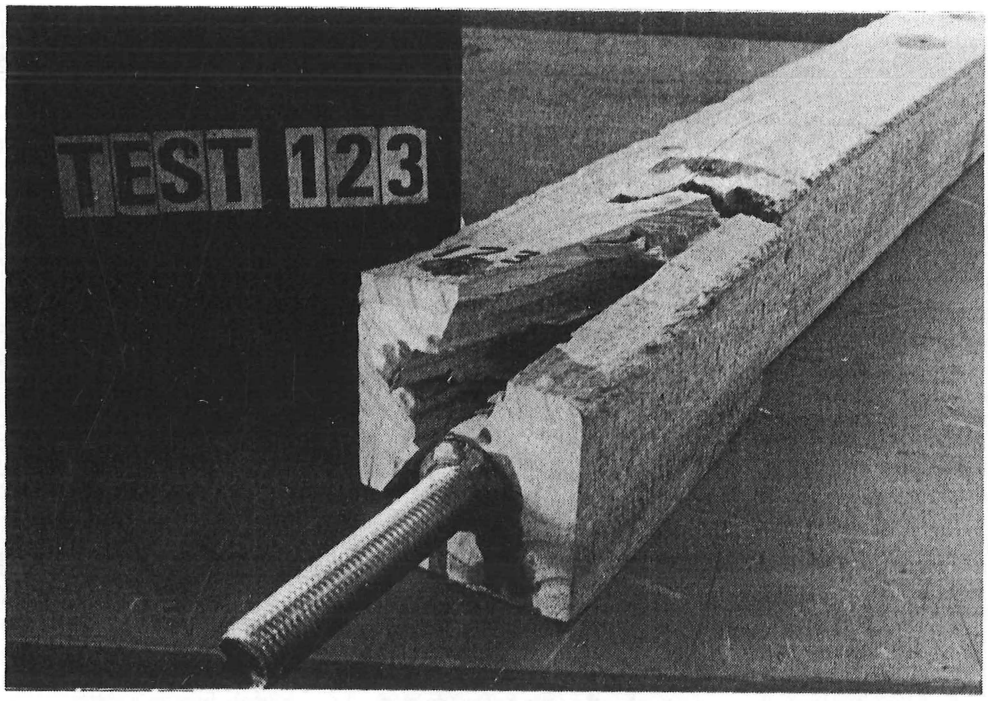

Figure 4.17. Confinement Failure with Extensive Splitting.

4.5.6 Failure at 300mm Embedment Length End.

At the high temperatures of approximately 70-80°C, three failures occurred in the 300mm embedment length end (two K80, one West epoxy). The failures were all combination bond and epoxy shear failures with large deflection pull-outs. As the specimen was being loaded the 200mm test end would extend as expected, then suddenly the 300mm end would also start to extend. Thus failure occurred at both ends, with extension of the bar from each end. It can be concluded from this result that at the higher temperatures (greater than 70°C), the difference in embedment length will not govern strength. Thus at the higher temperatures a longer embedment length will not guarantee more strength, as the epoxy has such a stiffness reduction that shear failure (and/or bond failure) will always occur.

4.5.7 Appearance Changes of the Epoxy.

The high temperatures of 80°C also changed the complexion of the epoxies. Once cooled to ambient temperatures, small sections of the K80 adhesive was found to be very crumbly and powdery. Its colour had partially changed from grey to white and had no strength to it. It could easily be picked away from the still intact grey coloured epoxy. The West epoxy, once cooled, had a more brown colour and was easily broken and picked off. This epoxy became very brittle and was glass like in the way it could be broken. Very different from its hard durable appearance on curing at room temperatures.

4.6 Strength Prediction Comparisons.

Deng (1993) developed a formula to predict tensile pull-out strength (see section 4.2.2) with the results of 138.8kN for K80 epoxy and 117.4kN for West epoxy. Figure 4.8 shows plotted trend lines for the oven tension test results and shows an ambient tensile strength of approximately 95kN. This shows the large scatter that must be expected when working with wood and this must be taken into account if using Deng's strength equation.

4.6.1 Timber Stiffness.

The differing range of stiffness in the timber was evident in the rate at which the specimen loaded itself. Though the Instron applied the deflection at a constant rate, the more stiff timber specimens would load quickly and usually fail quickly, in a brittle manner. Slowly loading specimens would normally fail by slow splits and cracks opening up. This difference

in stiffness of the wood can be attributed to its own strength and the difference in moisture content between specimens. The average moisture content was approximately 11% (table 4.2), though each specimen would have dried differently in the oven.

4.6.2 Cracking in Test Timber.

The low humidity heating of the oven caused drying of the timber specimens and cracking to occur. Most specimens had small cracks opening up on their exteriors, due to the low moisture content. Some wood seemed to react quite badly to the heating process with large cracks opening up. Some of these cracks did seem to induce failure, especially if they were near the edges of the testing end. Cracks were sometimes 2-3mm in width and 100-200mm in length.

CHAPTER 5

FURNACE TESTS

5.1 Introduction.

To evaluate the strength of the epoxied steel rod connections under severe fire conditions, full scale furnace tests were conducted using the BTL (Building Technology Limited) pilot furnace at Judgeford, near Wellington. The furnace temperature follows the ISO834 Standard Fire.

Research by Avent & Issa (1984) had shown that results from small scale tests on epoxy did not relate to full scale tests. Thus it was important to ensure that the tension test data could be confirmed with full scale tests.

5.2 Furnace Test Method.

Both the West system and K80 epoxies were tested by constructing 6 splice connections, as shown in figure 5.1. Each epoxy was tested with three embedment lengths, 250mm, 300mm and 350mm. The completed splice had the dimensions of 156 x 134 x 2000mm. Two furnace tests were conducted, one test with three splices using West system epoxy and the other test with three splices using K80 epoxy. Only threaded bars were used for these tests as they provide more strength than deformed bars under a tension load (Deng, 1993). Thermocouples were glued to the threaded rods to measure the temperature of the epoxy inside the splice.

5.2.1 Splice Construction.

The six splice connections were constructed from cutting down a 490x134mm glulam beam into 12 pieces of size 134x156x1000mm. The glulam timber was previously stored in a large warehouse, where it was kept dry and well ventilated. The glulam timber was manufactured by Hunter Laminates Ltd, of Nelson. The glulam was constructed from laminations of 42mm thickness. Density measurements on 10 off-cut samples gave an average oven-dry density of 417kg/m^3. The moisture content was recorded over the construction period and varied little

from its initial 11% reading (see table 5.1).

Specimen No.	Density kg/m^3	Moisture Content %
201	389.8	12.9
202	418.3	11.4
203	427.8	9.1
204	401.2	10.7
205	425.5	8.5
206	409.9	13.2
207	445.6	9.6
208	416.0	10.9
210	429.9	12.3
212	409.2	8.8
Average	417.3	10.9

Table 5.1. Density and Moisture Content of Ten Timber Samples From Splice Tests.

Drilling the timber specimens, preparing the threaded rods and gluing followed the same approach as used in the oven tests (section 4.2). Due to a small 1-2mm gap expected between the spliced beams a fire-resistant caulking, Fyreflex (supplied by Wormalds, Christchurch), was applied on the ends of the timber members before they were butted together and glued in place. The caulking was a non-asbestos sealant that had been tested to AS1530/4 (Australian Standard of Fire Resistance Tests of Elements of Building Construction). A bead of 4-5mm in width was applied 3-4mm from the edge of the timber and the splices lightly clamped together to ensure good spreading of the fire-resistant sealant and to ensure no movement occurred in the splice while curing of the epoxy took place.

At the outer ends of the spliced specimens, threaded rods of the same embedment length were

epoxied in place. This is shown in figure 5.1.

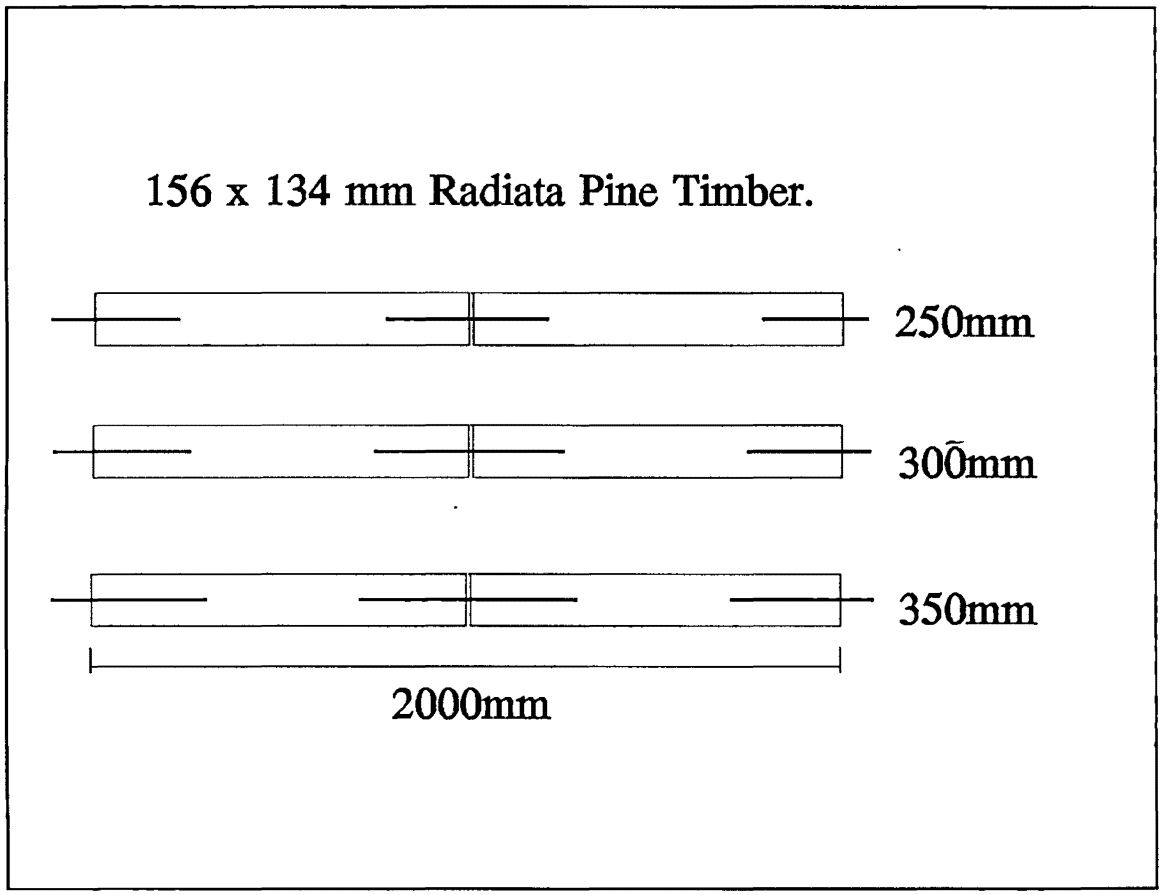

Figure 5.1. Embedment Lengths of Furnace Specimens.

To record temperatures inside the connection during the fire tests thermocouple wires were attached to the splice bar. These thermocouple wires were situated in the epoxy surrounding the bar so as to record the temperature rise within the epoxy (see figure 5.3). The wires were then passed through a 5mm hole drilled down the length of the splice (figure 5.2). Drilling of this small hole over a large distance proved to be difficult, but was achieved for four of the six splice beams.

5.2.2 Force Applied.

A tension load was applied based on the splice connection bars being designed for a stress level of 0.6 of their yield strength (f_y) under code specified loads. Under fire conditions, New Zealand Standards (SNZ, 1992) specify the gravity load conditions to be D + 0.4L (where D = dead load, L = live load). Under cold conditions the gravity loading is 1.2D + 1.6L. If it

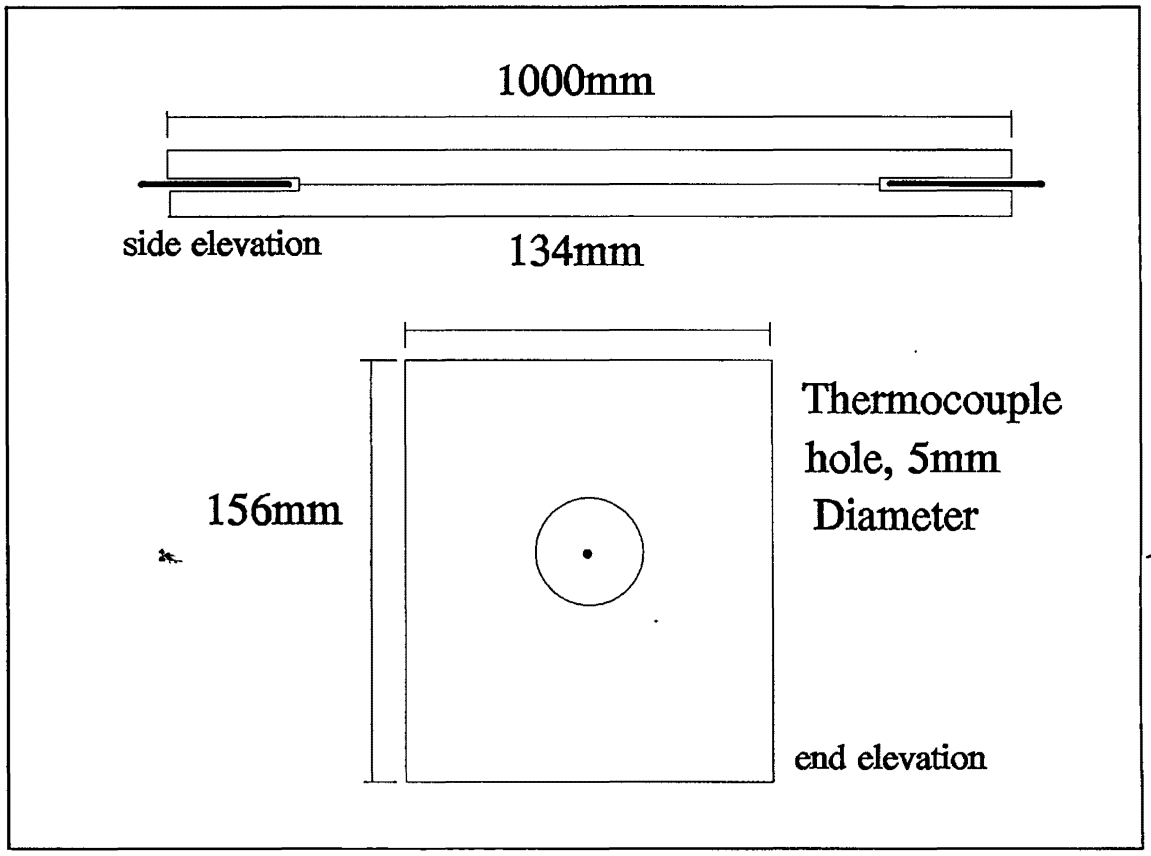

Figure 5.2. 5mm Hole Drilled in Splice Test Specimen to Position Thermocouple Wire.

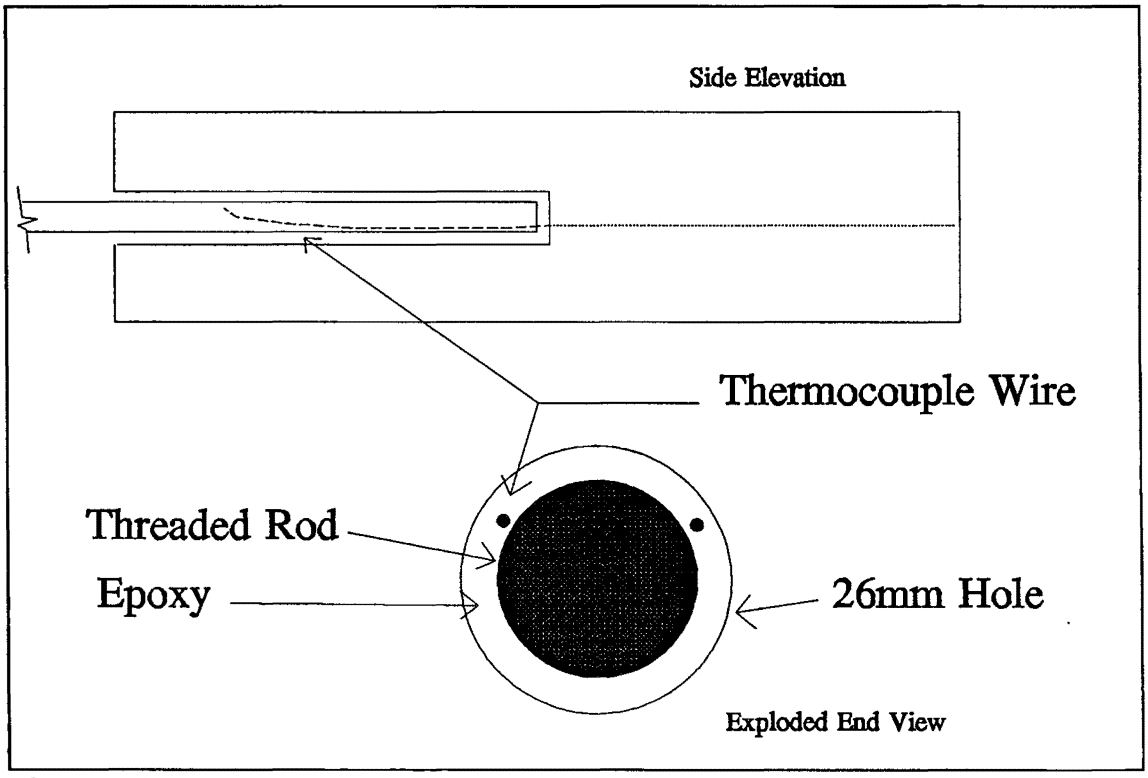

Figure 5.3. Location of Type K Thermocouple Wire.

is assumed that the dead and live loads are equal, then total cold gravity loading is 2.8D; and the total gravity load in fire conditions is 1.4D, i.e. half that of the cold conditions. Thus assuming a stress in the bar of $0.6f_y$ under 1.2D + 1.6L and a yield stress for steel of 680MPa, the load T carried under fire conditions will be,

$$T = 0.6 f_y A_c \; 1/2 \qquad 5.1$$

$$0.6 \times 680 \times 245 \times 1/2 = 49.98\text{kN}$$

where Ac = thread core area of 20mm rod.

Thus a tension load of 50 to 60kN was applied during the test. Based on strength predictions of 4.2.2, 50kN corresponds to 36% of K80's ultimate tension strength and 43% of West's ultimate tension strength.

These loads are quite severe as most connections would normally have steel of yield strength 300 or 430MPa, resulting in loads of 22.1kN and 31.6kN respectively. Thus the steel rod is not highly loaded, but the wood and epoxy are. This is to ensure failure occurs within the wood-epoxy connection and not in the steel.

5.2.3 BTL Furnace.

The pilot furnace situated in the fire testing laboratory at Building Technology Limited is diesel fuelled with the internal dimensions of 2200mm long x 1000mm wide x 450mm deep. The furnace has four internal thermocouples, shown in figure 5.4. The oxygen concentration inside the furnace during burning varies between 4% and 8%. The furnace is mounted such that it can be used either in a horizontal position or a vertical position. The horizontal position was used for these tests.

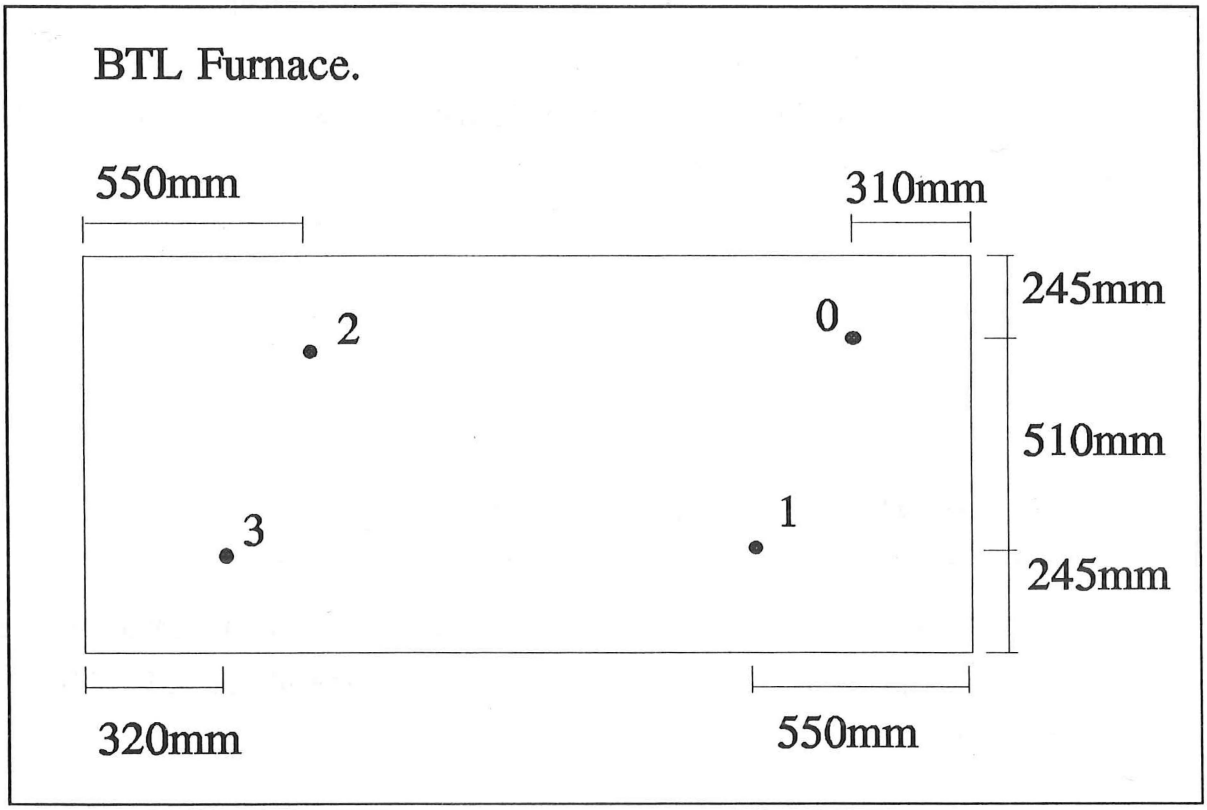

Figure 5.4. Location of Thermocouples in the BTL Pilot Furnace.

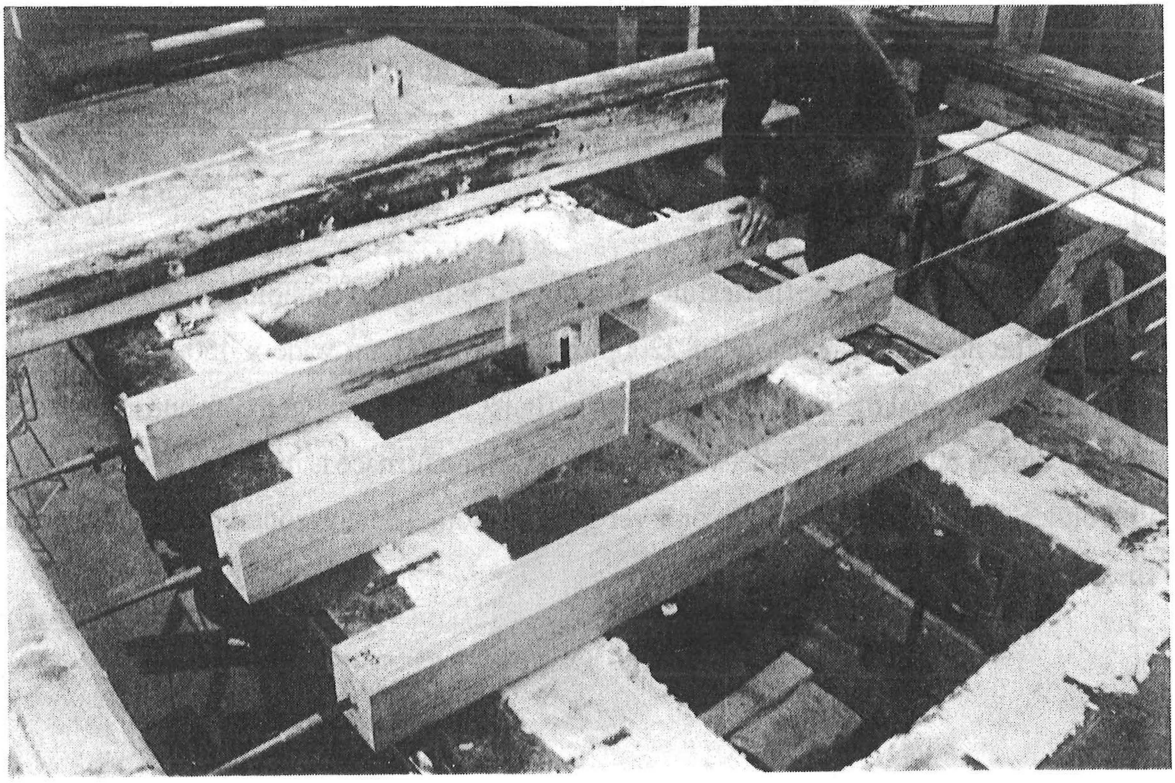

Figure 5.5. BTL Furnace and Splice Installation.

5.2.4 Test Specimen Installation.

The three specimens were positioned across the 2.0 metre length, with 500mm spacings between specimens. The test specimens were then anchored to one side of a reaction frame whilst the other end had a load-cell and jack applied the required force (figure 5.6).

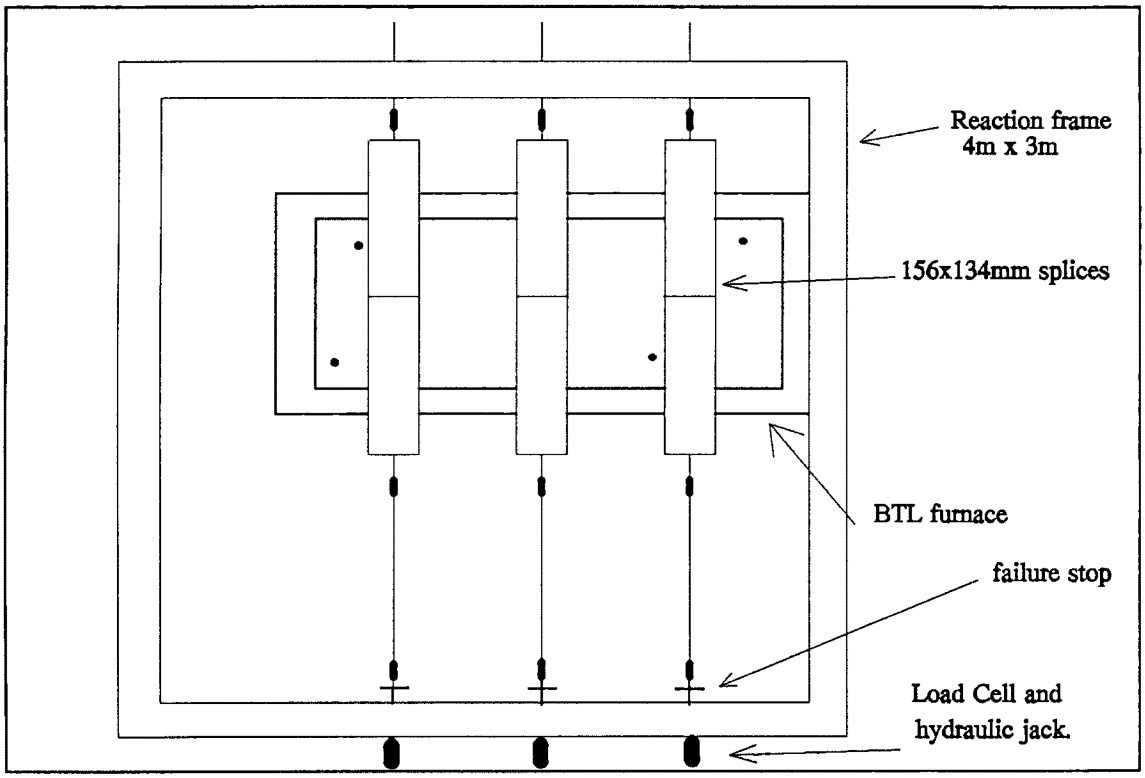

Figure 5.6. Schematic Diagram of BTL Furnace and Splice Location (not to scale).

The load was applied to each of the test splices using a hydraulic pump to apply the same pressure to each jack, resulting in similar loads. To measure the force applied, load-cells previously calibrated at the University of Canterbury were located between the jacks and the reaction frame. The pump was used to keep hydraulic pressure constant throughout the test. Stops were placed on the splice extension bars to limit movement to 30-40mm so that pressure in the hydraulic system would not be lost, even after one specimen had failed. Once the splice connection had moved the 30-40mm it could be deemed to have failed.

As the West specimens were being loaded before the test, the 300mm embedment length splice failed. The splice failed slowly at approximately 25kN. On inspection it was found that the glue had only partially cured in the splice. The failure was disappointing as it left only two West

system splices for comparison, but showed that even under laboratory conditions, problems can occur in the mixing of the epoxies. It appears that either the hardener had not worked properly, not enough hardener was added to the resin or it was not mixed properly. The accuracy required in measuring the quantities when mixing the epoxies is a problem that could limit use on a construction site.

Once the test specimens were attached to the reaction frame a heat containing lid was placed over the furnace. The lid was box shaped and had walls constructed of two sheets of 19mm gypsum plaster board. All gaps surrounding the lid were filled using fire resistant mineral fibre wool.

To record the movement in the splice, deflectometers were attached to the loaded end of each splice and anchored to the pilot furnace. The furnace was ignited and load was kept uniform until failure occurred in the splices.

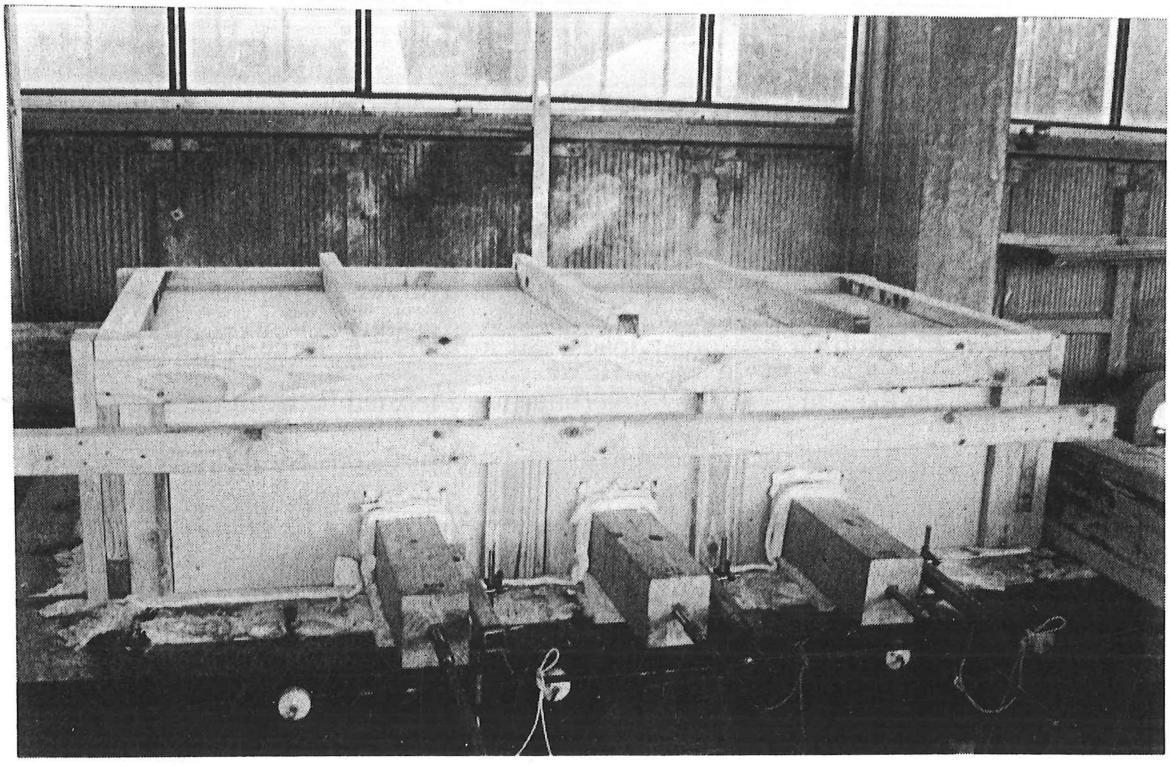

Figure 5.7. Furnace Test in Progress.

5.3 Observations and Test Results.

Loads on each of the test splices differed slightly due to the different piston sizes within the jacks, even though nominally they were the same. During failure the load drop-off was observed and hydraulic pressure on the load cells was kept constant throughout the failures.

5.3.1 Test 1, K80.

Maximum allowable movement in the splice was limited to 40mm and once this had occurred the splice connection was deemed to have failed. Failures occurred at the following times and epoxy temperatures,

250mm embedment length - 46mins	45.7°C
300mm embedment length - 48mins	50.9°C
350mm embedment length - 49mins	58.3°C

All failures were slow, taking 2 to 3 seconds to move the allowable 40mm. Once the test was completed, the furnace lid was removed and the samples extinguished with a fine water spray and the charred specimens removed. The failure mode was that of the epoxy softening and a shear failure occurring within the epoxy. A shear plane developed at the thread-top level, consistent with that seen in the earlier oven tension tests. Once removed from the furnace it could be seen that the epoxy was still bonded with both the threaded rods and timber. The epoxy had charred in the central area of the splice in the ensuing 5 minutes between the furnace stopping and the flames being extinguished by water. The epoxy did not ignite during the period that it was exposed to the ignited furnace.

Initial load applied during test was,

250mm -	56.5kN
300mm -	50kN
350mm -	46.7kN

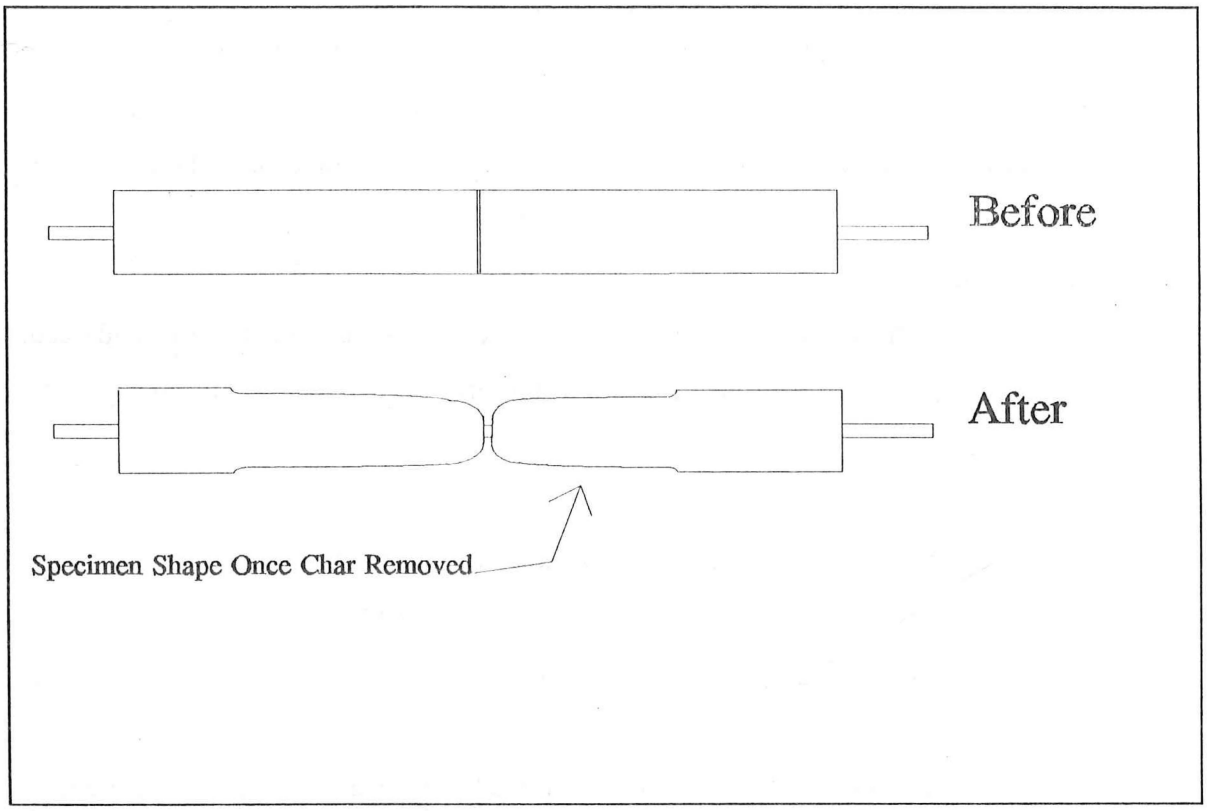

Figure 5.8. Shape of the Furnace Specimens Before and After Burning.

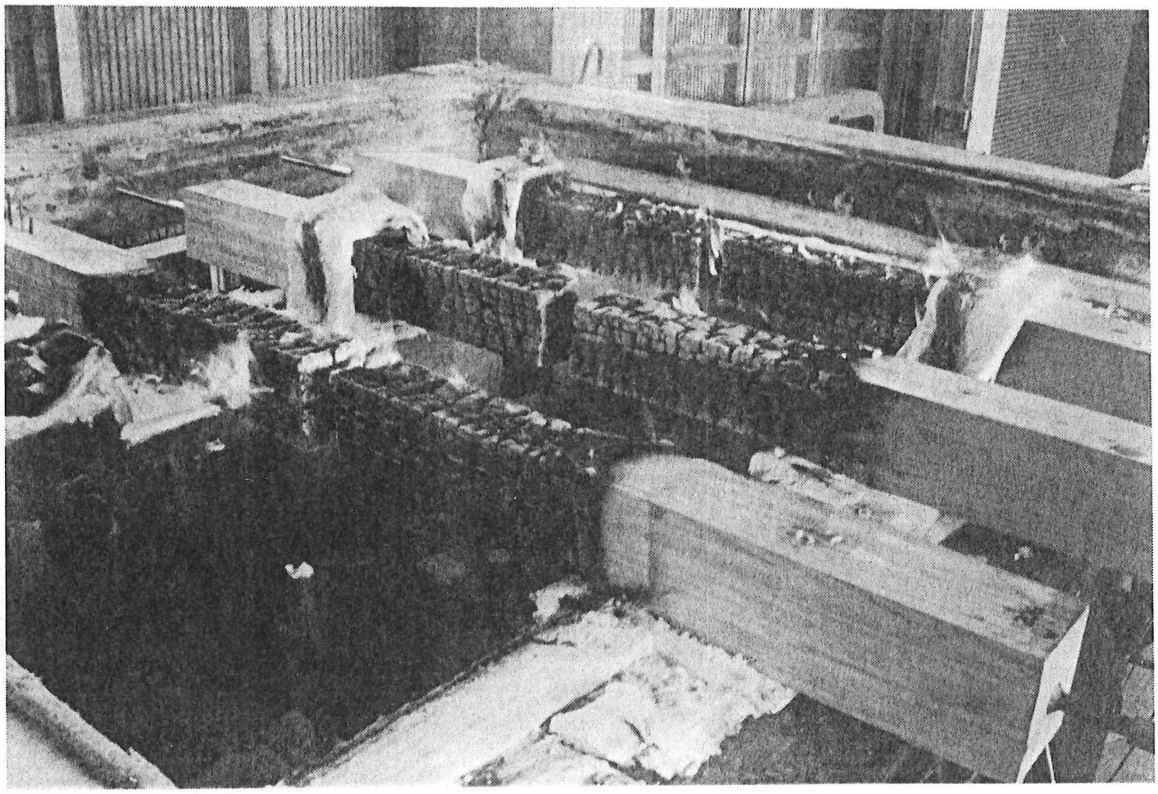

Figure 5.9. Completed Test with Furnace Lid Removed.

Each timber specimen burnt evenly across its section leaving residual sections with dimensions of 55-65 x 70-80mm. Char removal was achieved by scraping of the charcoal until the brown coloured, heat affected wood was exposed. The rate of charring increased towards the centre of the splice due to the heat re-radiating from each of the splice ends, causing an elevated rate of burning (figure 5.9). The fire protective sealant used to seal the 2mm gap in the splice would have offered some protection to the splice area, but obviously did not cope with the long burning period and heat generated in the burning timber.

Once the char was removed the stem of glue that had cured in the construction air-hole (see figure 4.2) was able to be seen. The K80 epoxy had charred at a lesser rate than the timber and was level with the outside edge of the char. This property of the epoxy is excellent as it does not provide a weakness for the fire to enter the timber, as would happen if the epoxy charred quickly and receded into the previously unburnt timber.

5.3.2 Test 2, West System.

The maximum allowable movement in the splice was limited to 35mm. Failures occurred at the following times and epoxy temperatures,

250mm embedment length -	42mins	40.2°C
350mm embedment length -	44mins	45.1°C

Average load applied during test was,

250mm -	61.6kN
350mm -	50kN

The 250mm embedment length specimen failed in a very fast brittle manner due to a bond failure at the timber epoxy interface. Once the specimen was removed from the furnace it could be seen that the epoxy was still completely bonded to the threaded bar and a small amount of wood up to 1mm thick, was attached to the outside of the epoxy in some places. The timber was split open on one side suggesting a typical confinement failure, but with the epoxy remaining intact around the bar. This failure suggests that a bond failure at the epoxy timber

interface occurred with a confinement failure, before the temperature had risen enough to weaken the epoxy sufficiently for a shear failure to occur within the epoxy.

The 350mm embedment length specimen failed by a slow shear failure in the epoxy with the splice moving the limiting 35mm in 2-3 seconds. The shear failure occurred by both shattering of the epoxy and movement along a shear plane at thread-top level. This failure mode was observed often in the oven tests.

Once char had been removed from the timber the residual sections were of the size 60-65 x 75-85mm. The charring rate was again faster towards the centre of the splice due to the fire protective sealant burning away and allowing the end-affect of re-radiation occurring (figure 5.9).

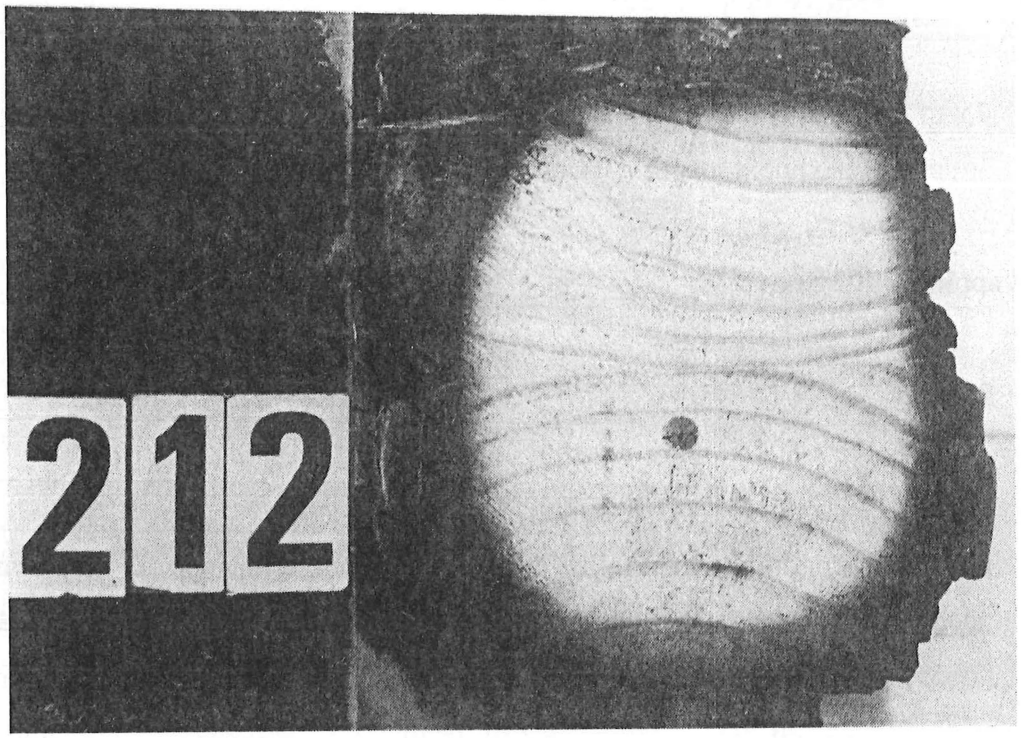

Figure 5.10. Cross-Sections Showing Charring and Heat-Affected Zone.

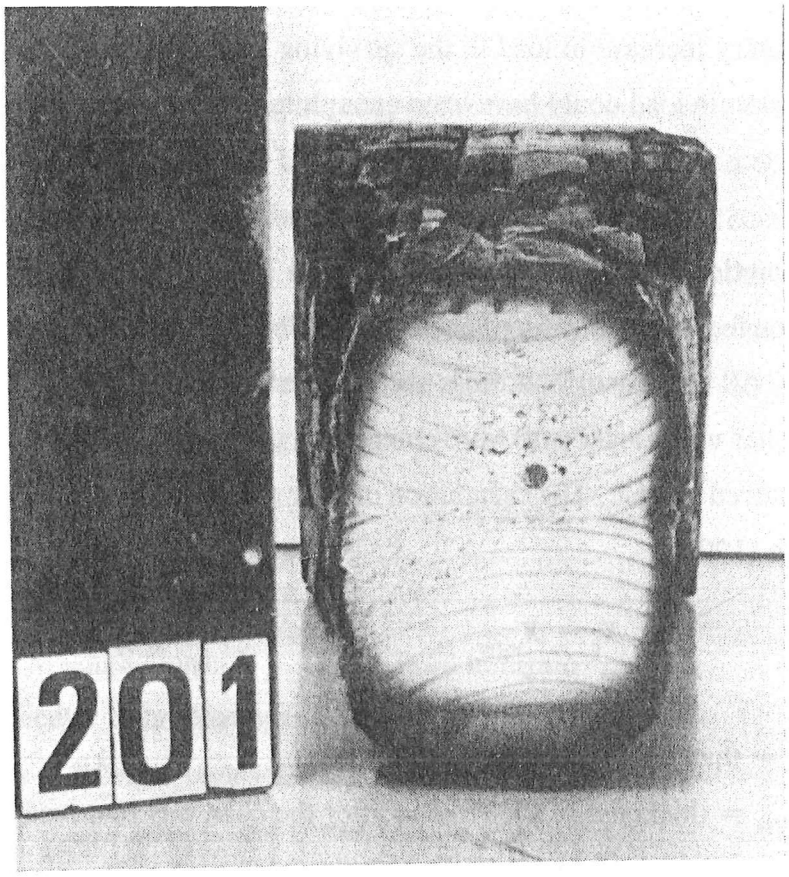

Figure 5.11. Cross-sections Showing Charring and Heat-Affected Zone.

As the char was removed around the air-holes it was evident that the West glue had charred faster than the timber. The timber was charred with no epoxy evident in the construction air-hole. The epoxy was found to be charred down to the level of the good, non-heat affected wood. Thus the rate of charring of the West system is faster than the charring rate of the timber and would enhance heat flow into the connection and surrounding wood via the construction air-hole. Once the lid was removed from the furnace the West system epoxy was observed to be burning freely at the splice opening. The K80 epoxy showed no signs of flaming in its furnace test.

5.3.3 Load At Failure.

Due to the closeness of the failures in each of the furnace tests load on the remaining tests specimens once one had failed, was unable to be measured. As all specimens were attached to a loading reaction frame it is likely that once one failed, the load would have increased on the remaining specimen(s). Thus the quick succession in failures in the K80 (and West) test could

be due to a momentary increase in load in the surviving specimens after the first and second failures. This increase in load could have been enough to induce premature failure within the surviving splice specimens.

5.3.4 Char Contraction.

The char contraction factor was measured once the samples had been extinguished and removed from the furnace. All specimens had cross-section cuts at a distance of 600mm from base. Measurements of char width and depth were completed, then samples were cut to measure the thickness of the charred sample. The calculation of char contraction factor is the same as used by Tran and White (1992),

$$f_c = \frac{X_c - X_{w,res}}{X_o - X_{w,res}} \qquad 5.2$$

where X_c = thickness of charred sample

$X_{w,res}$ = thickness of the residue after the char was removed

X_o = original thickness of the sample.

From the three specimens measured, an average char contraction factor of 0.706 was measured. Complete data is recorded in table 5.2.

Specimen No.	Original Size (mm)	Char Width (mm)	Residual Width (mm)	Char Contraction, f_c
201	156	135	93	0.666
201	134	115	63	0.732
207	156	125	70	0.640
207	134	110	55	0.696
212	156	140	84	0.777
212	134	115	65	0.725

Table 5.2. Measured Char Contraction Values From Furnace Tests.

5.3.5 Charring Rate.

The rate the wood charred at during burning in the furnace could easily be measured once the specimens were cut through their cross-section (see figures 5.10 and 5.11). The boundary between charred and uncharred timber is distinguishable by the heat-affected timber that is dark brown in colour. Measurements of the uncharred wood were taken at the boundary between charred and heat-affected wood. This is because the heat-affected wood still has some residual strength. All test specimens had cross-section cuts at a distance of 600mm from base and burning time was 50 minutes. Original Size 156x134mm.

Charring rates measured were,

Parallel to laminations: 0.68 mm/min

Perpendicular to laminations: 0.69 mm/min

(All data is listed in tables 5.3 and 5.4).

Specimen No.	Residual Size (ex 156mm)	Charred Wood, per side (mm)	Char Rate (mm/min)
201	93	31.5	0.63
203	98	29	0.58
207	70	43	0.86
209	89	33.5	0.67
210	95	30.5	0.61
212	84	36	0.72

Table 5.3, Charring Parallel to Laminations.

Specimen No.	Residual Size (ex 134mm)	Charred Wood, per side (mm)	Char Rate (mm/min)
201	71	35.5	0.71
203	67	33.5	0.67
207	79	39.5	0.79
209	70	32.0	0.64
210	63	31.5	0.63
212	69	34.5	0.69

Table 5.4, Charring Perpendicular to laminations

The charring rates are both slightly higher than the recently adopted New Zealand Timber Code (SNZ, 1993) rate of 0.65 mm/min for 420 kg/m^3 density. The charring rate is slightly higher perpendicular to the laminations, than parallel, which has been seen in fire tests by Odeen and Rogowski (1967) and Gardner and Syme (1991). This difference in charring rate has been explained by delamination in the glulam at the glue lines. There was no evidence of opening at the glue lines in the heat-affected timber. The large open fissures that were present in the already charred glue lines would increase heat penetration into the timber and this would explain some difference in char rate.

5.3.6 Residual Strength of Test Splices.

Once the sections had been extinguished and allowed to coll down (approximately 30 minutes), they were reloaded to see if the splices had any residual strength remaining. The remaining West splice connection that failed by shear/bond failure in the epoxy had no residual strength, with only 2kN of load increasing pull-out.

Two K80 splices were subject to tension load and both put up a small amount of resistance. The 300mm embedment length splice moved after 22kN of load was applied. The 250mm splice failed after 14kN of tension load was applied. From these results it can be assumed that once the epoxy connections have been severely heat affected that their strength properties are

greatly reduced.

5.3.7 Adhesive Lines in Timber.

The glulam timber used was produced with phenol formaldehyde adhesive, which is known for its resistance to fire. The samples removed from the furnace tests all showed little or no delamination at the glue lines (see figures 5.10 and 5.11). The adhesive charred at a rate equal to that of the timber and there was little evidence of the glue lines being a weakness in the timber, as it burns.

5.4 Comparison With Oven Tension Tests.

When the furnace data for load and temperature is plotted with the data from the oven tension tests, the general trend is followed (see figure 5.12).

The furnace data shows failure at lower temperatures than was occurring for the oven tests, for the same load. This difference could be due to the long term heating in the oven. As the oven test specimens were heated slowly over twenty four hours, the epoxy was able to stabilise at the one temperature. The splice specimens were heated quickly in the furnace which could lead to the epoxy being slightly weaker as it was not able to stabilise at one temperature, due to the rapid rate of heating.

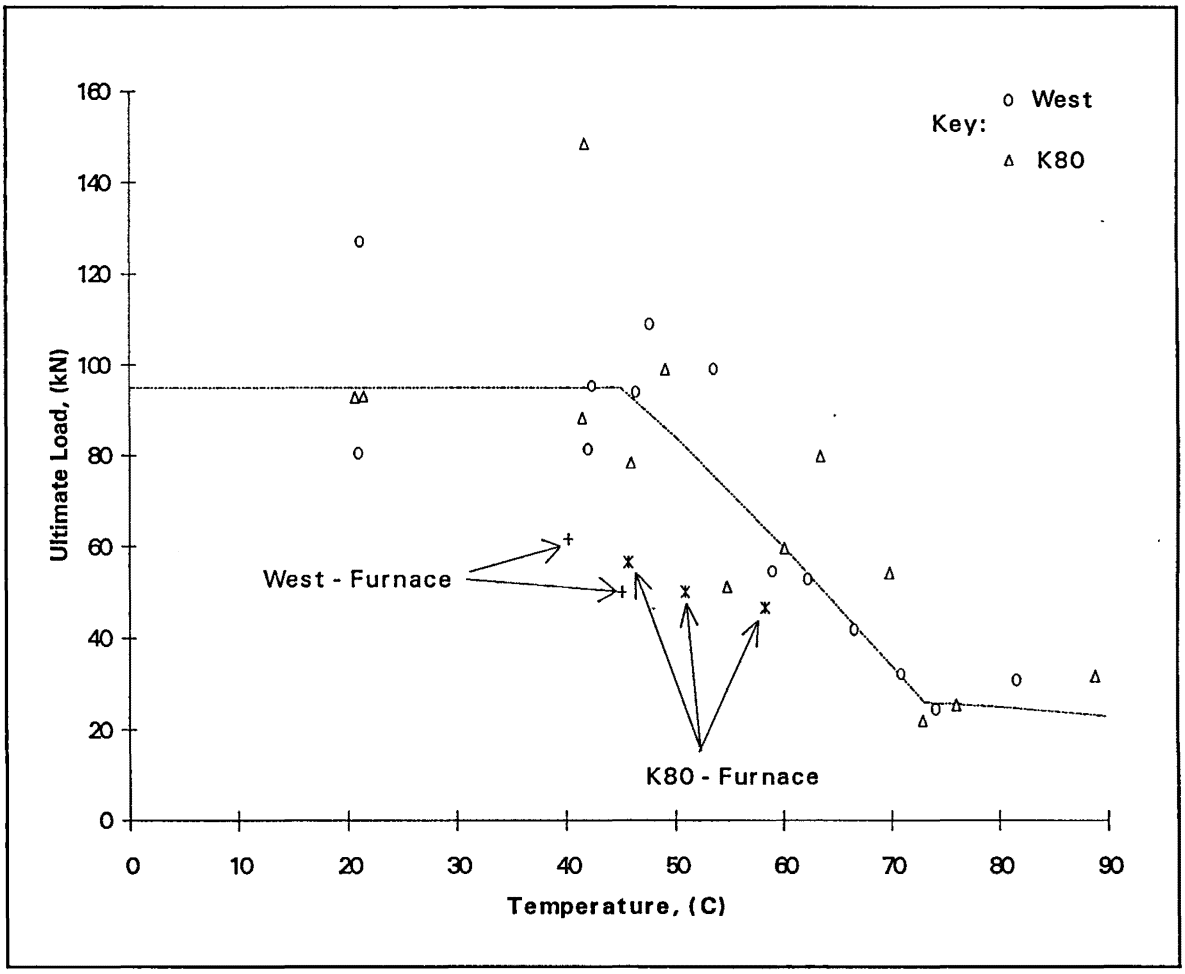

Figure 5.12. Oven Tension Test Data with Furnace Tension Test Data.

CHAPTER 6

TASEF MODELLING

6.1 Introduction.

To model the heat flow through a section of timber the heat transfer program TASEF was used. TASEF (Temperature Analysis of Structures Exposed to Fire) is a program designed to analyse structures exposed to fire, both two-dimensional and axisymmetric. Material properties such as thermal conductivity and specific heat are entered with their temperature dependence, giving a complete picture of how a material's properties change with temperature. It also has standard thermal properties for steel and concrete already calculated.

6.1.1 Modelling of Charring Using Non-Charring Program.

Modelling charring using an application program not specifically designed for this purpose has been attempted by White and Schaffer (1978). A rocket propulsion program normally used for thermal performance studies was utilised to study charring of timber. The thermal properties could be specified as a function of temperature and heat of pyrolysis could be included. The results of the program were compared with past experimental data on charring of oven-dried wood. The results were in good agreement but were limited by the input data on thermal properties.

6.1.2 TASEF Calculations.

The program is based on solving the transient two-dimensional Fourier heat transfer equation, by a finite element method (Sterner & Wickstrom, 1990). TASEF solves the matrices of the heat transfer equations via the forward differences approach, which is accurate and fast, but will have difficulties with large time steps. As with all finite element methods, a finer mesh will produce more accurate results, but at the expense of more computing time. The program allows any time-temperature curve to be entered and has the ISO834 standard fire curve pre-programmed, for easy use.

6.2 Modelling Pyrolysis.

To model the heat transfer and charring of the timber requires data on moisture content, density, specific heat and thermal conductivity of both wood and char. The burning of the timber was to be modelled over a large range of temperatures, ambient to approximately 900°C. With this in mind, small physical changes that affect the pyrolysis could be ignored, i.e. change in permeability of the wood as the char front proceeds.

The major change that does occur is the change in wood properties as it progresses from wood to char (see figure 6.1). The char front has been determined as 288°C by Schaffer (1984), but the exact transition between wood and char is unknown. Because of this uncertainty, it was decided to use wood properties up to 200°C and use char properties from 350°C upwards. The region between 200 and 350°C would be determined by linearly interpolating between the two points. This is approach taken by Knudson and Schniewind (1975) and Janssens (1993) in their modelling.

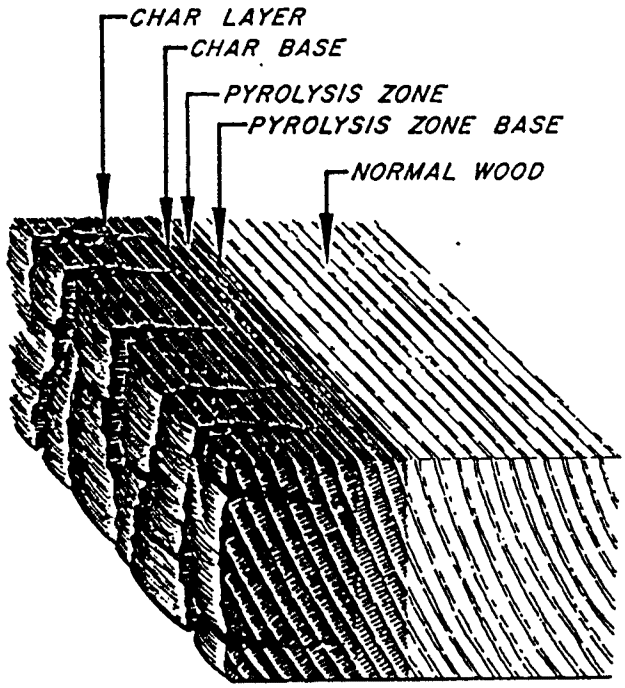

Figure 6.1. Progress of Char in Wood, (Schaffer, 1968)

6.2.1 Data Uncertainty.

The change in specific heat and thermal conductance over a large range of temperatures is the main uncertainty in the data input. Reviewing the literature it became obvious that

experimental work on conduction and specific heat of timber had produced a wide range of values and empirical equations. Also little or no work had been attempted on pinus radiata. A great deal of experimental work has been performed on southern pine, an American pine species. Data for southern pine has been used as the species are similar.

6.2.2 Data Selection.

Equations for thermal conductivity have been found from Parker (1988), Siau (1971) and Janssens (1993). Experimental work on the specific heat of wood has been more prevalent and many empirical equations were able to be found, Koch (1969), Knudson (1975), Parker (1988), Janssens (1993) (see section 2.4).

Janssens (1993) performed a comprehensive literature review of the experimental data and found equations over an extensive temperature range that accurately predicted the thermal properties of the wood. From his work the following equations were used,

specific heat of wood,

$$c_w(T) = 1159 + 3.867T \quad J/kg^oK \qquad 6.1$$

thermal conductivity of wood,

$$k\,(T) = (0.0237 + 2x10^{-4}\rho_o)\frac{T+273}{293} \quad W/m^oK \qquad 6.2$$

specific heat of char,

$$c_c = 714 + 2.32T - 8x10^{-4}T^2 - 3.69x10^{-7}T^3 \quad J/kg^oK \qquad 6.3$$

where T is in degrees celsius, for all of the above,
and ρ_o = oven dry density of timber (kg/m^3)

The thermal conductivity of char is defined by the char density,

$$\rho_c = \frac{\rho_o Y_c}{f_c} \qquad 6.4$$

where ρ_o = oven dry density of timber (kg/m^3)

Y_c = mass fraction of char

f_c = char contraction factor

Using the diagram shown (figure 6.2), the thermal conductivity of char can be found. A value of 0.24 was used for Y_c, based on the work by Tran and White (1992), using southern pine. Also Tran and White's char contraction value of 0.589 was used for comparison with that measured from the furnace tests. The emissivity of the wood during its change from uncharred to charred can be averaged over the transition period. Tran and White (1992) used a value of 0.88. This value was adopted for the TASEF modelling. An ambient temperature of 20°C was assumed. An oven-dry density of 420kg/m^3 was used for modelling (were it had not been determined beforehand). Moisture content evaporation as temperatures increased was based on data from the Wood Handbook (1987).

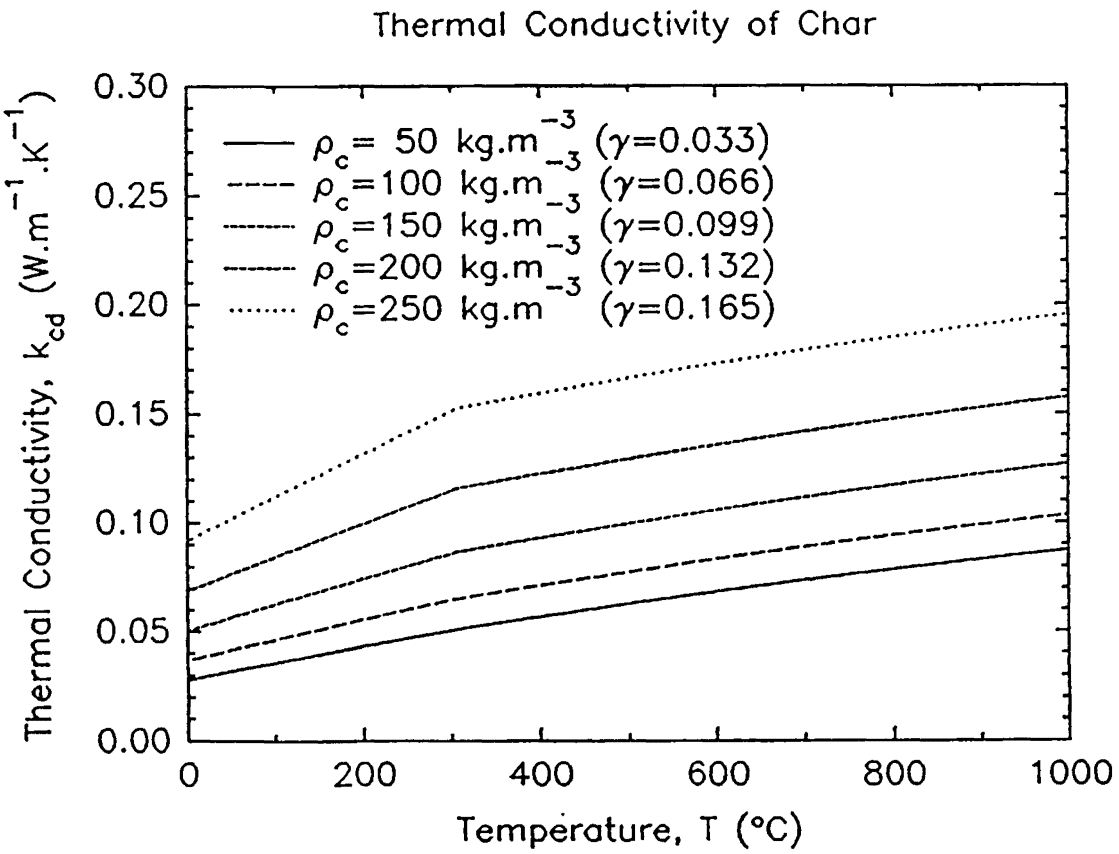

Figure 6.2. Thermal Conductivity of Char, (Janssens, 1993).

6.2.3 Data Input Limitations.

Physical changes in the wood as burning occurs that could not be modelled accurately included moisture content change at the char front and density change as charring occurs. As charring occurs, moisture content within the wood is increased as water is driven into the timber, as the char front advances. This small change in moisture as the temperature increases could not be modelled as it occurs over a small temperature range. The modelling in TASEF used relatively large temperature increments that would nullify this physical change. Also the high peak in specific heat as water changes from water to steam was not modelled. This relatively large change in specific heat over a short time period had an adverse impact on the modelling, so had to be ignored.

The change in density as wood converts to char was not modelled due to limitations in the type of input allowed in TASEF. This major reduction in density occurs between 400 and 600°C. TASEF allows for only increasing physical properties based on specific heat. As specific heat is directly related to density, the density reduction could not be accounted for directly. Density reduction is accounted for in the calculation of thermal conductivity, where Y_c is the mass fraction of char.

As the wood is converted to char and contraction occurs, the volume of material is reduced. The reduction in physical dimensions as charing progresses has not been modelled and cross section area is assumed to be constant over the duration of burning.

6.3 Epoxy Physical Properties.

To model the heat spread through the thin layer of the epoxy, the specific heat, density and thermal conductivity had to be found. Density of both West System and Nuplex K80 epoxy was found by direct measurement (see tables 6.1 & 6.2). Values for specific heat and thermal conductivity were found from references.

Specific heat	C = 1047 J/kg°K	(Hilado, 1990)
Thermal Conductivity	k = 0.167 W/m°K	(Hilado, 1990)

Specimen No.	Density kg/m^3
1	1140.5
2	1147.3
3	1136.5
4	1150.0
Average	1143.6

Table 6.1. Density Measurements for West System - Z105/Z206.

Specimen No.	Density kg/m^3
1	1599.1
2	1607.6
3	1602.2
4	1595.5
Average	1601.1

Table 6.2. Density Measurements for Nuplex K80 - Winter.

6.4 TASEF Input Method.

To perform a TASEF calculation on a section of material, the following process is carried out,

a, finite element mesh is constructed. If a line of symmetry is present in the section to be modelled, then this can be used to reduce the size of the section,

b, thermal properties are calculated for the materials being used. The properties need to cover the range of temperatures being investigated,

c, a time - temperature curve is either inserted by user or ISO834 can be used,

d, all data is compiled in the source code for TASEF,

e, output data is easily read as nodes, temperatures and times are compiled and shown.

6.4.1 Validation of TASEF Output.

To validate the output from TASEF, a block of pine was modelled burning under the ISO834 fire. The char front is located at 288°C and the complete charring process is considered to have occurred by 350°C. Thus tracing the 350°C isotherm through the block being modelled gave an indication of how quickly the charring process was taking place. Nodes of the finite element mesh were placed so that the 350°C isotherm could be traced easily (figure 6.3).

Using Janssens formulas (equations 6.1 - 6.4), a wood oven-dry density of 420kg/m^3, moisture content of 11%, char contraction factor f_c=0.589 and char yield Y_c=0.24, the modelled block produced the following char rate,

Char rate = 0.597 mm/min

This is in very good agreement with the expected 0.6-0.65mm/min charring rate expected in radiata pine of this density (Collier, 1992). The individual temperature profiles at the indicated nodes are shown in figure 6.4. Thermal properties entered in TASEF are listed in table 6.3.

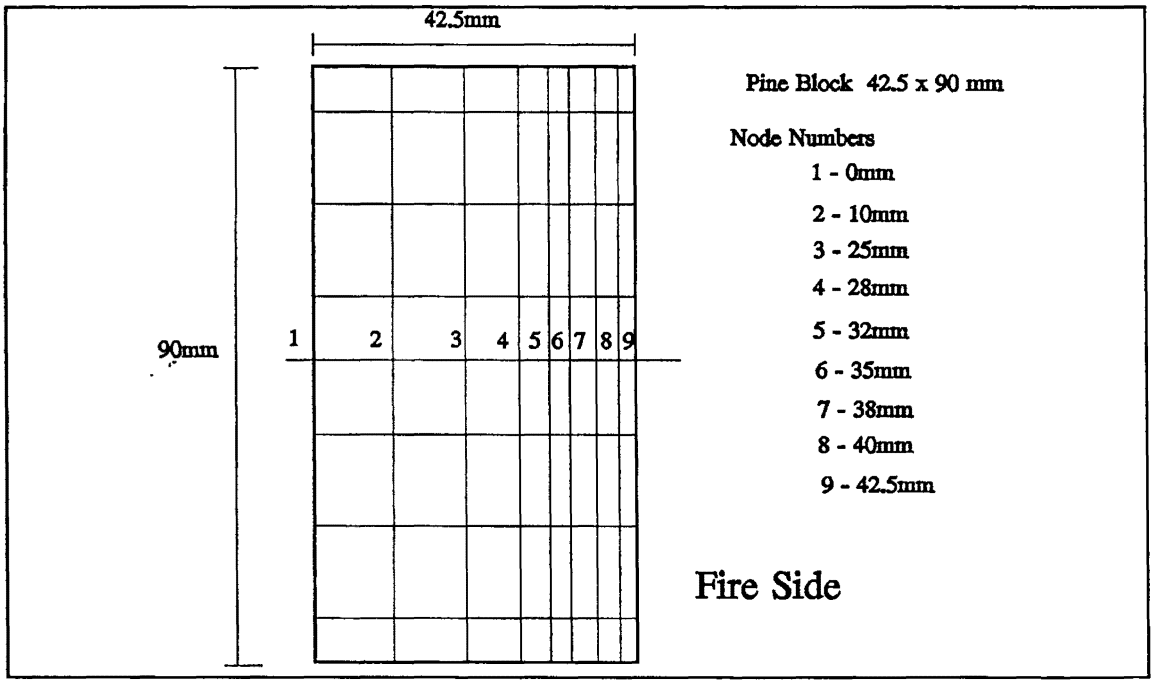

Figure 6.3. Wood Block Used to Validate TASEF Input. Finite Element Mesh is Shown. Data for Nodes 1-9 Used

Oven Dry Density	420kg/m^3	Density, 12% m.c.	452kg/m^3
Temperature (°C)	Moisture Content %	Specific Heat (J/kg°K)	Conductivity (W/m°K)
0	0.12	1159	0.106
50	0.08	1352	0.126
100	0.01	1546	0.145
150	0	1739	0.165
200	0	1932	0.184
350	0	1412	0.110
400	0	1490	0.113
500	0	1628	0.120
600	0	1738	0.128
700	0	1819	0.135
800	0	1869	0.140
900	0	1885	0.145

Table 6.3. Thermal Properties for Wooden Block Modelling, $Y_c = 0.24$, $f_c = 0.589$

6.5 TASEF Predictions of Furnace Tests.

Using the thermocouple data from the furnace tests, the TASEF output could be more readily validated. Using the pre-test data of density and moisture content, values for specific heat, wood conductivity and char conductivity could be determined. Thus TASEF modelling of the furnace test could be conducted.

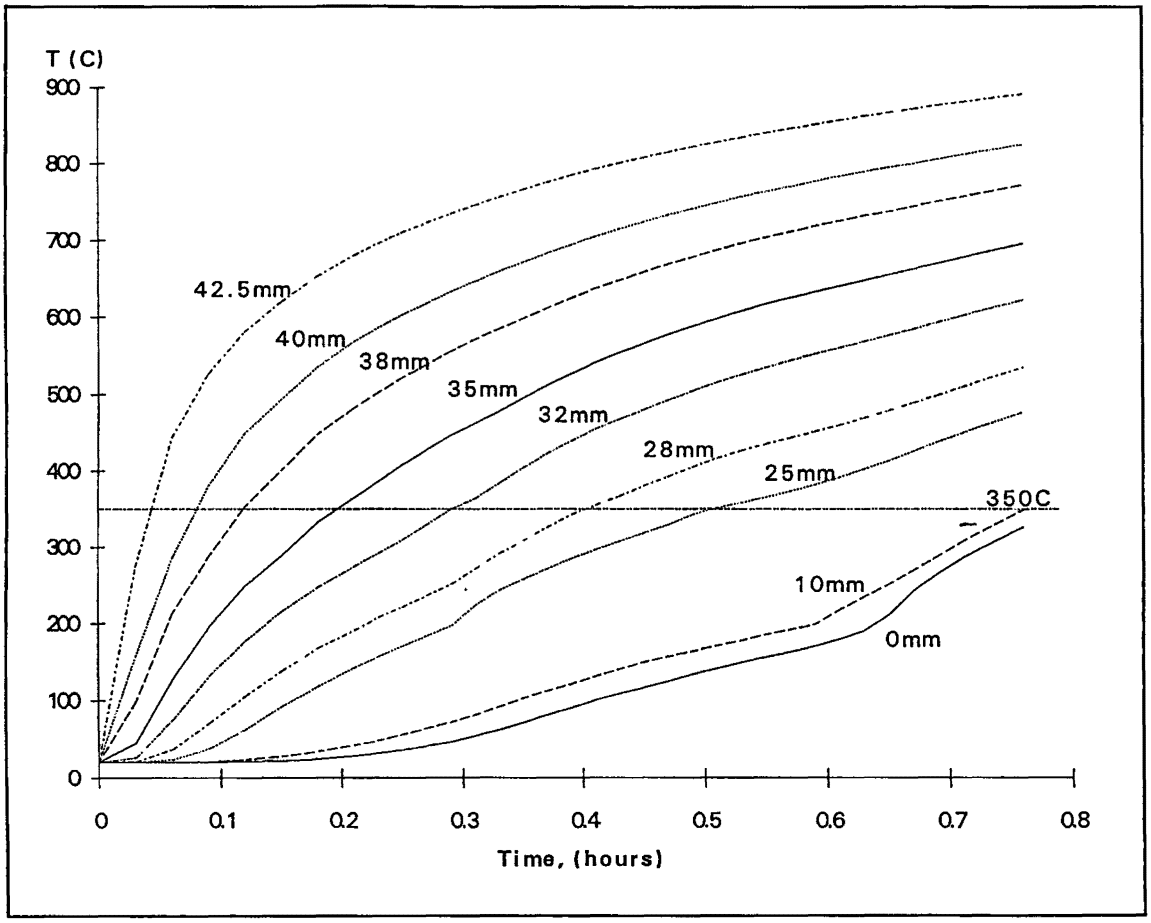

Figure 6.4. Node Temperatures for Modelling Wood Block Under ISO834, With 350°C Isotherm.

Two thermocouples were placed on the threaded rod at 45° from upright vertical, either side of the bar, within the epoxy (see figure 5.4). Both the 250mm and 350mm splice connections contained thermocouples. Thus to model the temperature at this position, the data from the node in the finite element mesh corresponding to the thermocouple was used. Finite element meshes developed for the splice connections and are shown in figure 6.7.

TASEF output (A, B) using Janssens equations 6.1 - 6.4 for the thermal properties and the thermocouple readings (T/C 250mm and 350mm embedment lengths) from the two furnace tests are plotted in figures 6.5 and 6.6. The two TASEF calculations are using the following relations,

TASEF runs A, B - Janssens formulas for specific heat and conductivity

- ρ = measured value from furnace test, 417kg/m^3
- m = moisture content 11%
- Y_c = 0.24 (Tran and White, 1988)

TASEF A - f_c = 0.589 (Tran and White, 1988)

TASEF B - f_c = 0.706 (measured from furnace test)

As can be seen from diagrams 6.5 and 6.6, the two TASEF calculations closely estimate both furnace tests and are on the safe side for predictions (TASEF temperatures slightly higher). Both plots of TASEF predictions show that estimation 'B' is a very good approximation to the temperature rise within the epoxy. Estimation 'A' gives higher temperature predictions in both cases, than estimation 'B'. Thus for all other modelling the thermal properties used for the TASEF B estimation will be used

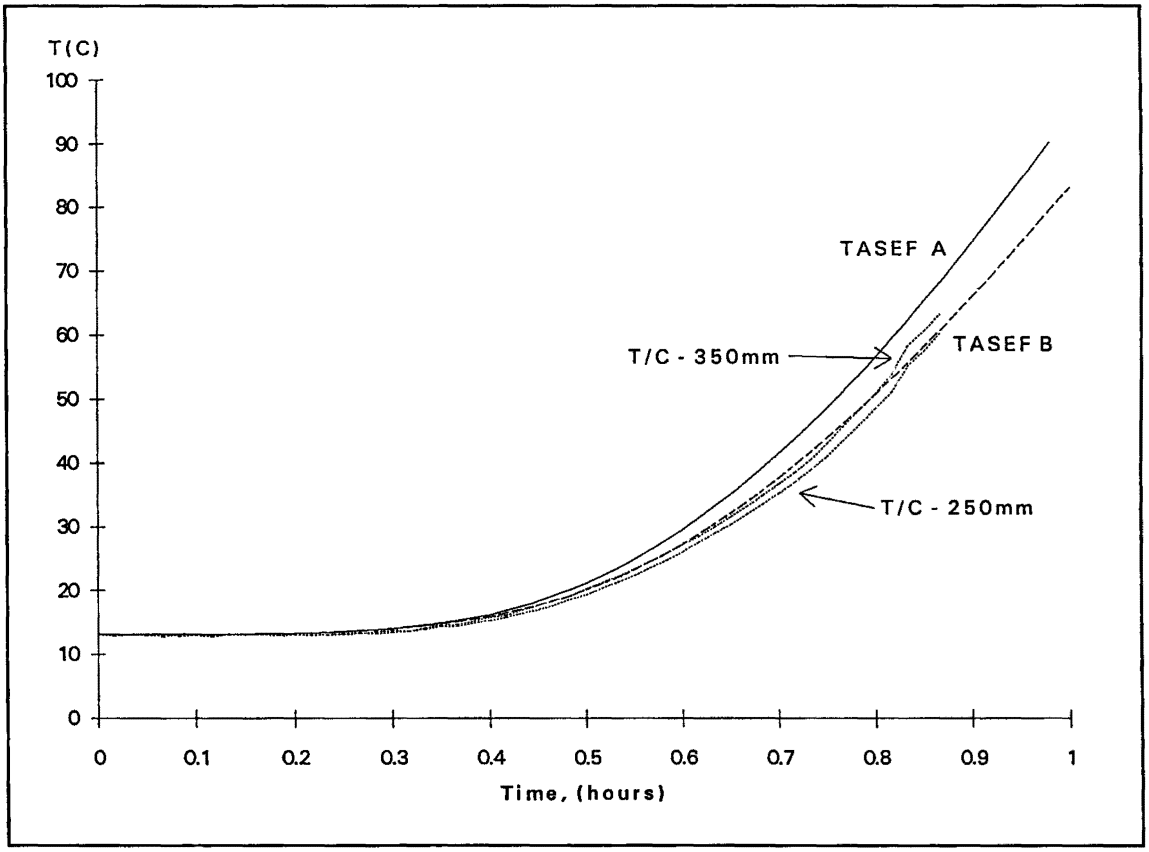

Figure 6.5. K80 Epoxy Test, Thermocouple Readings for 250mm and 350mm Embedment Length Specimens and TASEF Estimations.

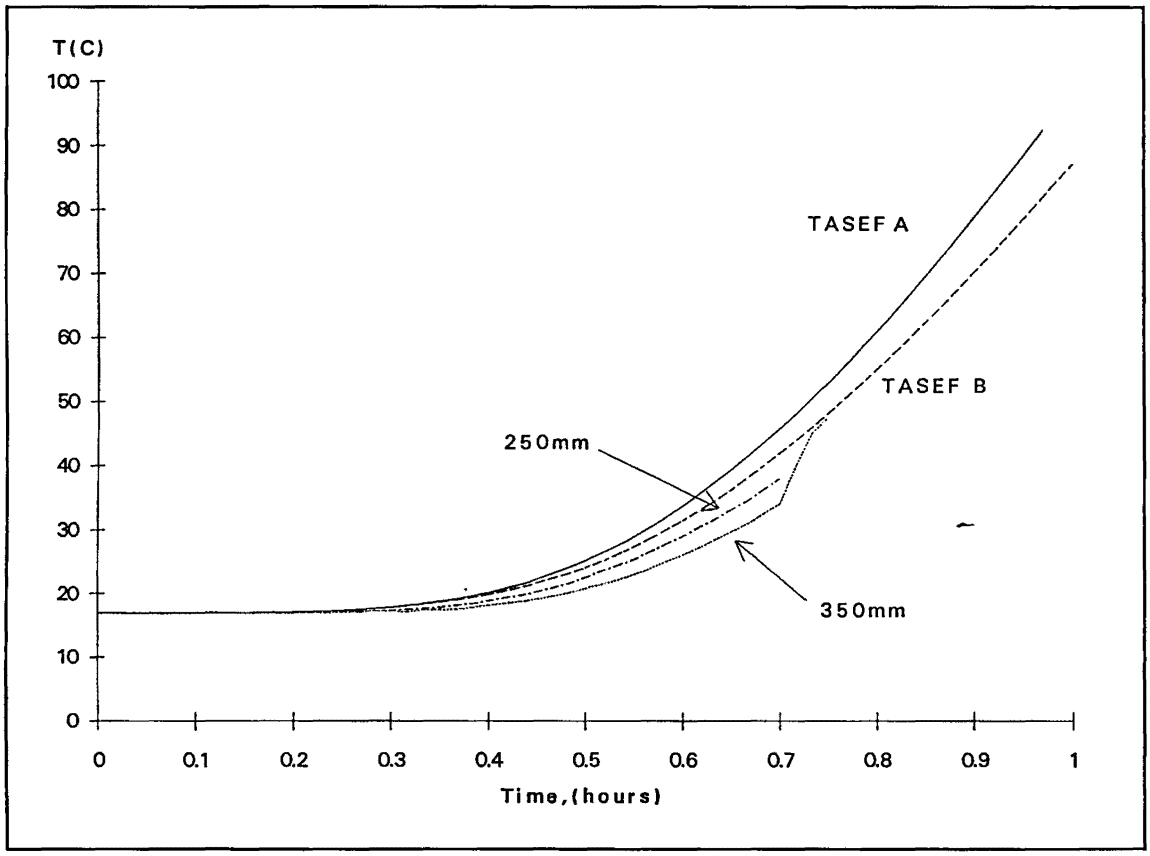

Figure 6.6. West Epoxy Test, Thermocouple Readings for 250mm and 350mm Embedment Length Specimens and TASEF Estimations.

6.6 Limitations of TASEF Modelling.

As with all modelling, the output is only as good as the input. Modelling the heat flow and physical changes in the wood as it burns is difficult due to the lack of exact information on the physical properties of wood, (unlike steel or concrete). Thus with there being uncertainty in the input data, there is difficulty in estimating the exactness of the output.

Refining the finite element meshes further would produce more accurate results, but the increased accuracy (1-2°C) is at the expense of a great deal of computer and operator time. Thus refining the mesh is not justified due to the uncertainty in the input, as changes in moisture content of 1-2% for example can change temperatures in the output by 5-10°C.

The nodes chosen as best representing the position of the thermocouples in the epoxy are

shown in figure 6.7. An average temperature of the four nodes is plotted in figures 6.5 and 6.6. The use of rectangles to approximate the diameter of the epoxy leads to only small errors in output temperatures. The four nodes recorded are dimensioned so that they are at the same position as the epoxy is, in the actual specimen.

The furnace tests show that the TASEF input data is estimating actual temperatures closely and on the safe side. The tracing of the 350°C isotherm also shows that the TASEF output gives a charring rate close to what is expected.

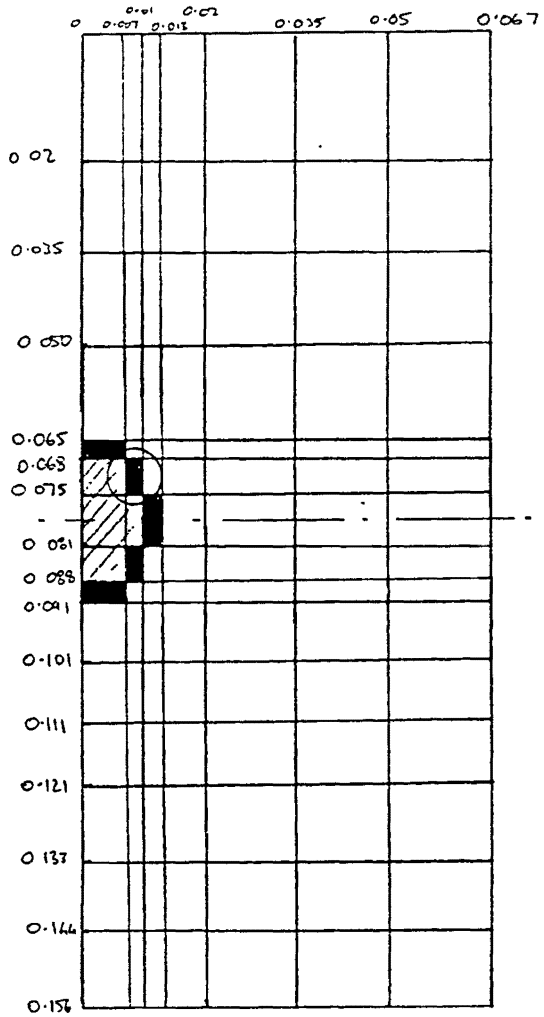

Figure 6.7. Finite Element Mesh for TASEF Modelling of Furnace Test Specimens. Dark Shading Represents Epoxy, Angled Shading Represents Steel. Nodes for Temperature Determination are Circled.

CHAPTER 7

DESIGN CALCULATIONS AND TASEF MODELLING

7.1 Introduction.

Assuming a critical temperature of failure for the epoxy dowel connection, modelling of actual connections using TASEF can be completed. Because the connections have already been used in a small number of buildings, it is important to check how these would cope in a fire situation.

The critical temperature of strength reduction is approximately 55°C for West System epoxy and 45°C for K80 epoxy (see figure 4.8), thus a temperature of 50°C was chosen as the critical temperature for the connection. Once this temperature is reached the connection can be assumed to be losing strength. Connections already designed have been used to model the temperature increase, under ISO834 fire conditions. The connection with the smallest edge distances was modelled in each case, thus providing a worst case situation for each beam section modelled.

7.2 Aqua Gym Connections.

The Aqua Gym complex in Christchurch is a portal frame structure with a span of 21m (see figure 7.1). The portals have curved knees and thus no moment resisting connection is required (Jellie Park Swimming Pool Complex is also similar; see Buchanan and Fletcher, 1989). The portal frames are fixed to the concrete foundation upstands by epoxy dowel connectors, constructed from galvanised threaded rods (see figures 7.2 & 7.3).

7.2.1 Modelling Aqua Gym Connections.

Two types of glulam connection were modelled,

496 x 115mm, 2 x R20mm Galvanised threaded rods, central
270 x 115mm, 2 x R16mm Galvanised threaded rods, central.

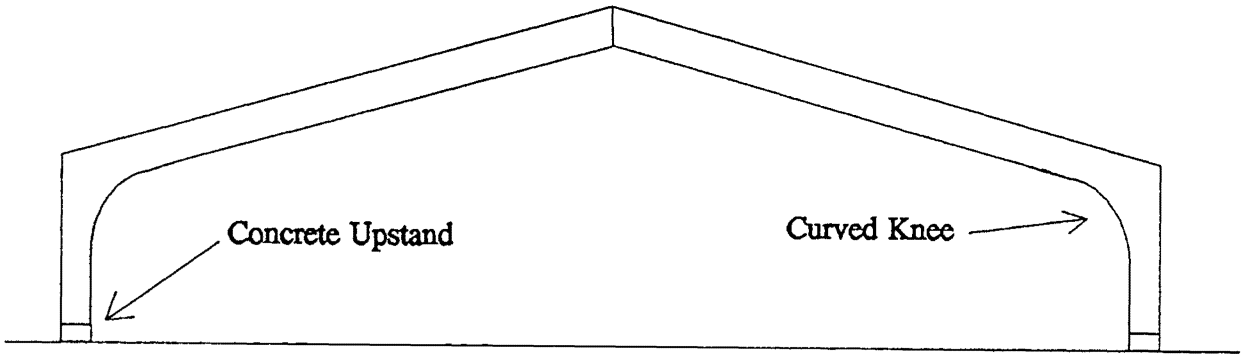

Figure 7.1. Aqua Gym Portal Frame Structure.

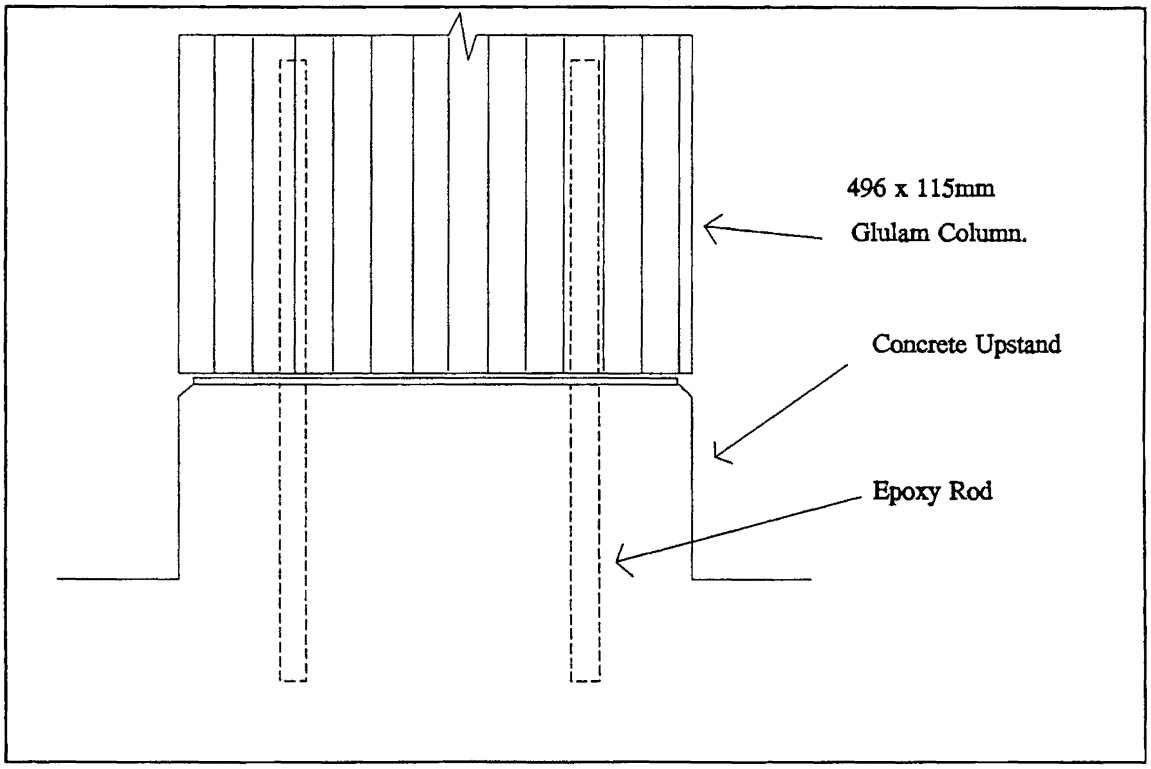

Figure 7.2. Concrete Upstand Base Support for Aqua Gym Glulam Column with Epoxy Dowel Connections.

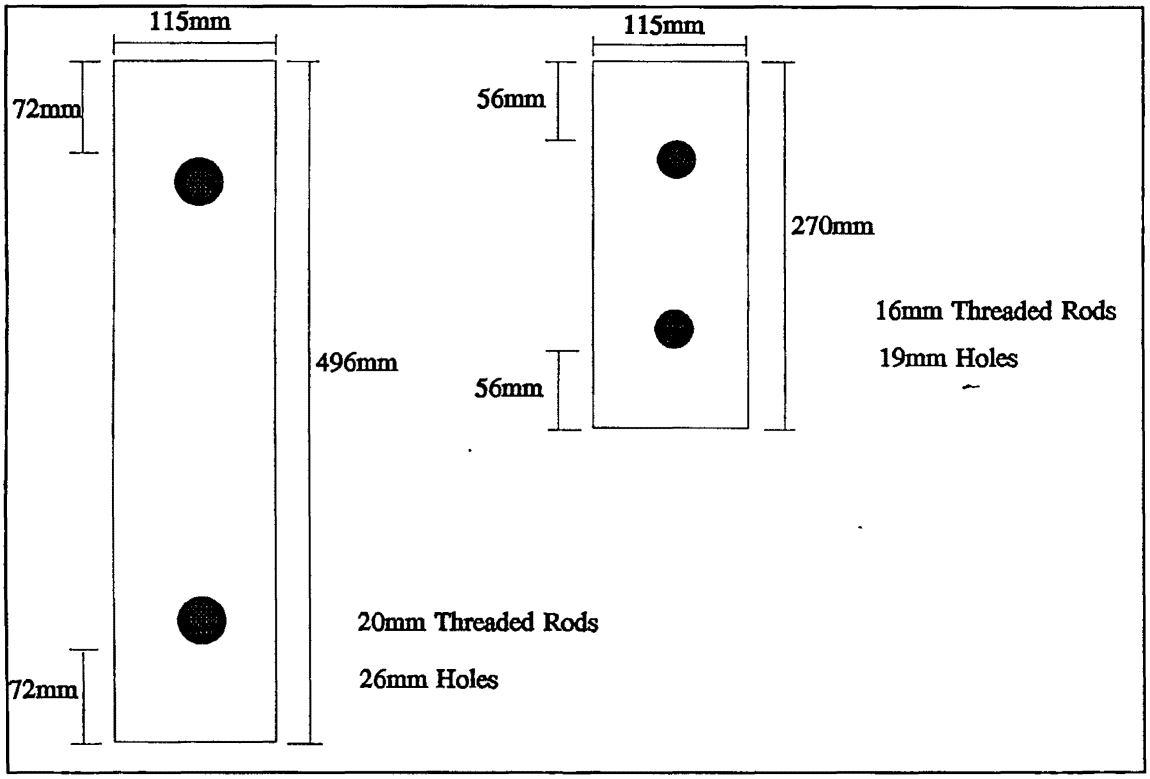

Figure 7.3. Cross Sections of Aqua Gym Connections, Modelled Using TASEF (edge distance dimensions to outside of epoxy).

These connections had finite element meshes constructed for them and the data entered in TASEF. Thermal properties are as listed in table 7.1. Finite element meshes are shown in figure 7.4.

7.2.2 Results of Modelling.

Plotting the time temperature curves for the nodes indicated in figure 7.4, gives the following results.

Critical temperature of 50°C is reached at the following times,

Aqua Gym Connection 1 -	37 minutes
Aqua Gym Connection 2 -	36 minutes

Oven Dry Density	420kg/m^3	Density, 12% m.c.	452kg/m^3
Temperature (°C)	Moisture Content %	Specific Heat (kJ/kg °K)	Conductivity (W/m°K)
0	0.12	1159	0.106
50	0.08	1352	0.126
100	0.01	1546	0.145
150	0	1739	0.165
200	0	1932	0.184
350	0	1412	0.090
400	0	1490	0.095
500	0	1628	0.100
600	0	1738	0.106
700	0	1819	0.110
800	0	1869	0.117
900	0	1885	0.125

Table 7.1. Thermal Properties for Aqua Gym Modelling.

The TASEF modelling shows that a 30 minute fire rating is achievable for the connection. As both these epoxy connections are designed resist the uplift from wind loads in the glulam portal frames, the epoxy connection is not critical as it is unlikely to be under high tension (uplift) forces, during fire.

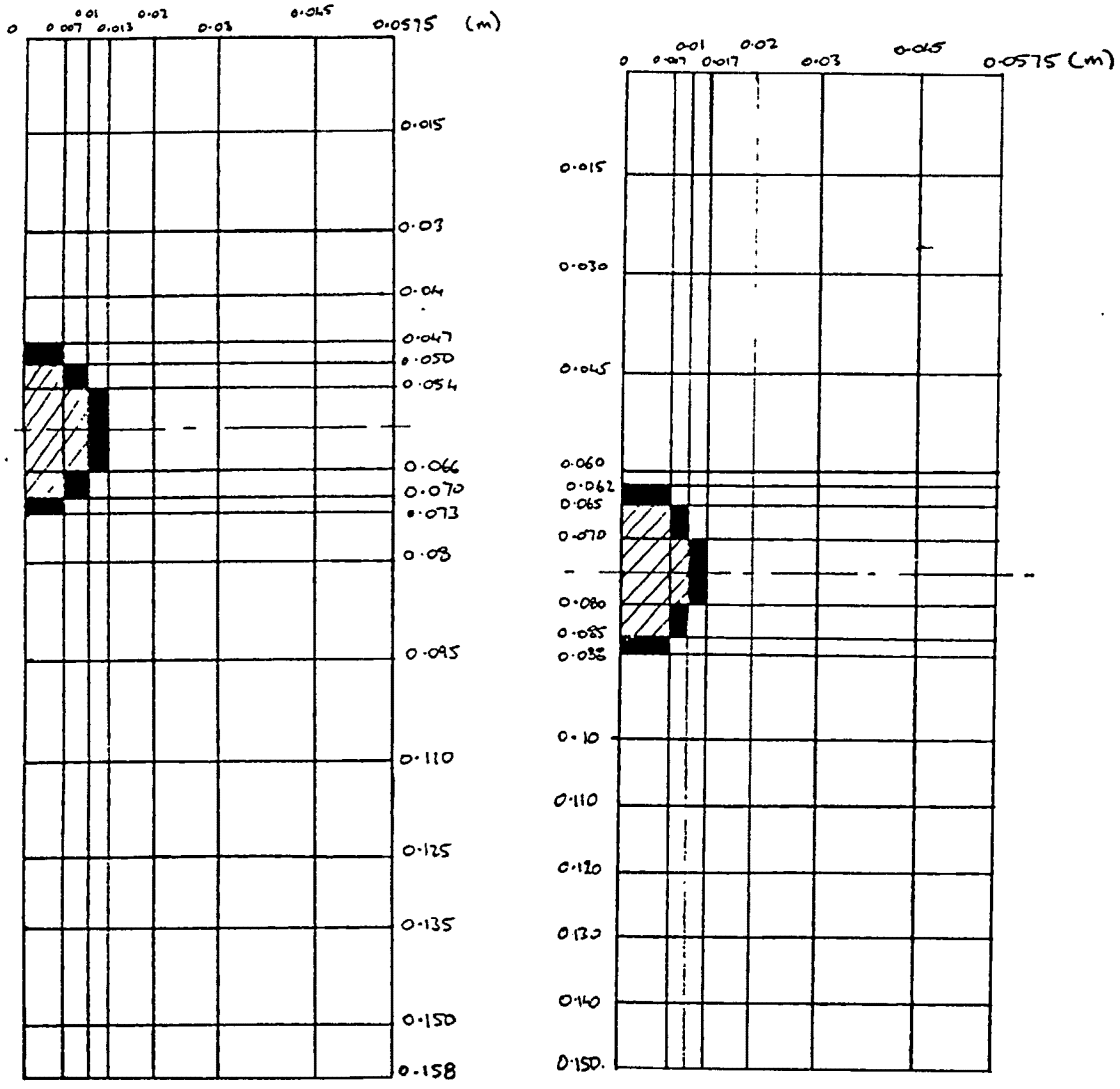

Connection 1 Connection 2

Figure 7.4. Finite Element Meshes For Aqua Gym Connections. Dark Shading Represents Epoxy, Angled Shading Represnts Steel. Nodes Used for Modelling are Circled.

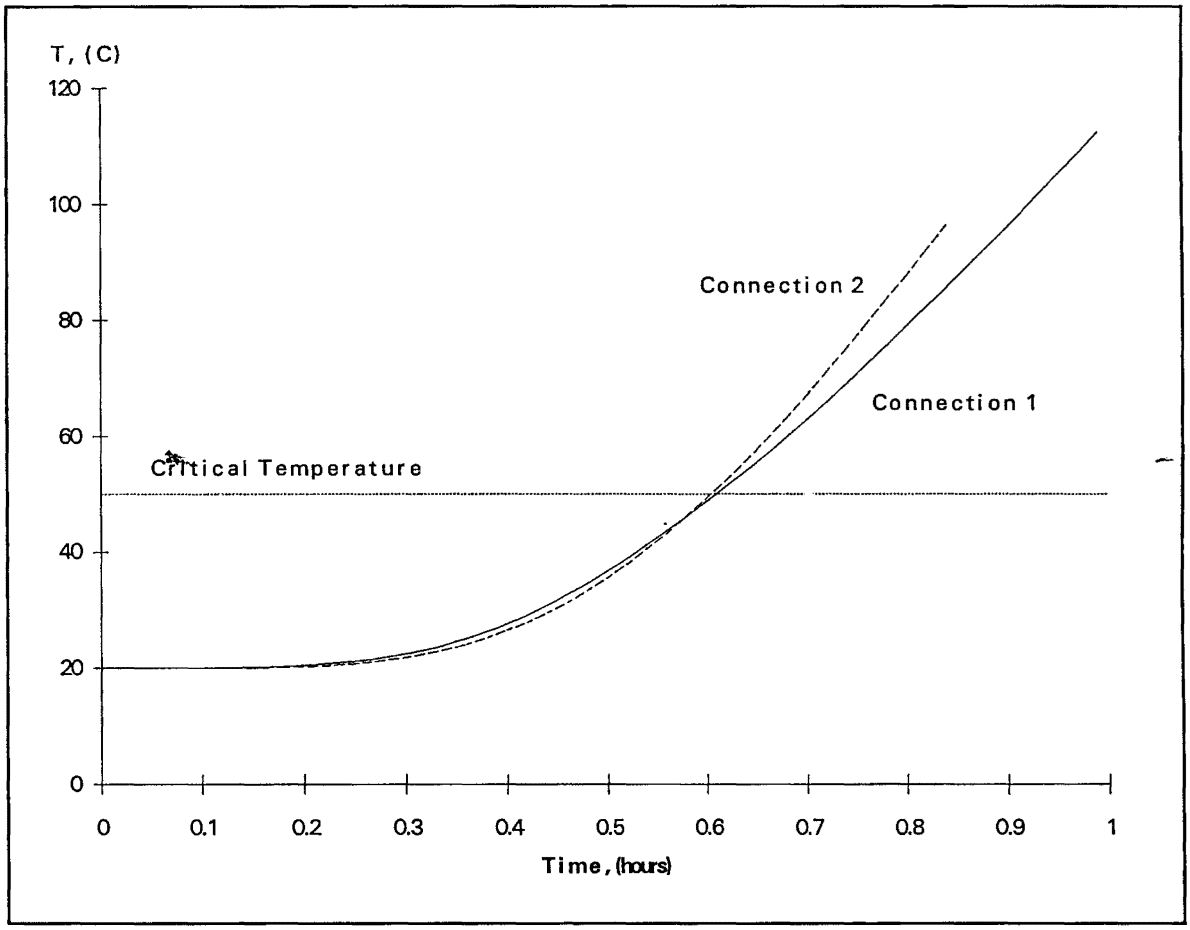

Figure 7.5. TASEF Estimations of Temperature Rise Within the Epoxy for Aqua Gym Connections, Modelled Under ISO834 Exposure.

7.2.3 Upstand Base Connection.

Use of the epoxy dowel connection in base upstands for fixing glulam portal frame or arch constructions is very advantageous. Due to the epoxy connection only resisting wind induced tension loads, the connection will still work well during long duration fires. The gravity and lateral forces will still be resisted by the connection, even when it has failed in the epoxy, due to bearing of the threaded rods in the wood.

7.3 Modelling Design Guide Connections.

A design guide for epoxy dowel connections using steel connecting brackets has been written by Buchanan and Fairweather (1992) for use in all building types. Hole spacings for 90, 135 and 180mm width beams are listed in table 7.2.

Beam size	D_e (mm)	D_v (mm)	D_m (mm)
90	45	50	
135	35	50	65
180	57.5	50	65

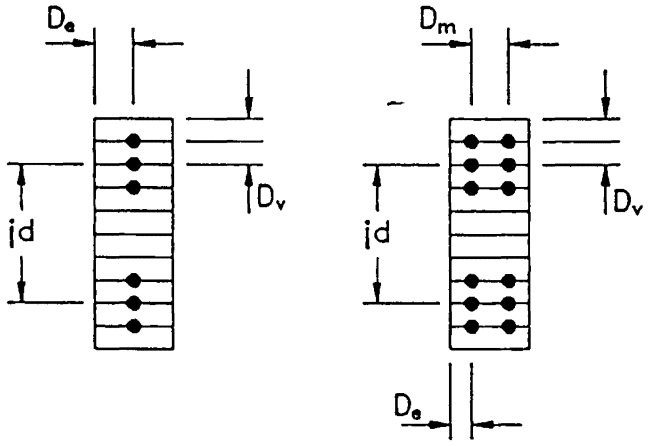

Table 7.2, Hole Spacings in Glulam Beam Ends.

All connections were modelled with 20mm threaded rods and 26mm diameter hole, the same specifications as the oven tension tests and furnace tests. The edge distances to the epoxied rods are shown in figure 7.6. TASEF input data is the same as that used for the Aqua Gym connections (table 7.1). Finite element meshes used are shown in figure 7.7. Each connection was modelled under ISO834 with an assumed initial temperature of 20°C.

Three connections were modelled using TASEF,

90mm beam width, one threaded rod, central.
135mm beam width, one threaded rod, central.
135mm beam width, two threaded rods, central.
180mm beam width, two threaded rods, central.

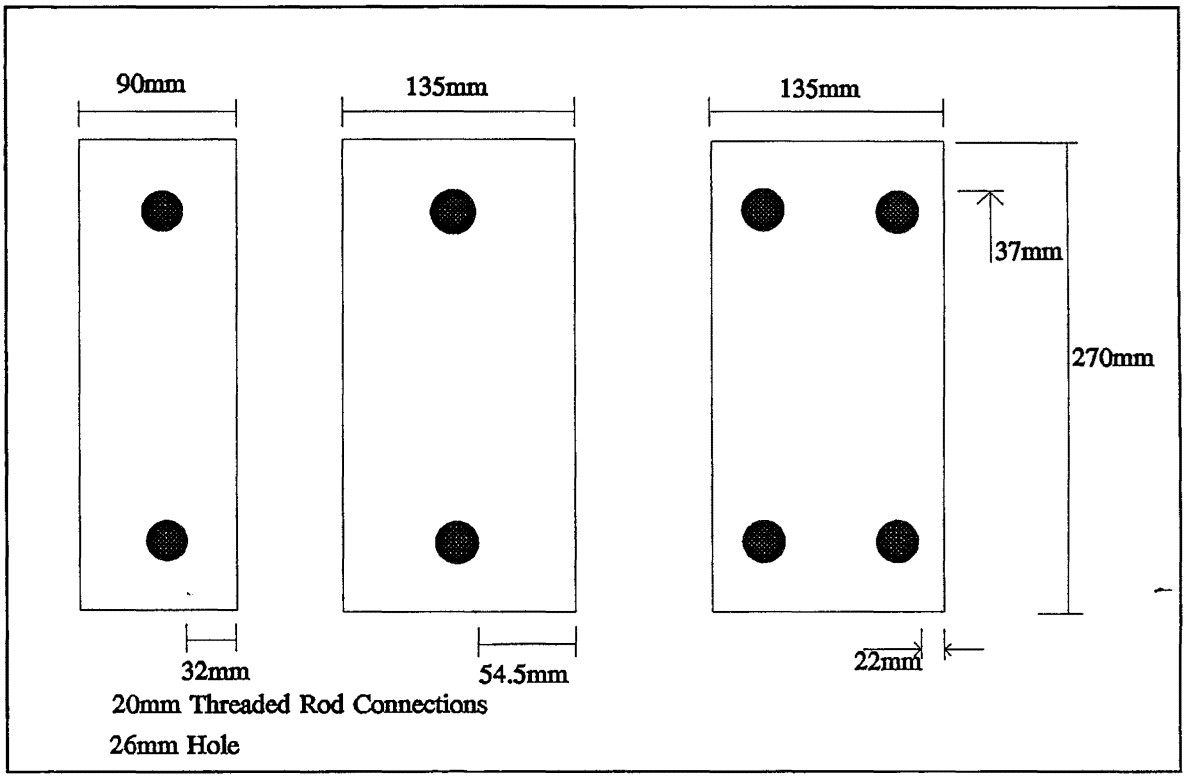

Figure 7.6. Design Guide Connections Modelled Using TASEF (edge distances indicated are to the outside edge of the epoxy).

7.3.1 Results of Modelling.

Using the data from the node indicated in the finite element meshes (figure 7.7), the following data resulted. The time temperature curves and critical temperature of 50°C are plotted in figure 7.8.

The critical temperature of 50°C is reached at the following times,

90mm - single rod	22 minutes
135mm - single rod	31 minutes
135mm - two rods	15 minutes
180mm - two rods	28 minutes

As can be seen the glulam connections with small edge distances perform poorly due to the heat conduction. These results are for the external threaded rods closest to the edges, which would be in the worst conditions during fire. But the exterior rods near the edges of the beams also carry the most load under bending, as they are closet to the extreme fibre of the

section. Thus these threaded rods are the most important as they will be under tension stresses during bending of the section.

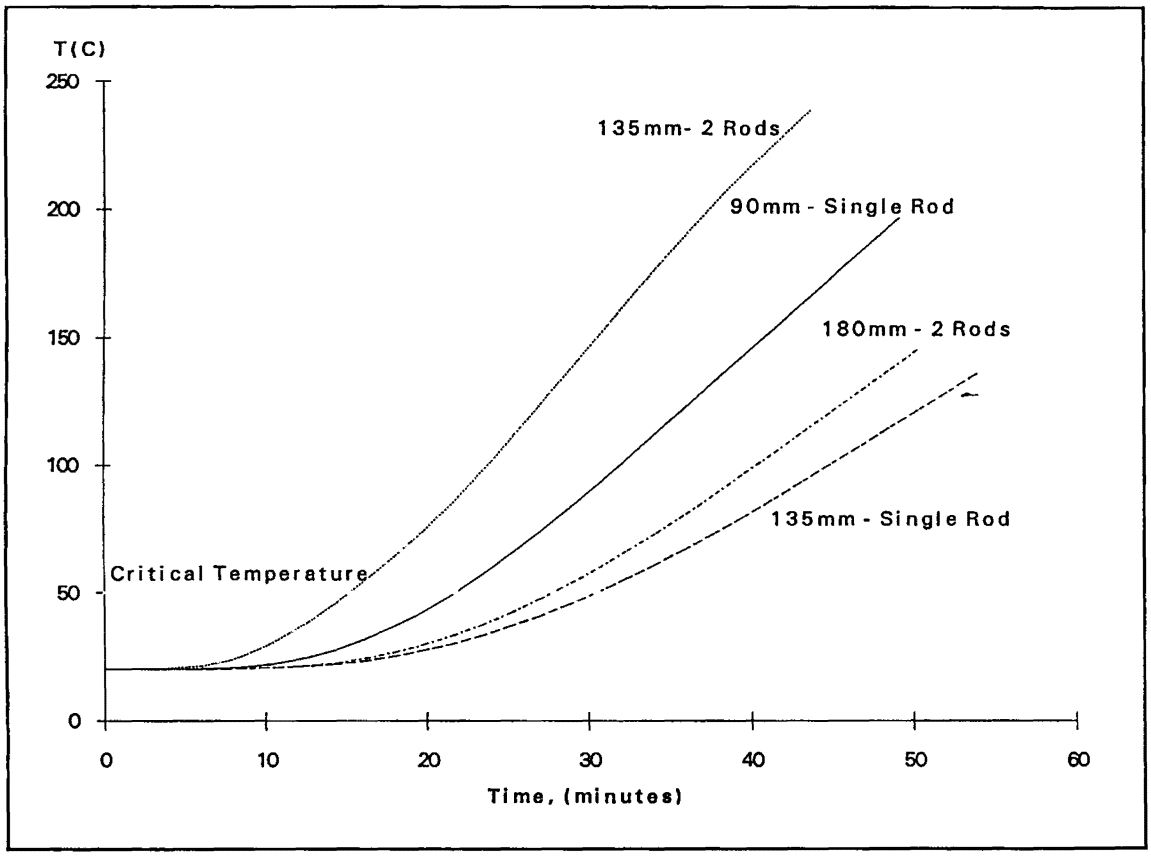

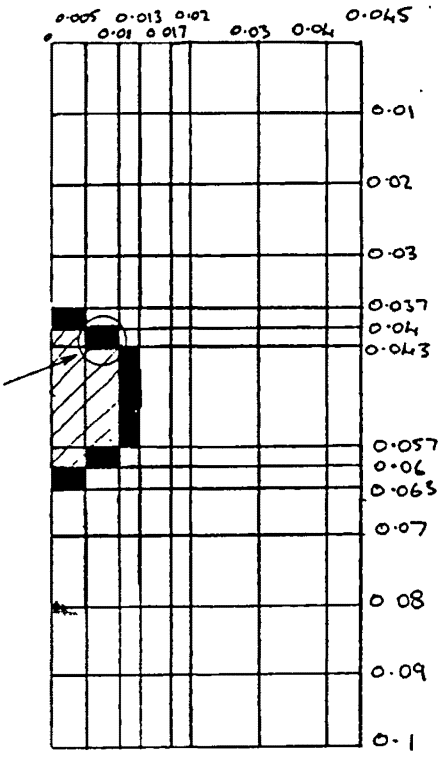

90mm - Single Rod

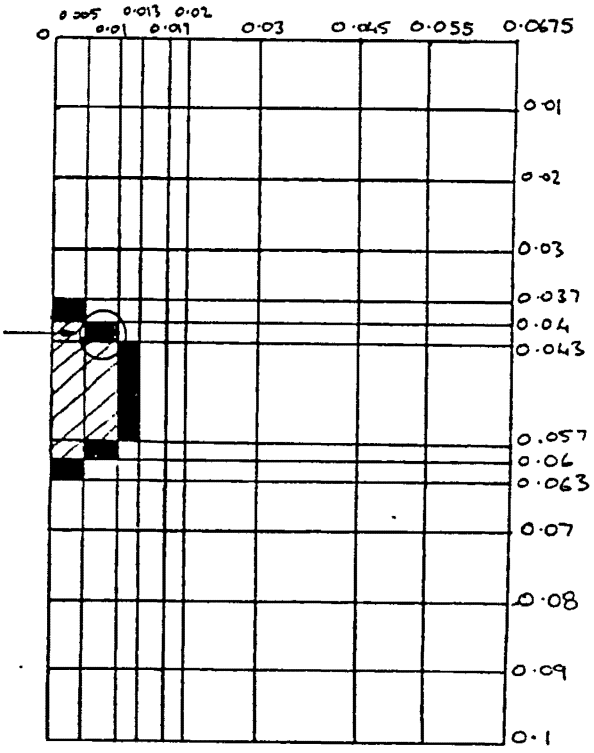

135mm - Single Rod

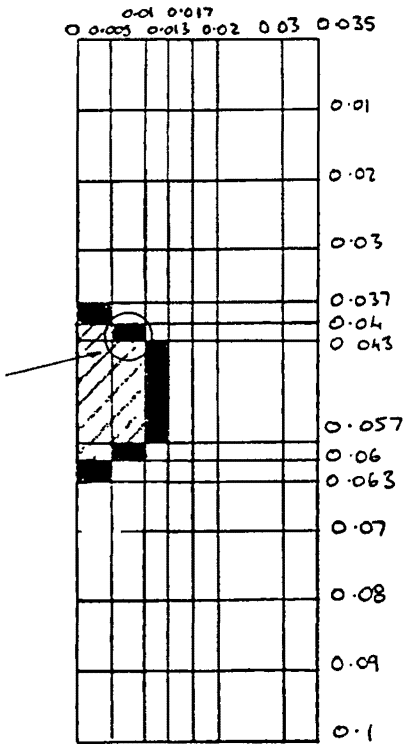

135mm - 2 Rods

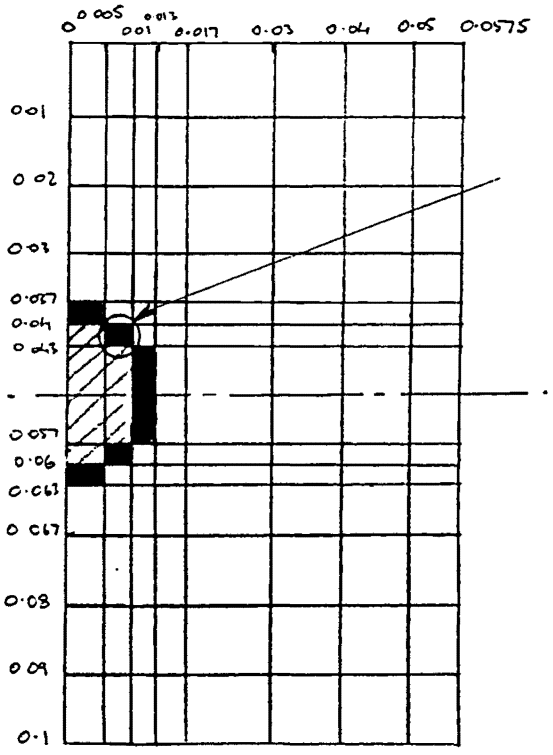

180mm - 2 Rods

Figure 7.8. Finite Element Meshes For Design Guide Connections. Dark Shading Represents Epoxy, Angled Shading Represents Steel. Nodes Used for Modelling are Circled.

7.4 Designing With TASEF Predictions.

Using a different critical temperature will lead to differing results for the various edge distances modelled. To account for the difference in side and edge distance, the distance from centreline of the bar to fire exposed corner is used, as shown if figure 7.9. Plotting the different radial distance values against time for critical temperatures of 40, 50 and 60°C, the following graph results (figure 7.10).

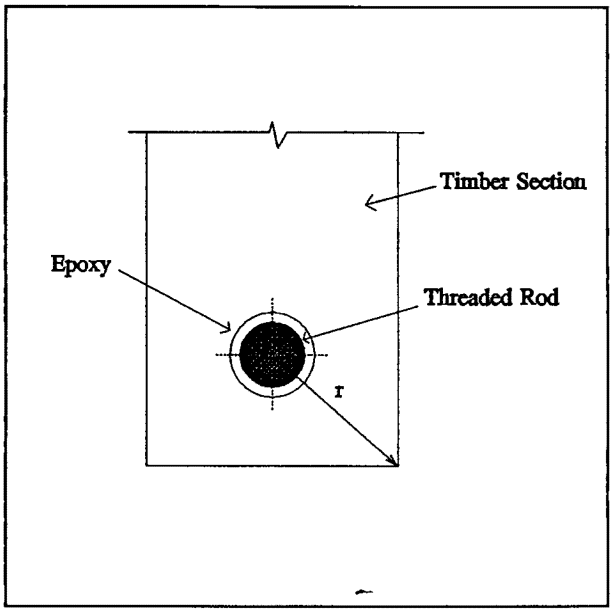

Figure 7.9. Radial Distance From Centreline of Bar to Edge of Timber Section.

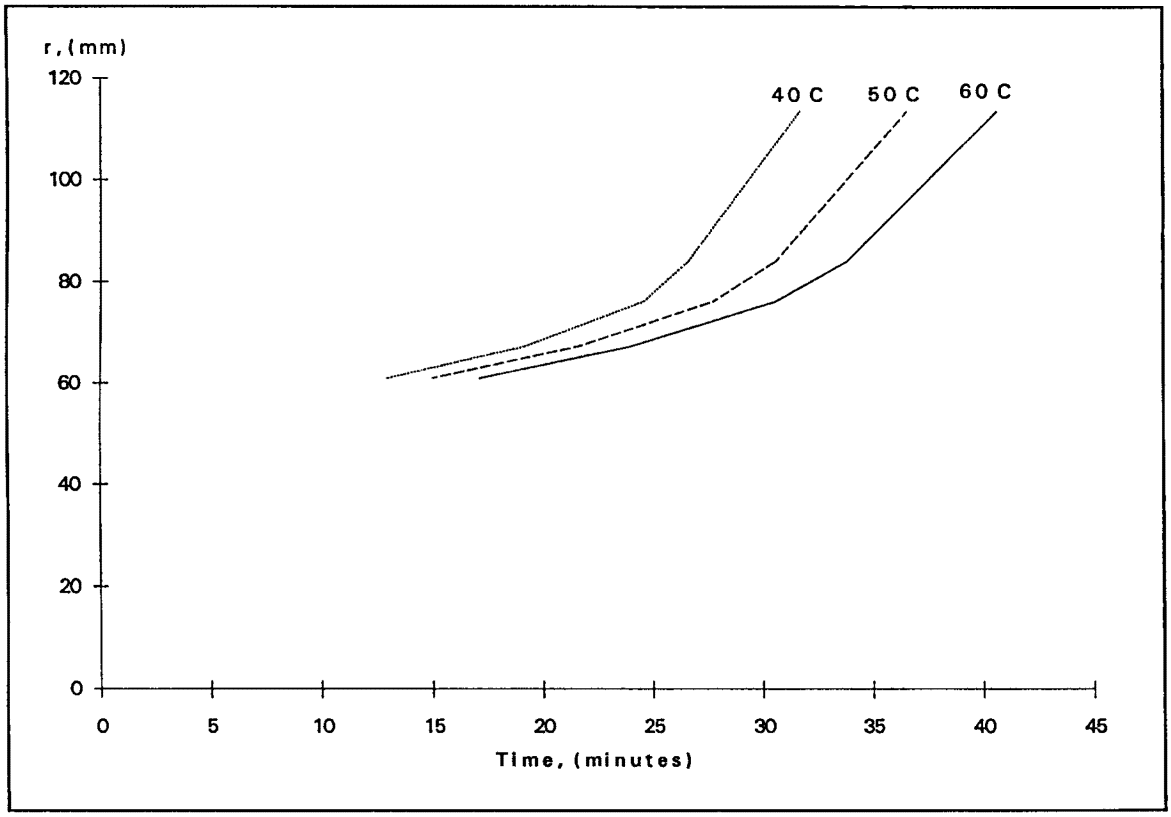

Figure 7.10. Radial Distance (mm) from Centreline of Bar to Fire Exposed Edge vs. Time, for Three Critical Temperatures.

7.4.1 FRR of Timber Section.

Using the width dimensions of the design guide connections and assuming some working loads and a depth for each section, the fire resistance of the timber members can be determined. A constant char value of 0.65mm/min and load factors from NZS3603:1993 (SNZ, 1993) have been used to construct a spreadsheet to make calculations easier. Values for fire resistance of the three timber sections, assuming three sides burning are as follows;

Stress Capacity of Member: $\phi f_u = \phi k_1 k_4 k_8 k_9 f_b$

where ϕ = Capacity reduction factor = 1.0 (fire conditions)

k_1 = Load duration factor = 1.0 (fire conditions)

k_4 = Parallel support factor = 1.32 (>8 laminations)

k_8 = Stability factor = 1.0 (Compression edge restrained)

k_9 = Glulam size factor = 0.86 (calculated from $(300/d)^{0.167}$)

f_b = Characteristic stress in bending, 17.7Mpa

Dead load = 10 kN/m

Live load = 4 kN/m

Load Combination in fire: Dead + 0.4Live

Member Size (mm)	Capacity Stress (Mpa)	Fire Resistance Time (mins)	Applied Stress (Mpa)	Deflection (mm)
765 x 90	20	43	19.4	80
765 x 135	20	72	19.3	76
765 x 180	20	100	19.5	72.5

Table 7.3. Fire Resistance of Design Guide Specification Beams.

Comparing timber fire resistance with epoxy connection fire resistance,

Member Size	Radial Distance, r (mm)	Timber Fire Resistance	Connection Fire Resistance
90mm - single rod	67.3	43mins	22mins
135mm - single rod	84.0	1hr 12 mins	32mins
135mm - two rods	61.0	1hr 12 mins	15mins
180mm - two rods	76.2	1hr 40mins	28mins

Table 7.4. Fire Resistance of Timber and Epoxy Connections.

From the following results it is clear that epoxy connections have a fire resistance rating of less than half that of the timber section, for the specified radial edge distances.

7.5 Increasing The Fire Resistance.

A simple method of increasing the fire resistance is to coat the wood sections with intumescent paint. This paint can be clear in appearance (like a varnish) but when its temperature reaches approximately 250°C reactions take place transforming the paint into a foam. This foam protects the wood from flame spread, charring and reduces heat conduction. With this in mind, a TASEF model was designed to mimic a section covered with intumescent paint.

7.5.1 Properties of Intumescent Paints.

Thermal properties of intumescent paints, once foamed proved to be difficult to find. Low conductivity thermal insulation such as fibre wool, insulation board and glass wool all have thermal conductivities of approximately 0.05 W/mK. Thus a value of 0.05W/mK was used. Foams and lightweight rubbers have specific heats of approximately 700 J/kgK and densities of approximately 150 kg/m^3 (Thomas, 1980).

Once the temperature of the foam has reached 500 to 600°C the foam resemble a carbon type char. Thus to model the changing thermal conductivity, the foam was given wood char

properties above 600°C. For modelling purposes the paint was assumed not to exist at temperatures of ambient to 250°C. The very thin layer of paint will not affect temperatures within the wood.

Temperature of Intumescent Paint, °C	Thermal Conductivity, W/mk
250	0.05
300	0.05
400	0.05
500	0.05
600	0.05
800	0.117 (Wood Char)
900	0.125 (Wood Char)

Table 7.5. Thermal Conductivity Values for Intumescent Paint.

7.5.2 Results Of Modelling.

Two Design Guide connections were modelled, a 90mm width and 135mm width, both with a single rod. The critical temperature of 50°C was reached within the epoxy at the following times,

90mm - single rod	28 minutes
135mm - single rod	37 minutes

This can be compared to the unprotected times for the epoxy to reach 50°C (see figure 7.11),

90mm - single rod	22 minutes
135mm - single rod	31 minutes

Thus time fire resistance is increased, though not by a large proportion (approximately 20%).

The results show that whilst intumescent paints will reduce flame spread, smoke output and reduce overall char time, they do not have enough influence on thermal conductivity to increase the fire resistance.

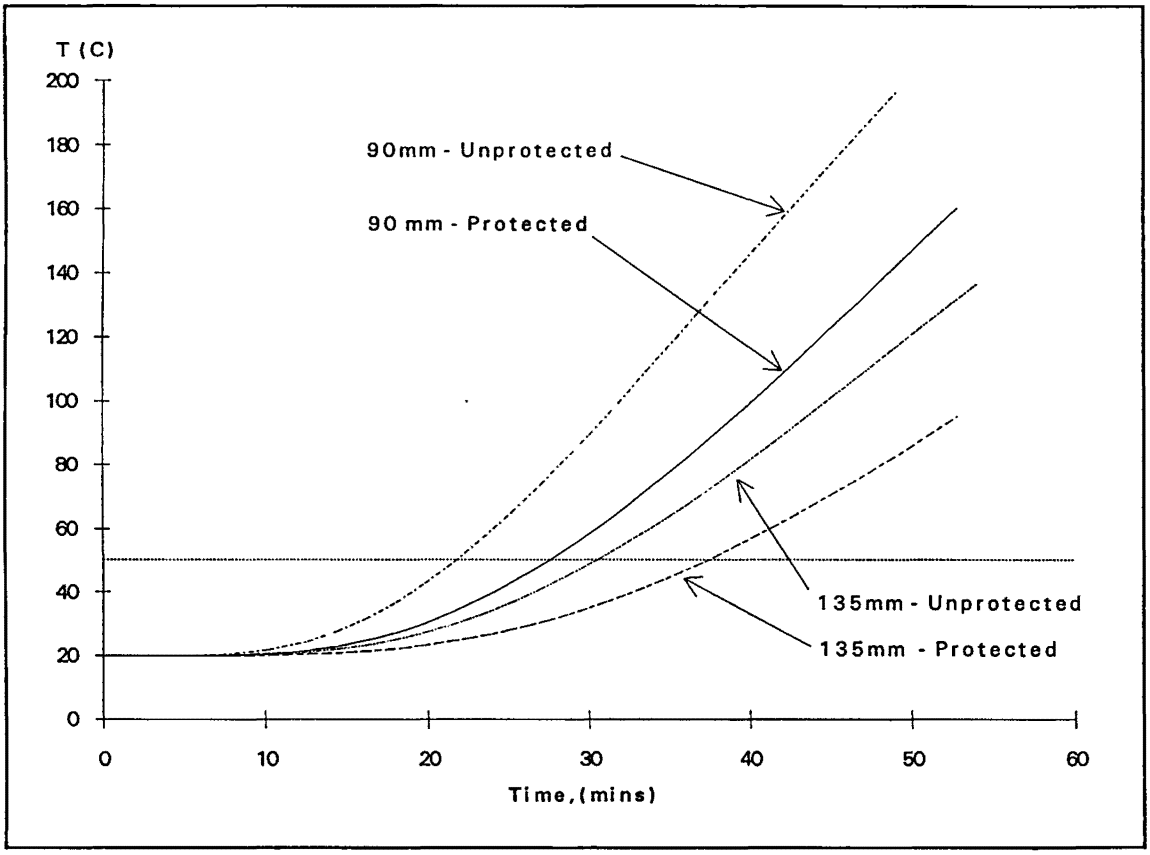

Figure 7.11. Comparison of Epoxy Temperature in Design Guide Connections Coated With Intumescent Paint and Unprotected Connections.

This modelling though must be taken with some caution as the thermal properties used are assumptions and not actual intumescent paint properties. It would be recommended that all sections be coated with intumescent paint, to increase the timber sections fire resistance.

7.6 Performance Under Real Fires.

Swedish research by Magnusson and Thelandersson (1970) has produced time temperature curves that mimic conditions in real fires. These time-temperature curves are based on a fire load and ventilation factor. Three types of time temperature curves have been used to model real fires. All are based on a high fire load of 720MJ/m^2 use three differing ventilation factors (m$^{1/2}$) to produce high, medium and low ventilated fires (figure 7.12).

7.6.1 TASEF Modelling of Real Fires.

Using the three differing fires as time temperature input for TASEF two design guide type connections were modelled, a 90mm width section and a 135mm width section with one rod (figure 7.6). Using the same thermal properties as was used for modelling under ISO834, the following times resulted for the epoxy to reach the critical temperature of 50°C (table 7.6 and figures 7.13 and 7.14).

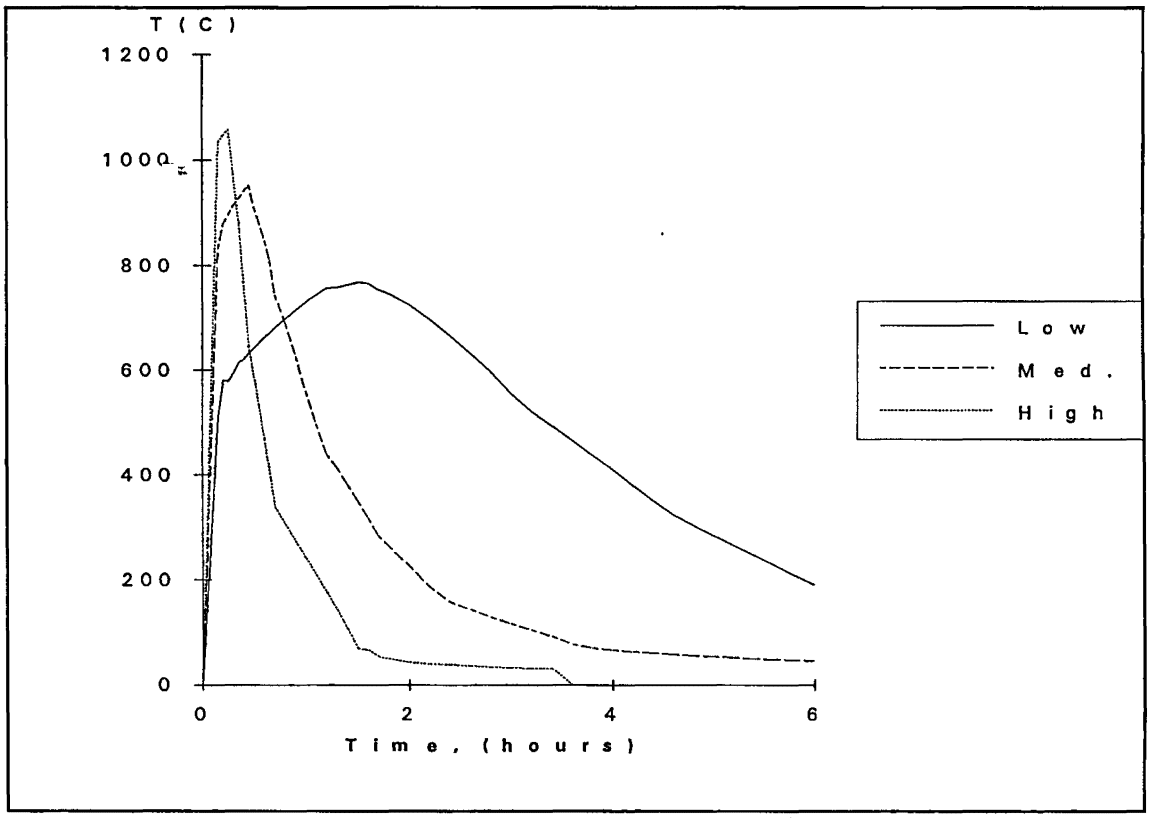

Figure 7.12. Real Fires Based on Fire Loads of 720 MJ/m^2 and Ventilation Factors of 0.02 (low), 0.06 (medium) and 0.12 (high).

The results show that the low ventilated fire gives a better performance for the epoxy rod connection. This is due to this fire staying at relatively low temperatures (500 to 600°C) for a long period whilst the medium and high ventilated fires reach temperatures of 900 and 1000°C respectively, within the first 20 minutes. The relatively high temperatures over a short time period for the highly ventilated fire still affect the epoxy adversely as the temperatures are above 500°C for the first 30 minutes, enough time for continued heat to penetrate into the connection.

	Time to reach Critical Temperature, (minutes)	
Fire Type	90mm Width Section	135mm Width Section
High	17	24
Medium	19	27
Low	24	33
ISO834	22	31

Table 7.6. Time to Reach Critical Temperature of 50°C Based on Three Real Fires.

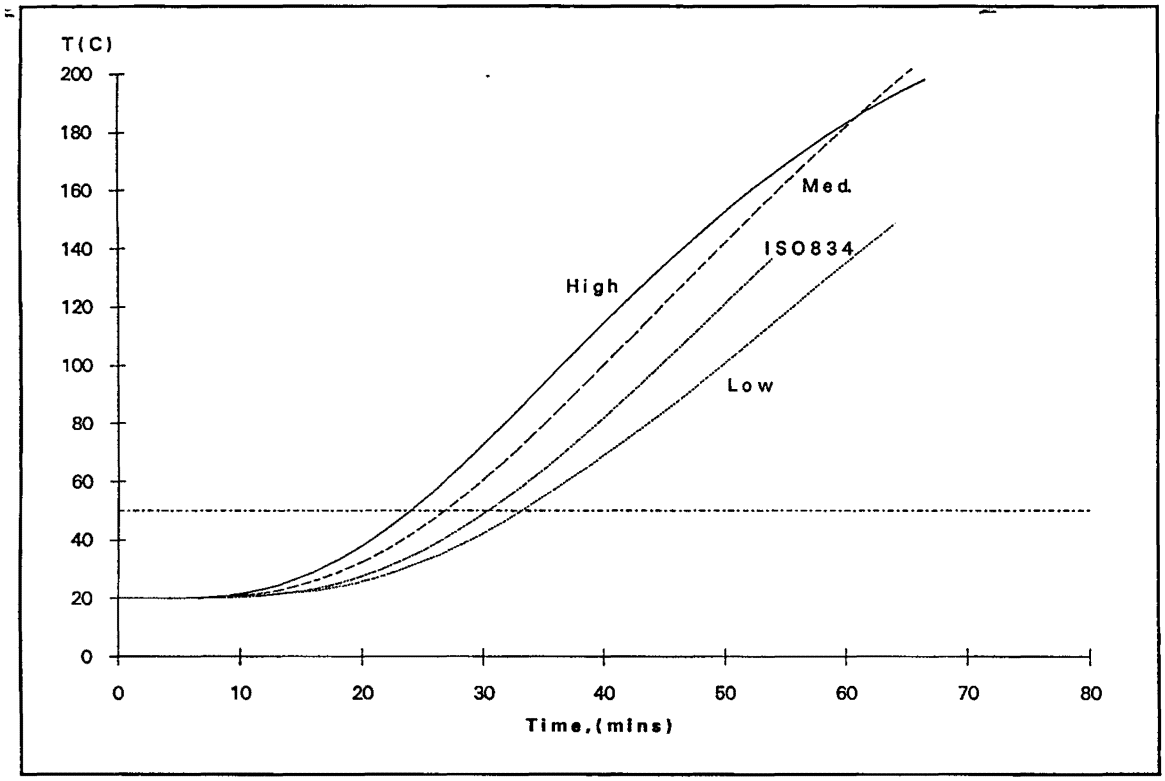

Figure 7.13. 135mm Design Guide Connection Modelled Using Real Fires and ISO834.

When the fires are modelled for their complete duration of six hours the lag in epoxy temperature, behind the fire temperature is more evident. Plots of fire temperature for the 135mm width specimen with a single bar are shown in figures 7.15 to 7.17.

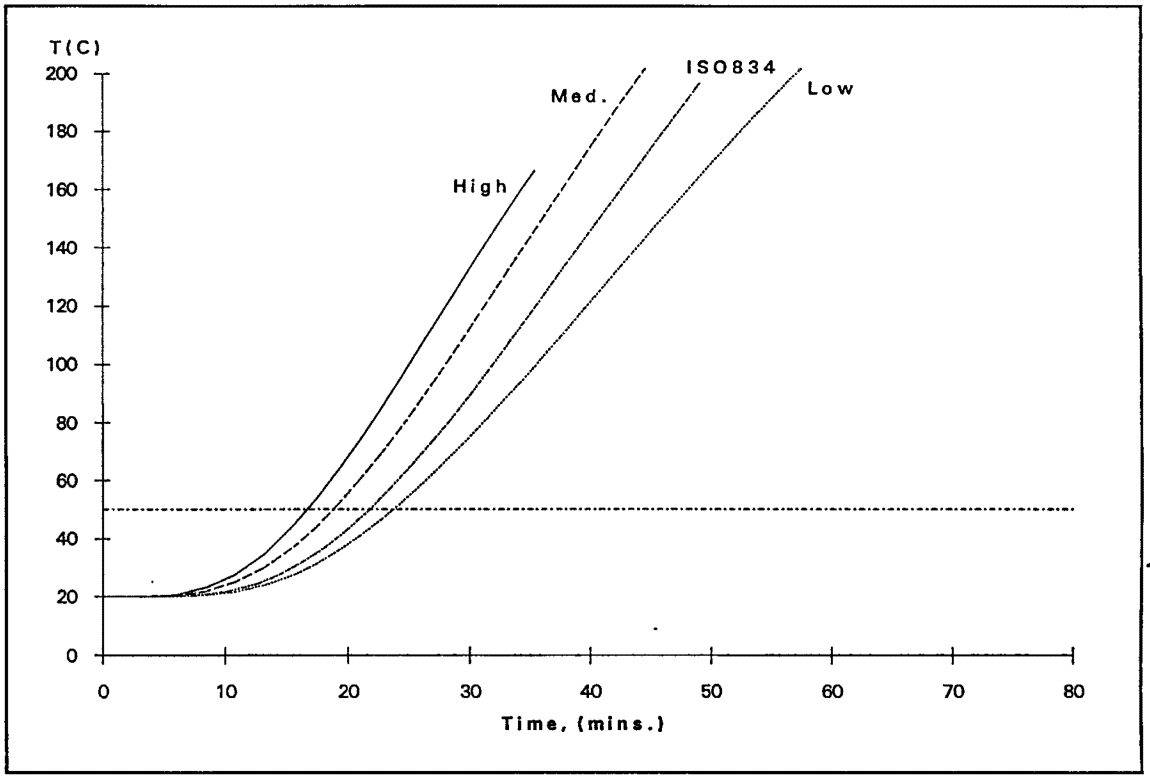

Figure 7.14. 90mm Design Guide Connection Modelled Using Real Fires and ISO834.

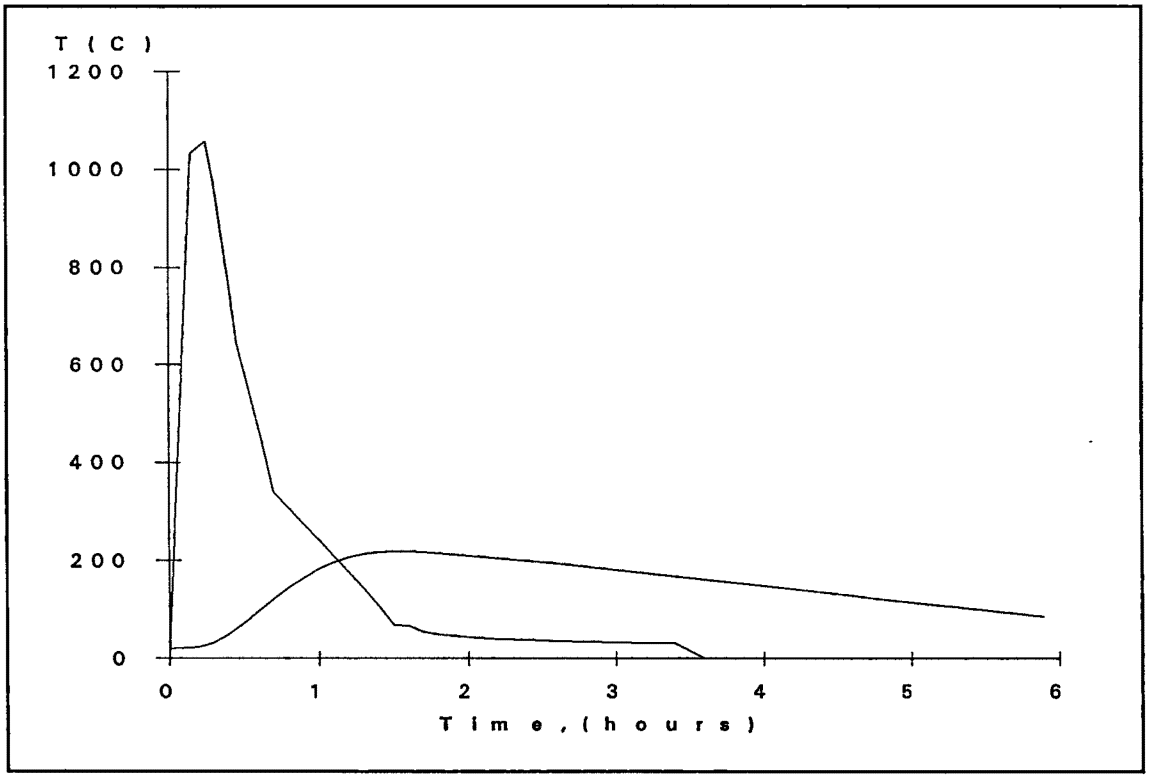

Figure 7.15. High Ventilation Fire and Corresponding Epoxy Temperature (135mm - Single Rod).

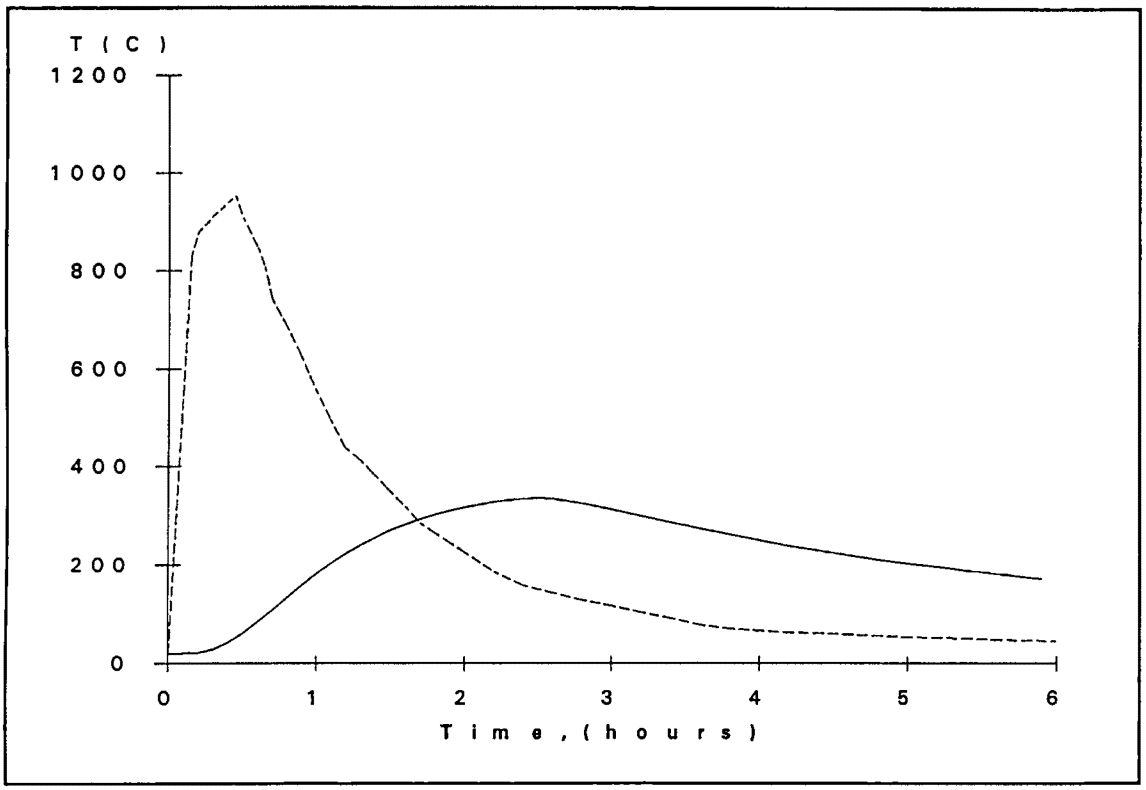

Figure 7.16. Medium Ventilation Fire and Corresponding Epoxy Temperature (135mm - Single Rod).

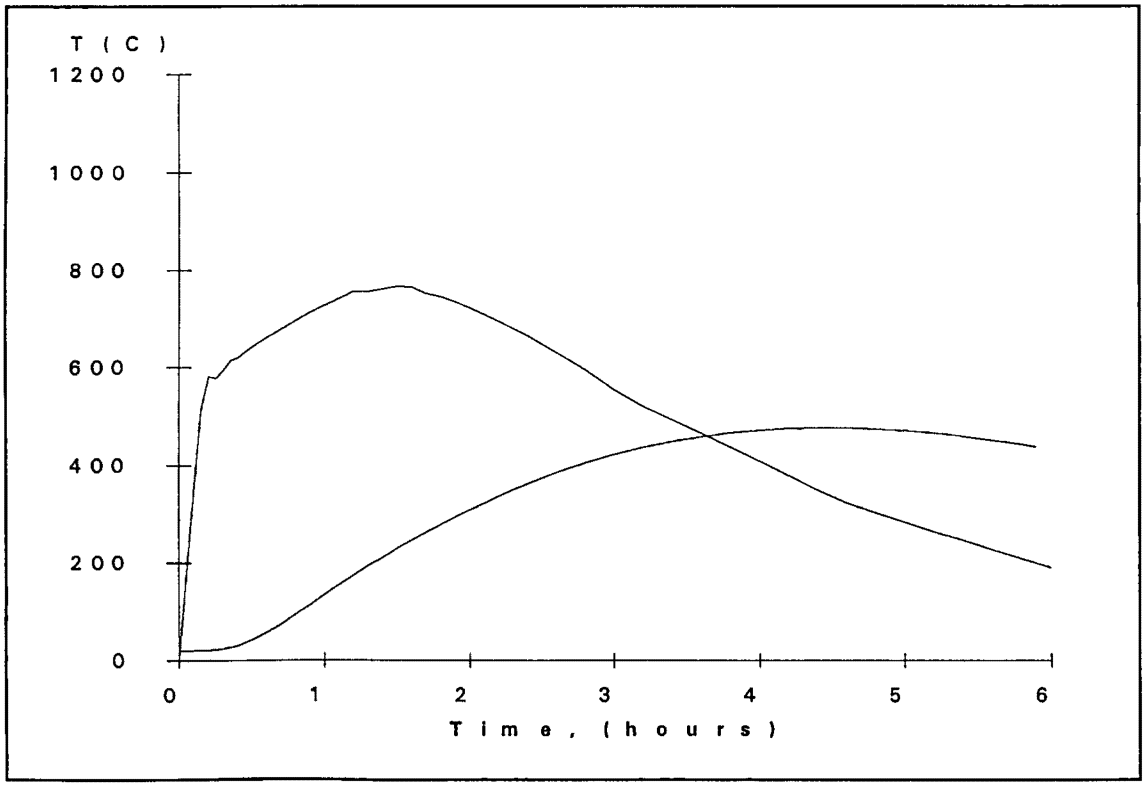

Figure 7.17. Low Ventilation Fire and Corresponding Epoxy Temperature (135mm - Single Rod).

CHAPTER 8

CONCLUSIONS AND SUMMARY

8.1 Summary.

This research was carried out to investigate the reaction of epoxy dowel connections under fire conditions. Tension tests were carried out with test specimens heated in an oven to temperatures of 80°C. Furnace testing of full size connections under the ISO834 standard fire were used to confirm the oven test data. Computer modelling using TASEF was then used to predict fire resistance of connections used in practice, utilising both ISO834 and real fire time temperature curves.

8.2 General Conclusions.

1, Both the West System and Nuplex K80 epoxies reach a critical temperature at approximately 50°C (West at 55°C and K80 at 45°C). Strength decreases rapidly once this temperature is reached.

2, The mode of failure in the epoxy connection loaded in tension at elevated temperatures differs from that at ambient temperatures. Elevated temperature failure is by pull out due to shear within the epoxy and/or loss of bond at the wood epoxy interface. Failure at ambient temperatures is by tension failure in wood or by loss of confinement.

3, Tension failure at ambient temperatures is usually brittle. Failure at elevated temperatures is usually more ductile.

4, Epoxies are expected to creep at elevated temperatures due to a change in the modulus of elasticity. This is evident in tension testing.

5, Time to failure in fire conditions appears to be mainly dependent on epoxy temperature, with little or no effect of the applied load or the embedment length.

7, Modelling with real fire time-temperature curves produces very similar results to those from modelling with the standard time-temperature curve of ISO834.

8, A 30 minute fire resistance rating is easily achievable with this type of connection.

8.2.1 Fire Resistance.

Due to the heat conduction through the wood section, epoxy connections with small edge distances, are very susceptible to fire. Fire resistance can be increased by increasing member size, thus increasing edge distance or providing insulation to the connection via gypsum plasterboard or intumescent paint.

Unfortunately these solutions are not always practical. An increase in member size is an expensive exercise and bending forces in a section are most efficiently resisted by having the threaded rods placed close to the extreme fibre of the section, regardless of its size. Gypsum plasterboard is not an aesthetically pleasing solution as most glulam sections are designed to be exposed, not covered in plasterboard. Intumescent paint should be applied to the exterior of a section as this provides good protection in delaying charring and has the ability to lower heat conduction.

All structures utilising glulam sections should have sprinkler systems installed throughout, thus minimising the chance of a large fire. If a fire does grow in a sprinklered building it would be expected that the exposed glulam sections would be well cooled by the sprinklers, thus greatly increasing the fire resistance of the timber sections.

8.2.2 Relative Epoxy Strength.

Nuplex K80 has the ability to become plastic at elevated temperatures ($>50^{o}C$), then return to its more hardened phase once cooled. This gives the K80 connection some residual strength once temperature has returned to ambient. West System epoxy remains quite brittle at all stages of the heating process and only a small amount movement due to the epoxy softening occurs, thus failure is normally one of confinement. Thus once connections with West system have failed, there is normally little residual strength left, especially if splitting in the timber has occurred.

Thus K80 has an advantage of greater residual strength after the fire than West epoxy appears to, though the level of residual strength is low once the epoxy has cooled (approximately 20kN).

8.2.3 Embedment Length.

Tests at ambient temperatures by Townsend (1990), Fairweather (1992) and Deng (1993) have all shown a direct relationship between ultimate tensile pull-out strength and embedment length. The elevated temperature tests have revealed that this direct relationship does not hold, once a critical temperature is reached. Once temperatures are above a critical value the embedment length no longer governs pull-out strength, but epoxy stiffness does. Epoxy stiffness is directly related to the increase in temperature.

8.3 Further Research.

Research should also be carried out into the following topics,

i, K80 and West compression and tension strengths at a range of temperatures from ambient to 100°C, using standard test cylinders.

ii, A test must be developed that determines epoxy shear and bond strength with timber.

iii, More oven tension tests carried out to expand the present work. Also testing above 100°C and testing with longer embedment lengths.

iv, Thermal properties of radiata pine be specifically determined, i.e. thermal conductivity and specific heat tests.

v, High temperature epoxies could be investigated for strength and heat resistance.

vi, Cement based epoxy-grouts could be investigated as to their strength and heat resistance. Also fibreglass reinforced epoxies could be investigated.

vii, Various types of intumescent paints could be furnace tested to see their performance in enhancing fire resistance.

References

Avent R.R & Issa C.A., 1984; Effect of Fire on Epoxy-Repaired Timber. Journal of Structural Engineering, Vol. 110, No. 12, pp 2858-2875.

Baber H.L. & Fowkes A.H.R., 1984; Fire Resistance of Load Bearing Timber Walls. Proceedings of Pacific Timber Engineering Conference, Vol II, pp708-714.

Barnett C., 1984; Review of Chemical and Physical Characteristics. Proceedings of Pacific Timber Engineering Conference, Vol II, pp691-702.

Bender D.A., Woeste F.E., Schaffer E.L. & Marx C.M., 1985; Reliability Formulation for the Strength and Fire Endurance of Glued-Laminated Beams. USDA Research paper, FPL 460, Wisconsin.

Buchanan A.H. & Fletcher M.R., 1989; Glulam Portal Frame Swimming Pool Construction. Proceedings of the Second Pacific Timber Engineering Conference, Auckland, New Zealand, 1989, Vol. 1 pp 245-249.

Buchanan A.H. & Fairweather R.H., 1992; Glulam Portal Frames With Steel Knee Joints - Design Guide. Report prepared for Hunter Laminates Ltd, Nelson.

Buchanan A.H. & Fairweather R.H., 1994; Seismic Design of Glulam Structures. Bulletin of New Zealand National Society for Earthquake Engineering, March.

BS 5268: Part 4.1, 1978; Method of Calculating Fire Resistance of Timber Members. British Standards Association.

Caley P., 1993; Ciba-Geigy (NZ) Limited, Auckland, Data Sheet for Ciba-Geigy (NZ) Ltd.

Charleson A.W. & Patience D.B., 1993; Review of Current Structural Timber Jointing Methods - An Architectural Perspective. New Zealand Timber Design Journal, Issue 3, Vol.2, 1993.

Chow S.Z., 1969; A Kinetic Study of the Polymerization of Phenol-Formaldehyde Resin In the Presence of Cellulosic Materials. Wood Science, Vol 1, No. 4, pp215-221.

CIB, 1986; Design Guide - Structural Fire Safety. Fire Commision of the Conseil International du Bâtiment (CIB W14), Fire Safety Journal, Vol. 10 No. 2, pp 79-136.

Collier, P.C.R., 1992; Charring Rates of Timber. BRANZ Study Report No. 42, Building Research Association of New Zealand, Judgeford, New Zealand.

Collins M.J., 1983; Density Conversions for Radiata Pine. FRI Bulletin No. 49, Forestry Research Institute, Rotorua.

Cown D.J. & McConchie D.L., 1983; Radiata Pine Wood Properties Survey (1977 - 1982). FRI Bulletin No. 50, Forestry Research Institute, Rotorua.

Crawford R.J., 1987; *Plastics Engineering - Second Edition.* Pergamon Press, England.

Cutter B.E. & McGinnes E.A., 1981; A Note on Density Change Patterns in Charred Wood. Wood and Fiber, Vol 13 No.1, pp 39-44.

Deng J, 1993; Unpublished Ph.d. Dissertation, University of Canterbury.

Drysdale D.D., 1985; *An Introduction to Fire Dynamics.* Wiley, New York.

Fairweather R.H., 1992; Beam Column Connections for Multi-Storey Timber Buildings. Research Report 92-5, Department of Civil Engineering, University of Canterbury.

FEDG, 1993; Fire Engineering Design Guide - Draft. Editor A.H. Buchanan, Centre for Advanced Engineering, University of Canterbury, Christchurch.

Gardner W.D. & Syme D.R., 1991; Charring of Structural Timbers of Eight Australian Species and the Effect of 13mm Gypsum Plasterboard Protection on Their Charring. Project Report, Forestry Commission of New South Wales.

Hilado C.J., 1990; *Flammability Handbook for Plastics, fourth edition.* Technomic, Pennsylvania.

Imaizumi K., 1963; Stability in Fire of Protected and Unprotected Glued Laminated Beams. Reprint from Norsk Skogindustri, No.4, 1962, New Zealand Forest Service Information Series No. 47, Wellington.

Janssens M.L., 1993; Development of a Simple Model for the Charring of Fire-Exposed Wood Members. Presentation at University of Canterbury, Unpublished.

Johnson R.P., 1970; The Properties of an Epoxy Mortar and its Use For Structural Joints. The Structural Engineer, Vol. 48 No.6, pp 227-233.

Kenna L.F., 1973; Timber Structures and Fire. Research Paper, Building Research Association of New Zealand, Wellington.

Knudson R.M. & Schniewind A.P., 1975; Performance of Structural Wood Members Exposed to Fire. Forest Products Journal, Vol. 25 No. 2, pp23-32.

Koch P., 1969; Specific Heat of Ovendry Spruce Pine Wood and Bark, Wood Science. Vol 1, No. 4, pp203-214.

Kung Hsiang-Cheng, 1972; A Mathematical Model of Wood Pyrolysis. Combustion and Flame, Vol.18, pp185-195.

Lee H. & Neville K., 1957; *Epoxy Resins.* McGraw-Hill, New York.

Lie T.T., 1977; A Method For Assessing the Fire Resistance of Laminated timber Beams and Columns. Canadian Journal of Civil Engineering, Vol 4, pp 161-169.

McIntosh K.A., 1989; From Theory to Reality - 30 Years in Glulam Manufacture. Proceedings of the Second Pacific Timber Engineering Conference, Auckland, New Zealand, 1989, Vol. 1 pp 229-234.

Majamaa J., 1991; Calculation Models of Wooden Beams Exposed To Fire. Research Notes No.1282, Technical Research Centre of Finland.

Magnusson S.E. & Thelandersson S., 1970; Temperature-Time Curves of Complete Process of Fire Development. Lund Institute of Technology, ACTA Polytechnia Scandinavica No. 65, Stockholm, Sweden.

Mikkola E., 1990; Charring of Wood. Research Paper 689, Technical Research Centre of Finland.

Moss P., 1982; Structural Uses of Epoxy Resin Adhesives. Department of Civil Engineering Research Report, No. 82-3, University of Canterbury.

Nielsen P.C. & Olesen F.B., 1982; Tensile Strength of Finger Joints at Elevated Temperatures. Report No.8205, Institute of Building Technology and Structural Engineering, Aalborg, Denmark.

Nuplex, 1993; Nuplex Industries Data Sheet - K80 Winter, Product Information.

Odeen K., 1967; Fire Resistance of Glued, Laminated Timber Structures. Fire and Structural Use of Timber in Buildings - Proceedings of the Symposium held at the Fire Research Station Boreham Wood, Hertsfordshire, England.

Parker W.J., 1988; Prediction of the Heat Release Rate of Wood. (Ph.D. Dissertation), The George Washington University, Washington D.C., USA.

Potter W.G., 1975; *Uses of Epoxy Resins.* Newnes-Butterworths, London.

Rogowski B.F.W., 1967; Charring of Timber in Fire Tests. Fire and Structural Use of Timber in Buildings - Proceedings of the Symposium held at the Fire Research Station Boreham Wood, Hertsfordshire, England.

Schaffer E.L., 1968; A Simplified Test for Adhesive Behaviour in Wood Sections Exposed to Fire. U.S.D.A. Forest Service Research Note, FPL-0175, Forest products Laboratory, Madison, Wisconsin, USA.

Schaffer E., 1977; State of Structural Timber fire Endurance. Wood and Fibre, Vol. 9 No. 2, pp 145-170.

Siau J.F., 1971; *Transport Processes in Wood.* Springer - Verlag, New York.

SNZ, 1992; NZS4203:1992 New Zealand Loadings Standard. Standards New Zealand, Wellington.

----------, **1993;** NZS3603:1993 Code of Practice for Timber Design. Standards New Zealand, Wellington.

----------, **1989;** MP9:1989, Fire Properties of Building Materials and Elements of Structure - Part 1. Standards New Zealand, Wellington.

Sterner E. & Wickstrom U., 1990; TASEF User's Manual. SP Report 1990:05, Swedish National Testing Institute, Sweden.

Swedish Finnish Timber Council, 1981; Swedish and Finnish Redwood and Whitewood. Performance in Fire, The Swedish Finnish Timber Council, Retford.

Tabor L.J., 1978; *Effective Use of Epoxy and Polyester Resins in Civil Engineering Structures.* CIRIA, London.

Tenning K., 1967; Glue Laminated Timber Beams: Fire Tests and Experience in Practice. Fire and Structural Use of Timber in Buildings - Proceedings of the Symposium held at the Fire Research Station Boreham Wood, Hertsfordshire, England.

Thomas L.C., 1980; *Fundamentals of Heat Transfer.* Prentice-Hall, New Jersey.

Timms C., 1994; Adhesive Technologies Ltd., Auckland, Data Sheet for West System Epoxies.

Townsend P.K., 1990; Steel Dowels Epoxy Bonded in Glue Laminated Timber. Research Report 90-11, Dept. of Civil Engineering, University of Canterbury.

TRADA, 1971; Fire Performance of Timber: A literature Survey, Section 5, Section 6 & Section 7. Timber Research and Development Association, High Wycombe, England.

Tran H.C. & White R.H., 1992; Burning Rate of Solid Wood Measured in a Heat Release Rate Calorimeter. Fire and Materials, Vol 16. pp197-206.

Tsoumis G.T., 1991; *Science and Technology of Wood.* Van Nostrand Reinhold, New York.

TUM, 1989; Timber Use Manual. Editor A.H. Buchanan, New Zealand Timber Industry Federation, Wellington.

Wardle T.M., 1966; Notes on the Fire Resistance of Heavy Timber Construction. New Zealand Forest Service, Info. Series No. 53, Wellington.

West System, 1993; West System Epoxies Data Sheet - Z105/Z206 Product Information

White R.H. & Nordheim E.V., 1992; Charring Rate of Wood for ASTM E119 Exposure. Fire Technology, Vol 28 No. 1, pp 5-30.

White R.H. & Schaffer E.L., 1978; Application of CMA Program to Wood Charring. Fire Technology, Vol. 14 No.4, pp 279-290.

White R.H. & Schaffer E. L., 1981; Transient Moisture Gradient in Fire-Exposed Wood Slab. Wood and Fiber Vol. 13 No. 1, pp 17-38.

Wood Handbook, 1987; U.S. Department of Agriculture. Agriculture Handbook No. 72, Washington, D.C., USA.

APPENDICES

Appendix 1: Oven Tension Test Failure Descriptions.

Appendix 2: Load Deflection Curves for Oven Tension Tests.

Appendix 3: Furnace Temperatures.

Oven Tension Test Specimens.
Tension load applied at a rate of 2cm/min.

Test 101: K80, failure temperature 41.5°C ; Very stiff wood with fast loading, first cracking 36kN, large cracks opening, splitting failure along length.

Test 102: K80, failure temperature 89°C; Slow loading with first cracking 27kN, slight extension in epoxy at test end, then extension of epoxy also occurring at the control end, i.e. failure at both ends. No cracking at control end, timber-epoxy bond failure and shear failure in epoxy.

Test 103: K80, failure temperature 41.7°C; Stiff wood with fast load increase, first cracking 51kN, then continual small cracks before fast, explosive failure. Complete opening of the timber surrounding the epoxy.

Test 104: K80, failure temperature 76°C; Slow loading with splitting occurring over all parts of specimen. Oven heating had caused large cracks to open near the control end of the specimen. First cracking at 21kN and extension occurring at test end, then extension occurring at both ends at 28kN. Shear failure in epoxy and bond failure with timber.

Test 105: K80, failure temperature 55°C; Slow loading with first cracking at 37kN. Slow splitting failure occurring from 49kN as splits opened in the timber and connection failed.

Test 106: K80, failure temperature 73°C; Slow loading and small cracks opening up at 14kN. Bar extending from epoxy and slowly pulling out from the connection. Shear failure in epoxy as bar pulled from the connection.

Test 107: West, failure temperature 53.5°C; Very stiff wood with fast loading. First cracking at 63kN, then an explosive brittle failure with wood opening and shattering around the connection.

Test 108: West, failure temperature 42.4°C; Stiff timber with fast loading and cracking from 71kN. Large crack opened at 82kN, but continued to carry increasing load until an explosive failure, with large cracking surrounding all of the connection.

Test 109: West, failure temperature 42°C; Slow loading with first splitting occurring along already open cracks at 30kN. Large cracks opened at test end causing brittle failure.

Test 110: West, failure temperature 74.1°C; Large shrinkage cracks had opened before testing. First splitting at 23kN, bar extension from test end and large shrinkage cracks opening. Splitting down the shrinkage cracks, 200-300mm in length.

Test 111: West, failure temperature 81.4°C; Slow loading and first cracking at 20kN, then extension of bar from epoxy, then extension of bar from control end. No cracking occurring at the control end and only very small cracks at the test end. Shear failure in epoxy at both ends.

Test 112: West, failure temperature 71°C; Timber very cracked due to oven-drying. First splitting under load at 26kN, then bar extension from epoxy as shear failure and timber bond failure occurred in the epoxy. Splitting due to loading very small, though induced by the pre-test splitting due to oven-drying.

Test 113: West, failure temperature 21°C; Slow loading with first cracks occurring at 78kN. Brittle explosive failure at 81kN, with large cracks opening.

Test 114: K80, failure temperature 21°C; Very fast loading with first cracking at 67kN, continued by more splitting and major cracking occurring at 84kN. Very brittle failure as tension failure occurred in timber, with loud noise. Air hole as a weakness in the timber induced the tension failure.

Test 115: K80, failure temperature 20.7°C; Very fast loading with cracking at 60kN and continued cracking until explosive failure at 94kN. Large cracking occurring across the top of the test specimen.

Test 116: West, failure temperature 21°C; Slow loading with cracks appearing at 45kN. One large crack opened from test end to a length of 400mm at 117kN, but increasing load still carried. Fast brittle failure as connection opened up in splitting.

Test 117: K80, failure temperature 63.5°C; Fast loading with cracking occurring at 42kN. Splitting occurring up to failure with large splits across top of connection. Brittle failure after epoxy had extended.

Test 118: K80, failure temperature 70°C; Slow loading with first cracking at 35kN. As loading continued, bar extension from epoxy due to splitting around the connection. Slow splitting failure in the wood surrounding the connection.

Test 119: K80, failure temperature 46°C; Large splits occurring in the timber due to oven drying. Slow loading with cracks opening up from 29kN. Continued cracking around connection until failure as large splits opened up the whole connection. Extension in the bar as it pulled away from the epoxy.

Test 120: K80, failure temperature 49.1°C; Slow loading, first cracking occurring at 61kN. Continued cracking until brittle failure occurred with large splitting in timber. 300-400mm cracking along length of timber.

Test 121: K80, failure temperature 60.1°C; Slow increase in load and slow cracking occurring from 31kN. Large cracks of length 300mm opening up around connection and extension of the bar in the epoxy. Failure as bar extended from the epoxy and the connection opened up from the splitting.

Test 122: West, failure temperature 59°C; Very slow increase in load with first splitting at 39kN, then more splitting at 44kN. Failure due to slow splitting failure in timber and epoxy extension.

Test 123: West, failure temperature 48°C; Very fast increase in load, first cracking at 70kN, followed by more cracking until failure by brittle, explosive opening of timber.

Test 124: West, failure temperature 46.4°C; Slow loading, splitting from 30kN. Splitting continued with large cracks opening along the length of the timber. Cracks 300-400mm in length. Failure at 96kN very brittle, with opening up of the timber.

Test 125: West, failure temperature 62.3°C; Large cracks opened up during oven heating. First cracking at 31kN. Splitting occurring during failure as bar extends out of the epoxy and connection opens up. Slow failure.

Test 126: West, failure temperature 66.6°C; Very slow loading with splitting occurring from 35kN. Slow cracking occurring around connection as epoxy extends out of the connection. Slow failure due to extension of epoxy and opening up of connection, due to splitting.

Load Deflection Curves

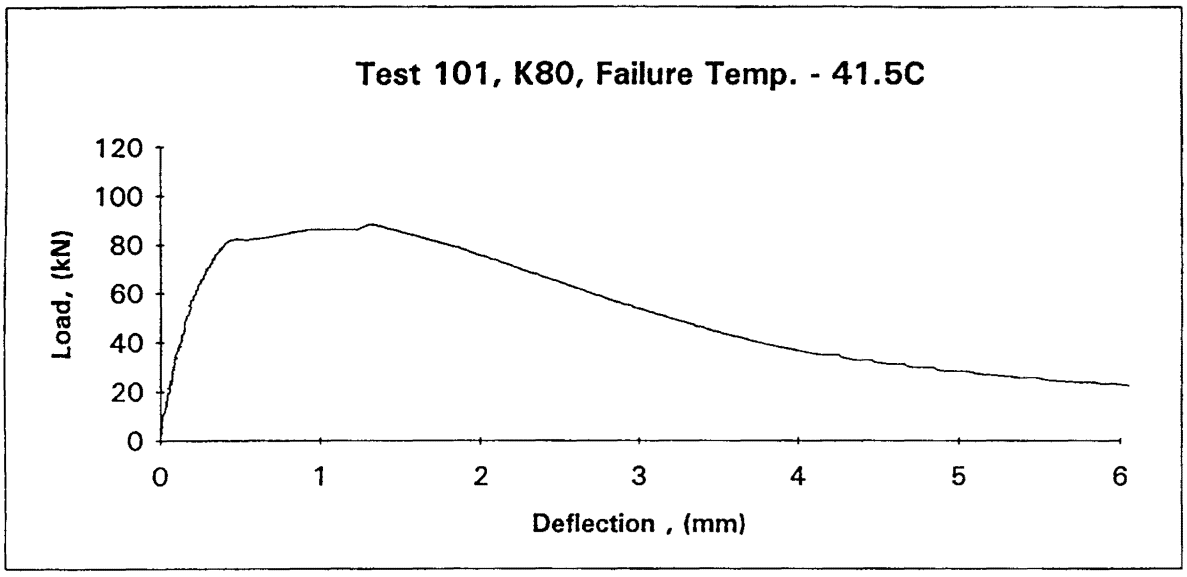

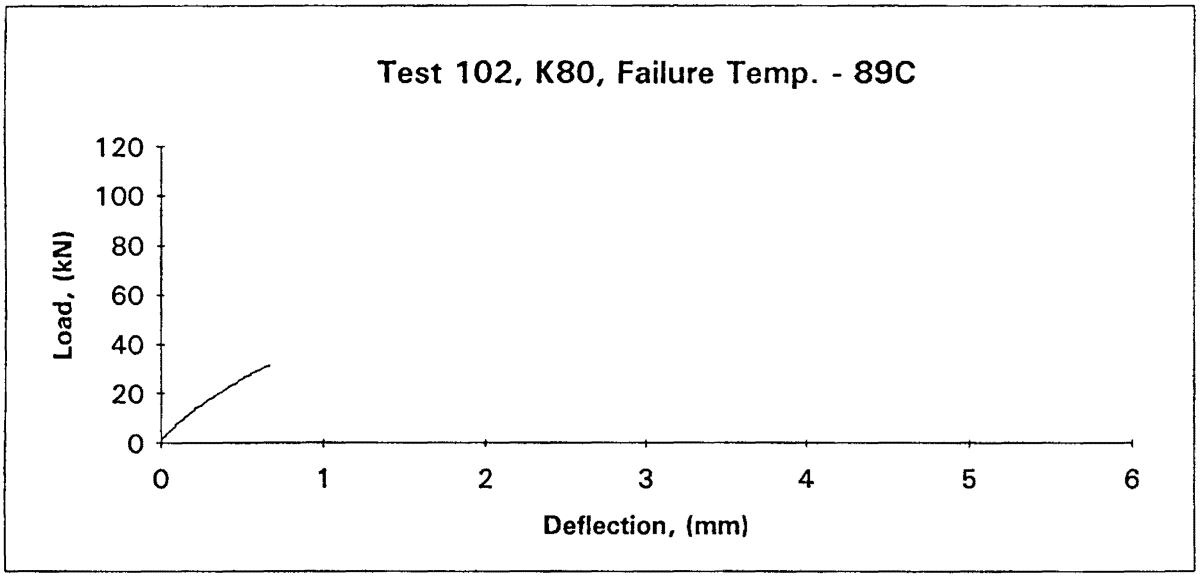

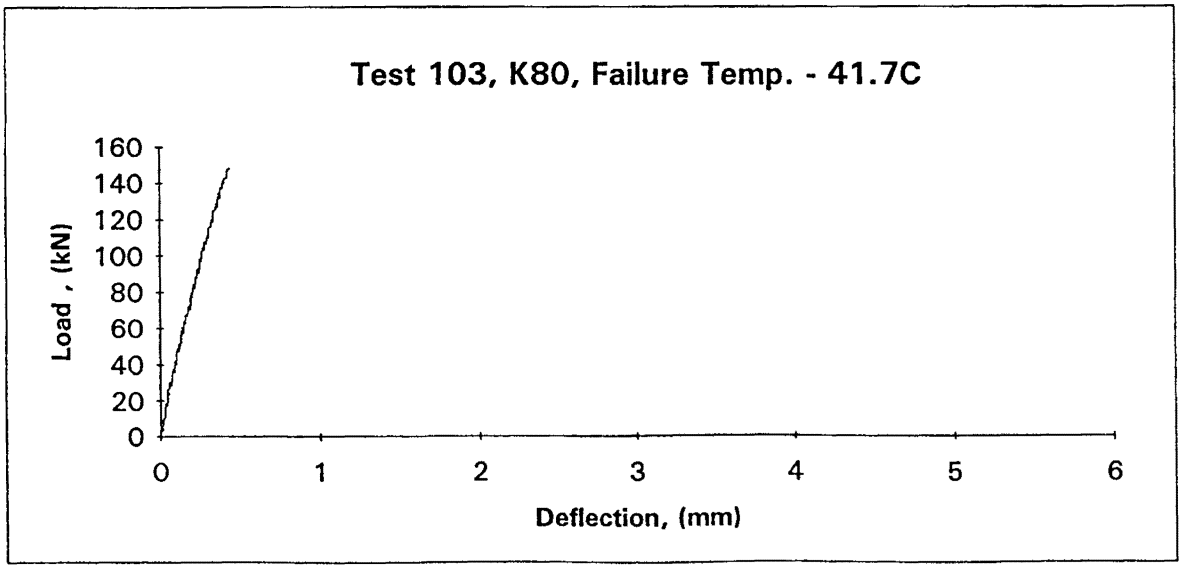

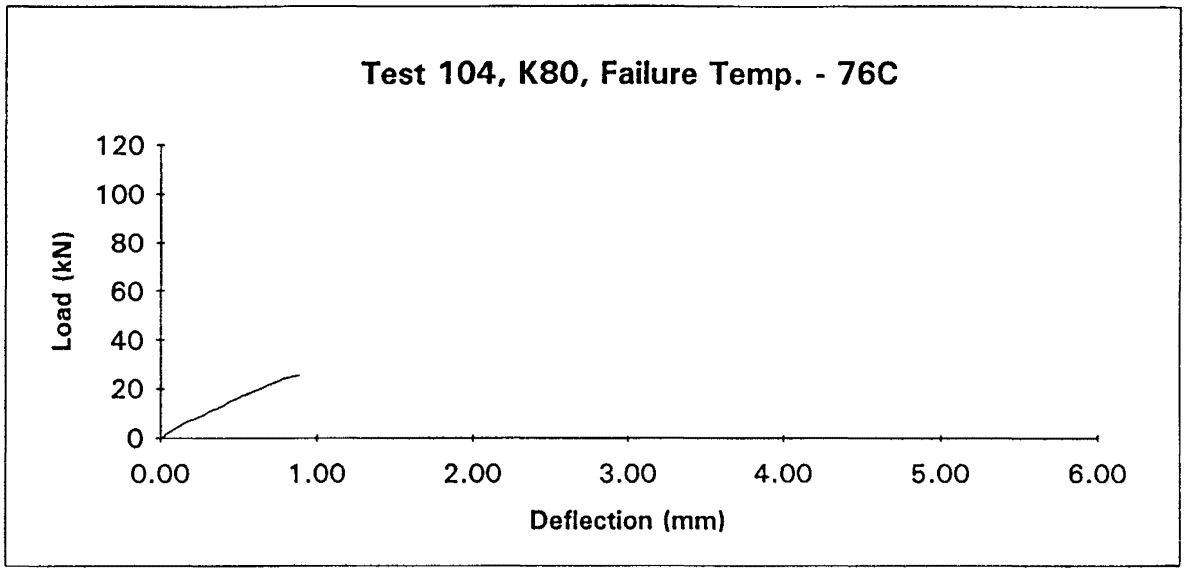
Test 104, K80, Failure Temp. - 76C
Load (kN)
120
100
80
60
40
20
0
0.00
1.00
2.00
3.00
4.00
5.00
6.00
Deflection (mm)

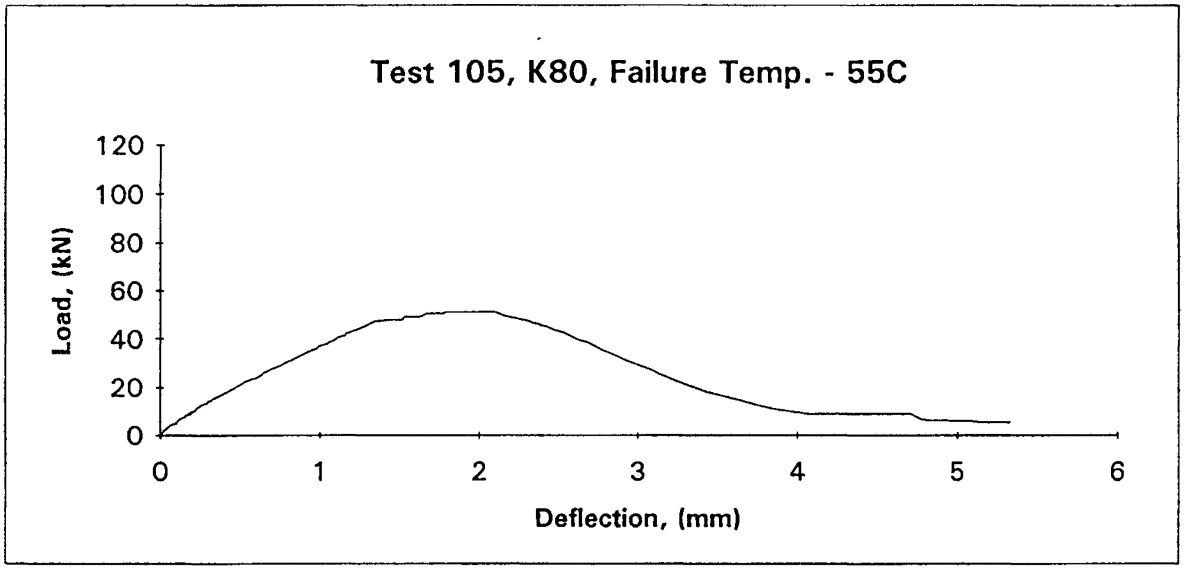
Test 105, K80, Failure Temp. - 55C
Load, (kN)
120
100
80
60
40
20
0
0
1
2
3
4
5
6
Deflection, (mm)

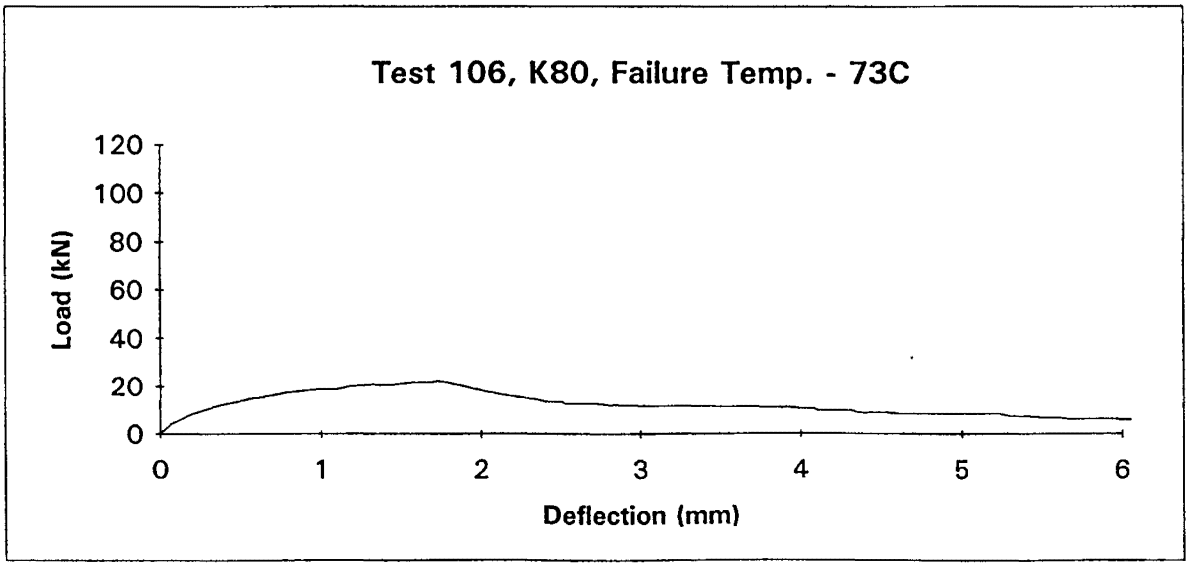
Test 106, K80, Failure Temp. - 73C
Load (kN)
120
100
80
60
40
20
0
0
1
2
3
4
5
6
Deflection (mm)

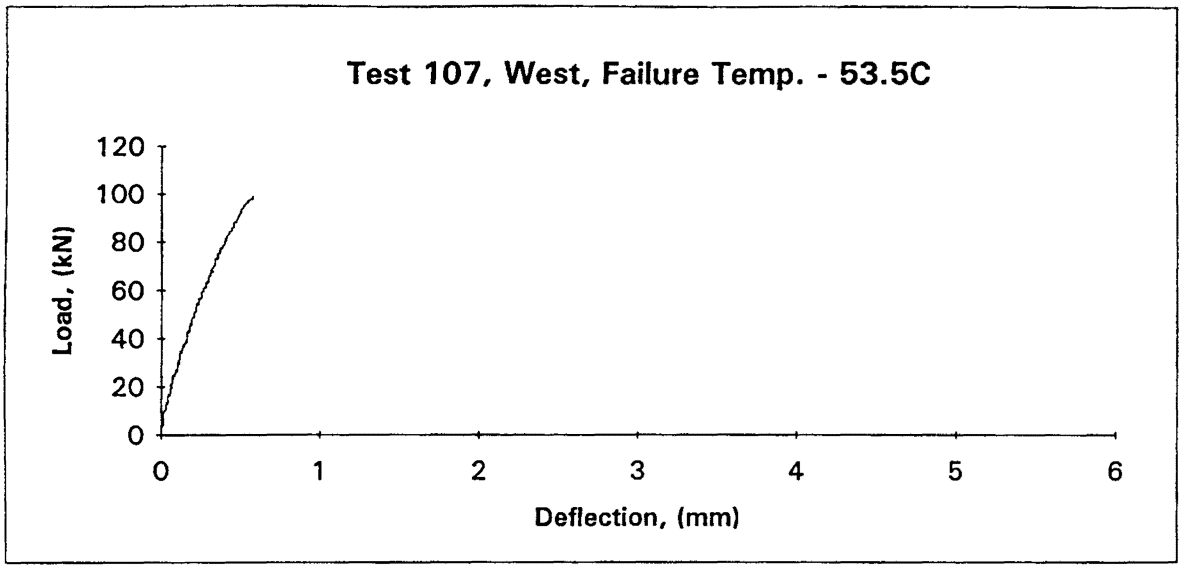
Test 107, West, Failure Temp. - 53.5C
Load, (kN)
120
100
80
60
40
20
0
0
1
2
3
4
5
6
Deflection, (mm)

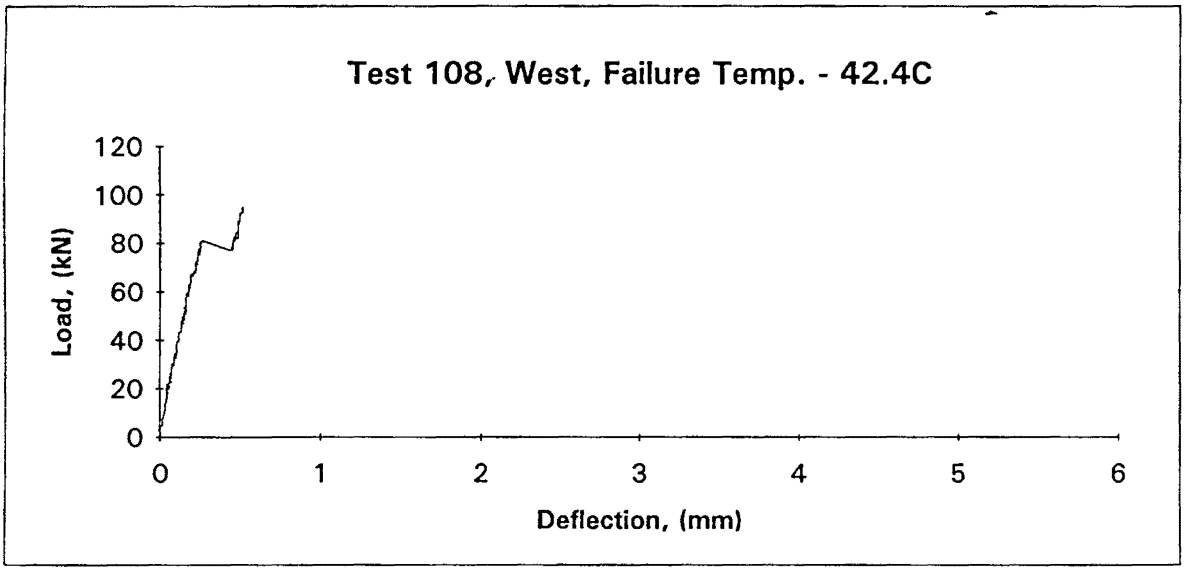
Test 108, West, Failure Temp. - 42.4C
Load, (kN)
120
100
80
60
40
20
0
0
1
2
3
4
5
6
Deflection, (mm)

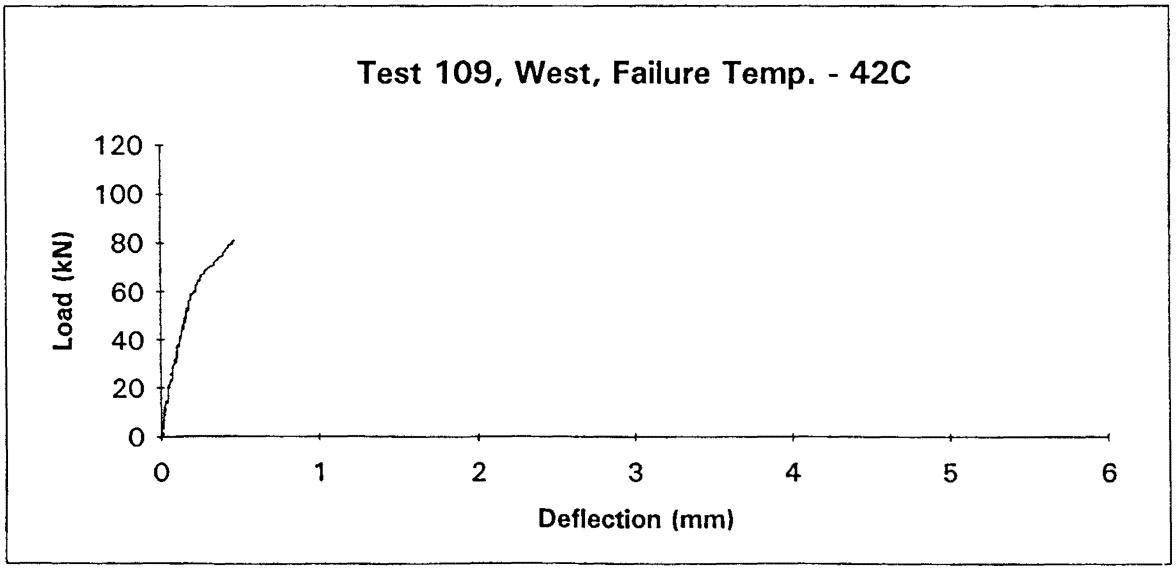
Test 109, West, Failure Temp. - 42C
Load (kN)
120
100
80
60
40
20
0
0
1
2
3
4
5
6
Deflection (mm)

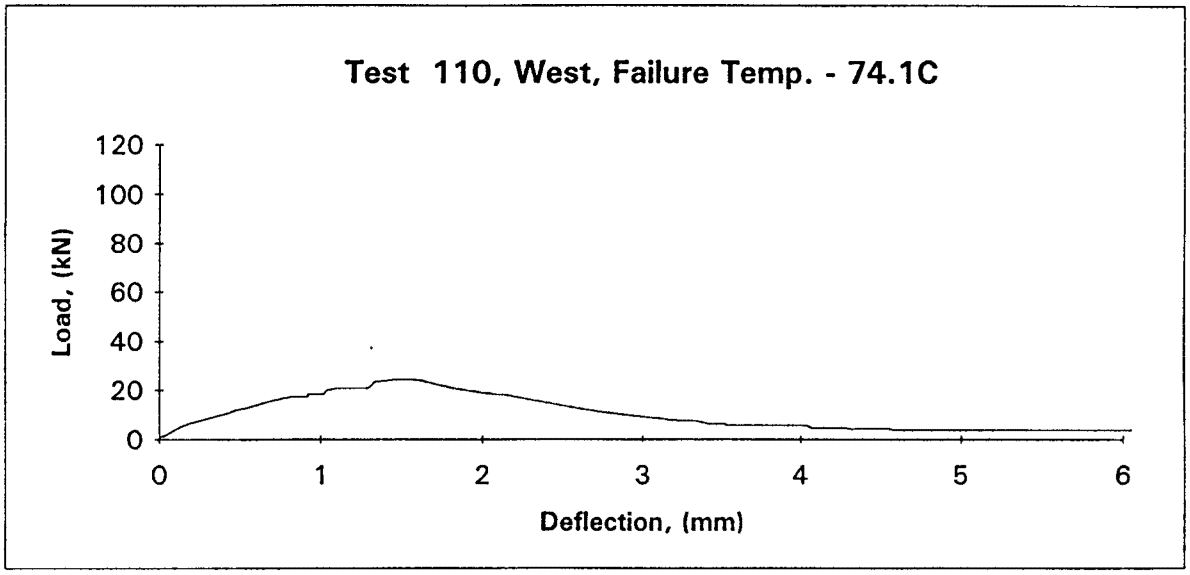
Test 110, West, Failure Temp. - 74.1C
Load, (kN)
120
100
80
60
40
20
0
0
1
2
3
4
5
6
Deflection, (mm)

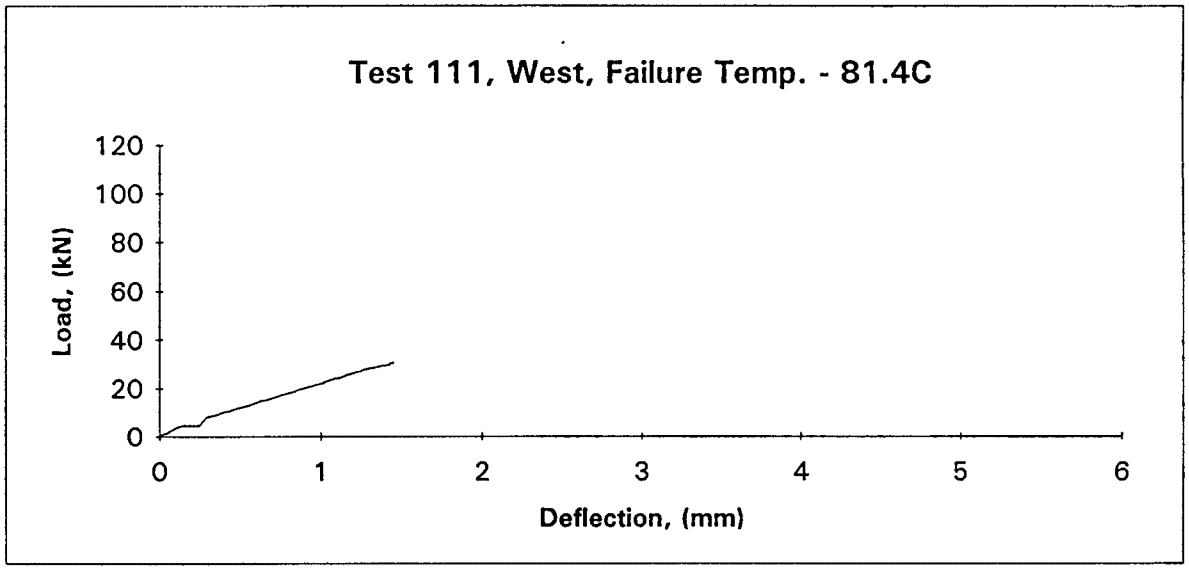
Test 111, West, Failure Temp. - 81.4C
Load, (kN)
120
100
80
60
40
20
0
0
1
2
3
4
5
6
Deflection, (mm)

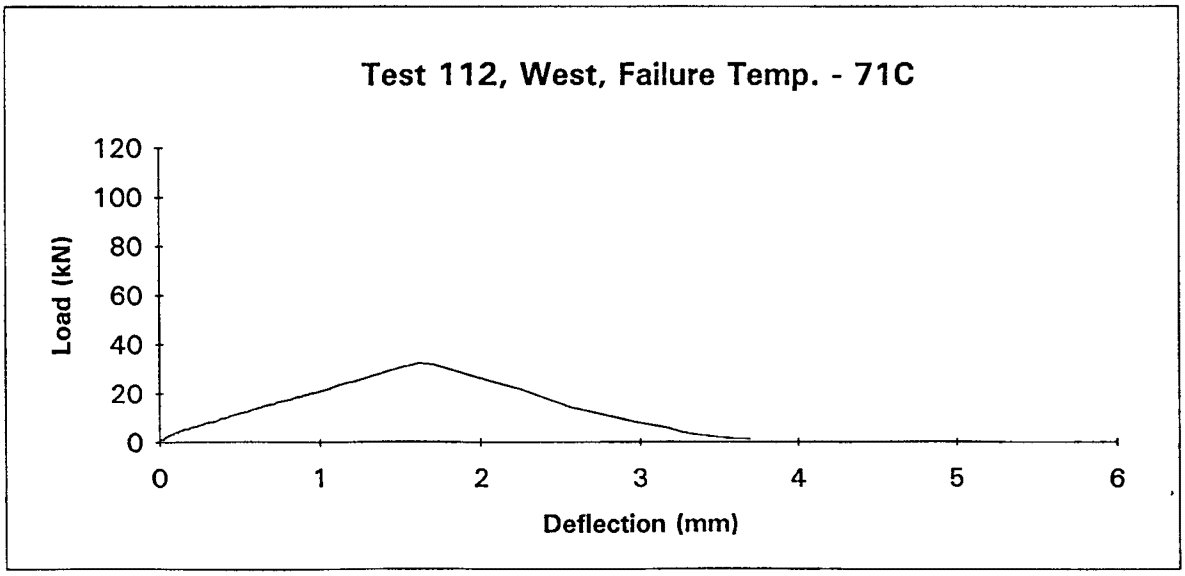
Test 112, West, Failure Temp. - 71C
Load (kN)
120
100
80
60
40
20
0
0
1
2
3
4
5
6
Deflection (mm)

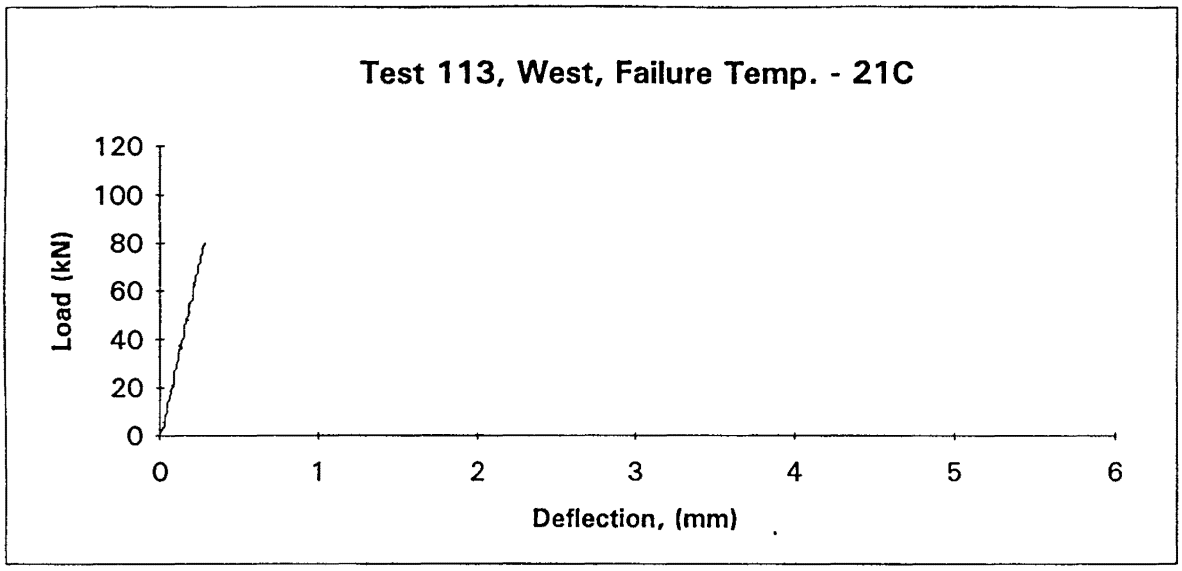
Test 113, West, Failure Temp. - 21C
Load (kN)
120
100
80
60
40
20
0
0
1
2
3
4
5
6
Deflection, (mm)

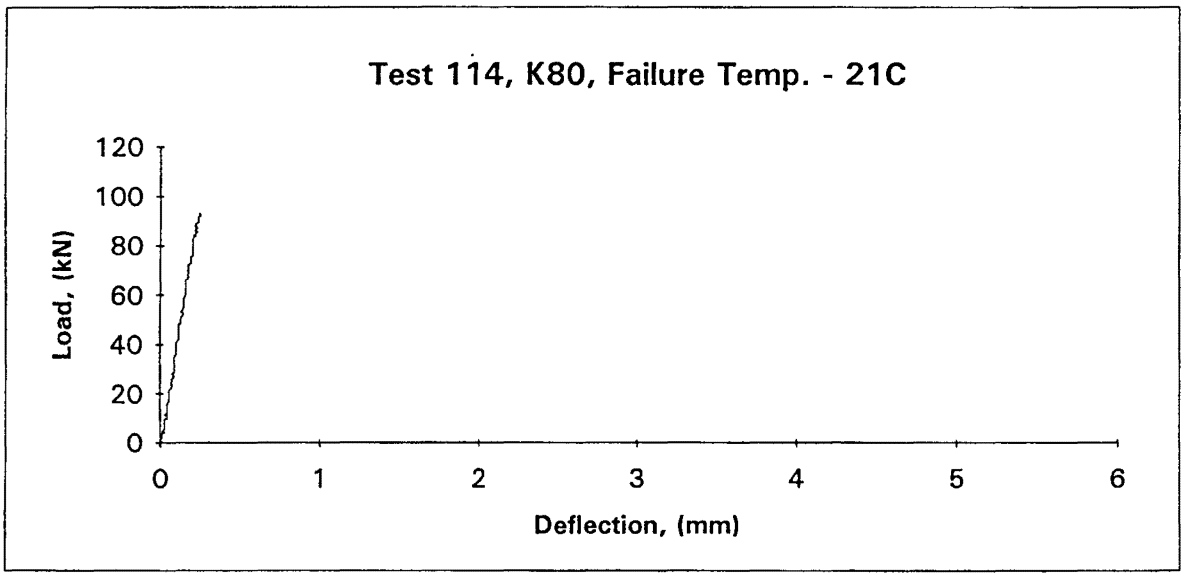
Test 114, K80, Failure Temp. - 21C
Load, (kN)
120
100
80
60
40
20
0
0
1
2
3
4
5
6
Deflection, (mm)

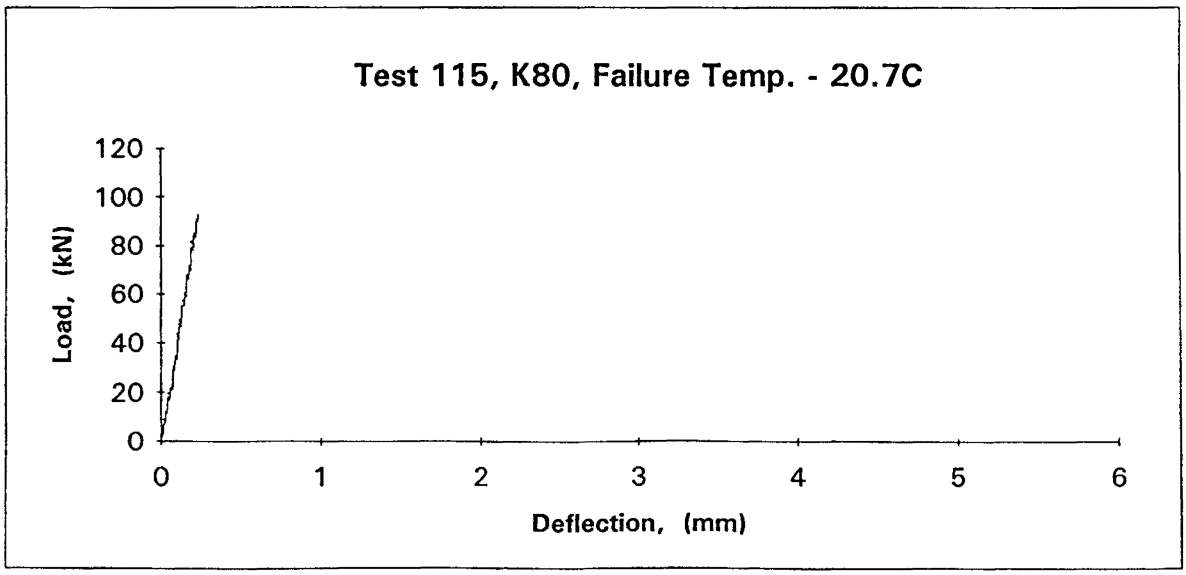
Test 115, K80, Failure Temp. - 20.7C
Load, (kN)
120
100
80
60
40
20
0
0
1
2
3
4
5
6
Deflection, (mm)

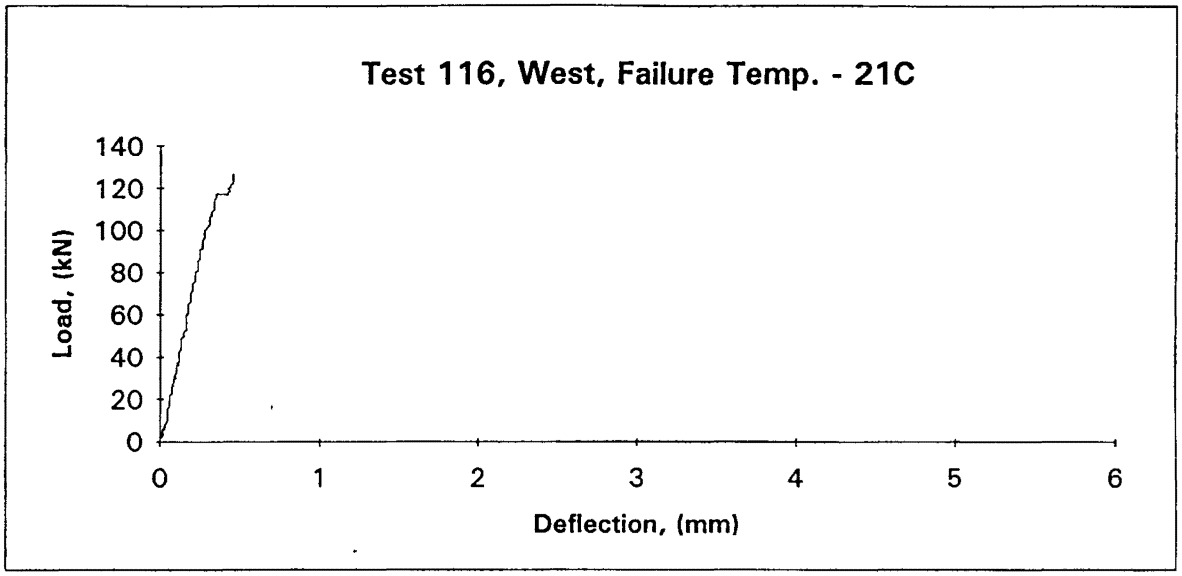
Test 116, West, Failure Temp. - 21C
Load, (kN)
140
120
100
80
60
40
20
0
0
1
2
3
4
5
6
Deflection, (mm)

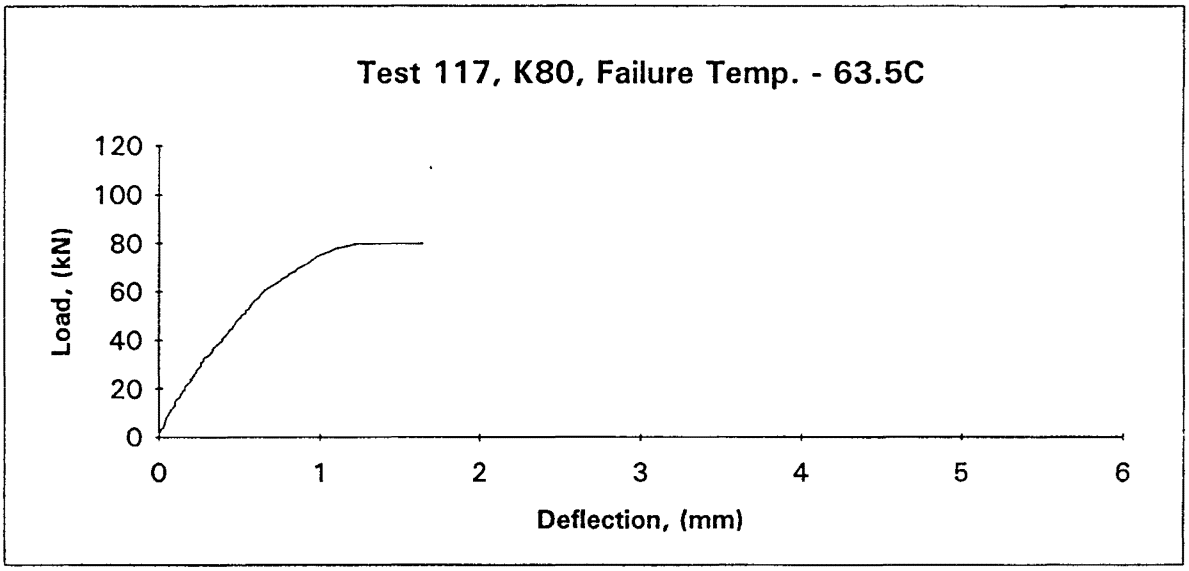
Test 117, K80, Failure Temp. - 63.5C
Load, (kN)
120
100
80
60
40
20
0
0
1
2
3
4
5
6
Deflection, (mm)

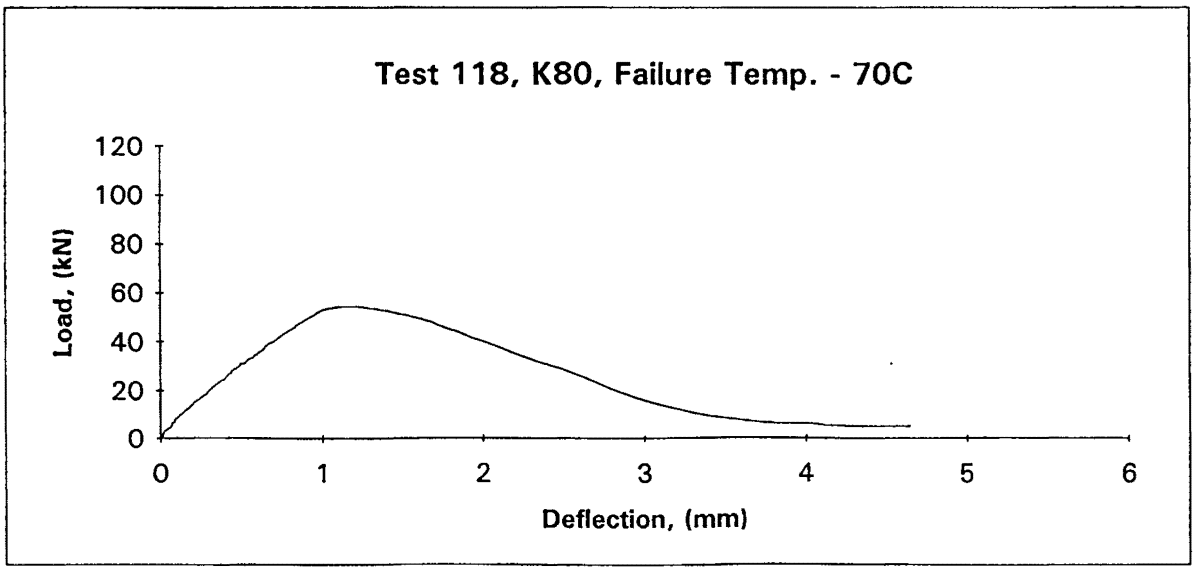
Test 118, K80, Failure Temp. - 70C
Load, (kN)
120
100
80
60
40
20
0
0
1
2
3
4
5
6
Deflection, (mm)

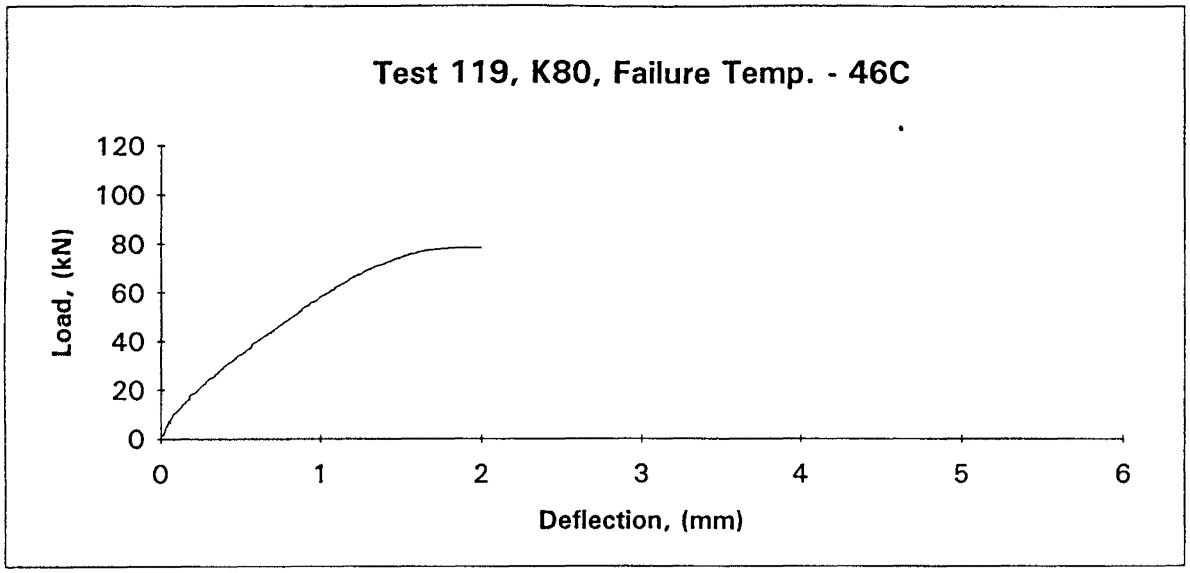
Test 119, K80, Failure Temp. - 46C
Load, (kN)
120
100
80
60
40
20
0
0
1
2
3
4
5
6
Deflection, (mm)

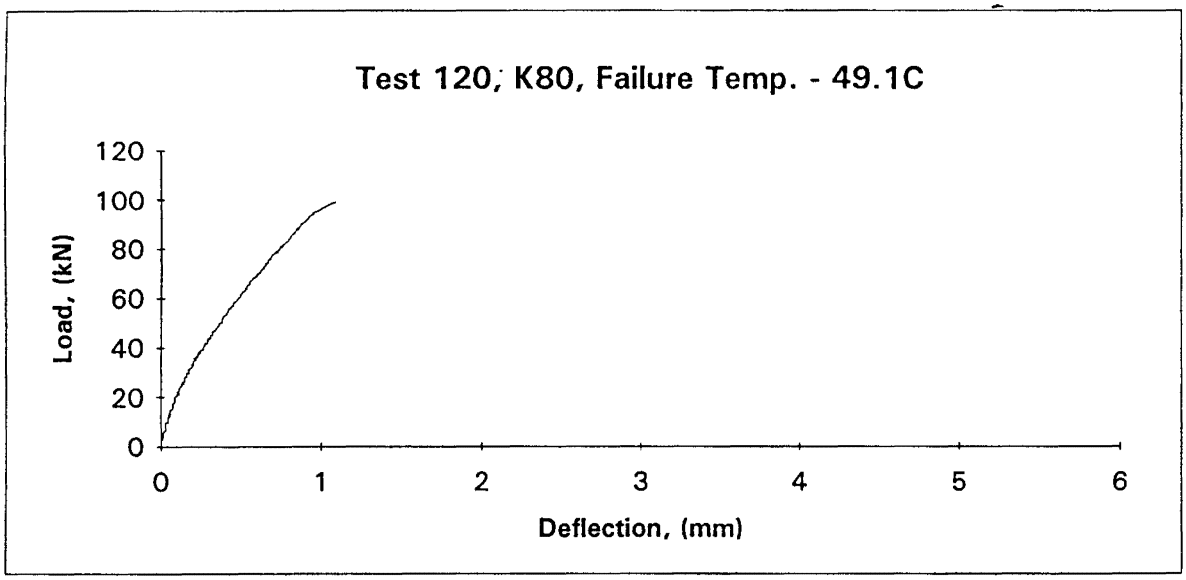
Test 120, K80, Failure Temp. - 49.1C
Load, (kN)
120
100
80
60
40
20
0
0
1
2
3
4
5
6
Deflection, (mm)

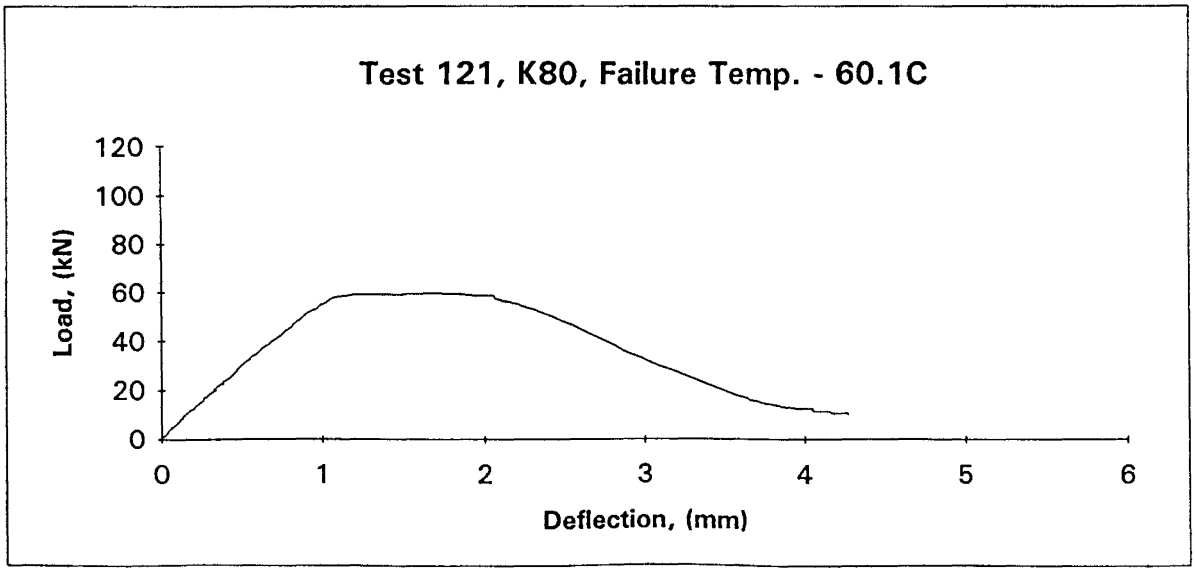
Test 121, K80, Failure Temp. - 60.1C
Load, (kN)
120
100
80
60
40
20
0
0
1
2
3
4
5
6
Deflection, (mm)

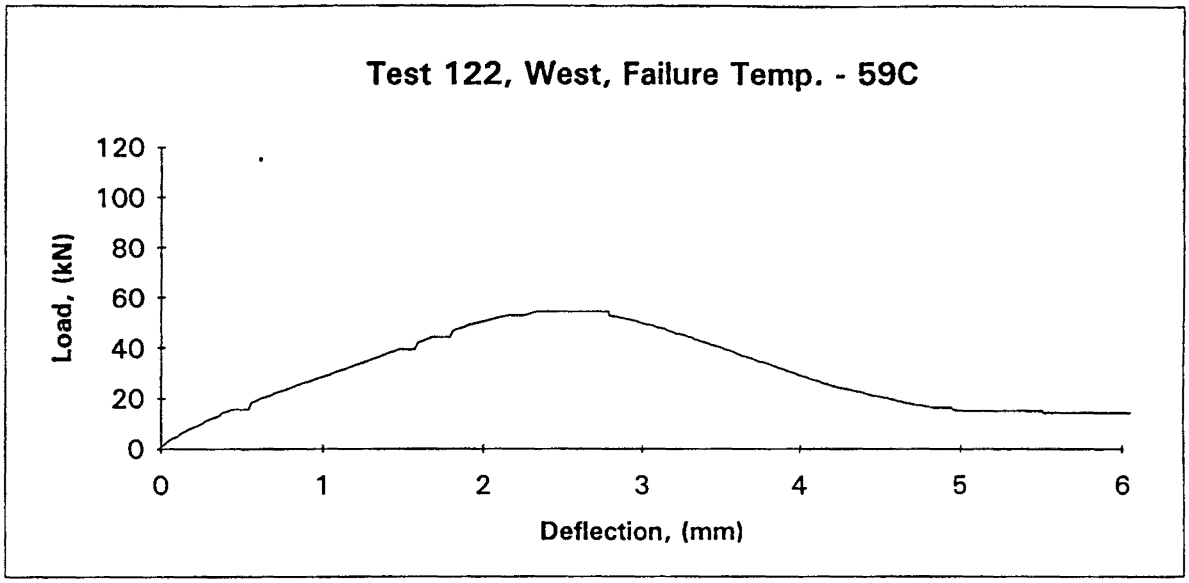
Test 122, West, Failure Temp. - 59C
Load, (kN)
120
100
80
60
40
20
0
0
1
2
3
4
5
6
Deflection, (mm)

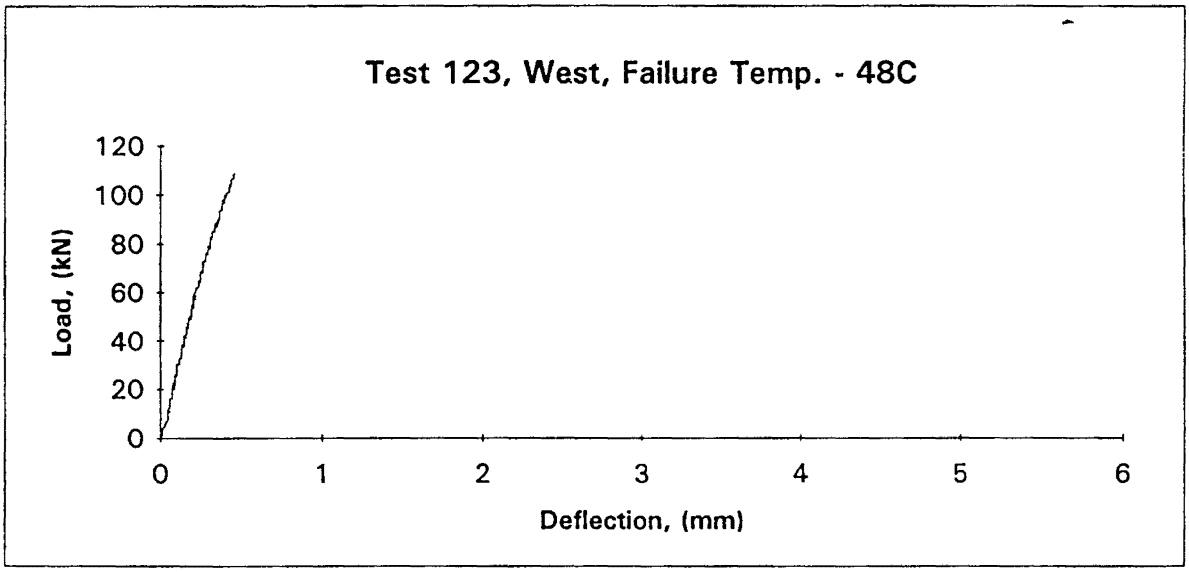
Test 123, West, Failure Temp. - 48C
Load, (kN)
120
100
80
60
40
20
0
0
1
2
3
4
5
6
Deflection, (mm)

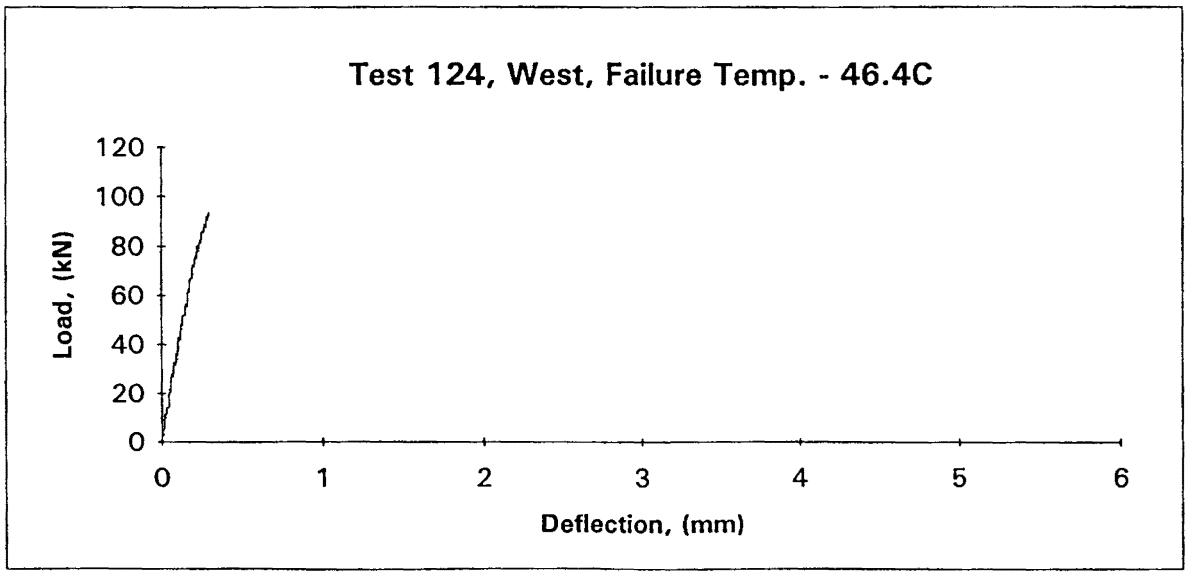
Test 124, West, Failure Temp. - 46.4C
Load, (kN)
120
100
80
60
40
20
0
0
1
2
3
4
5
6
Deflection, (mm)

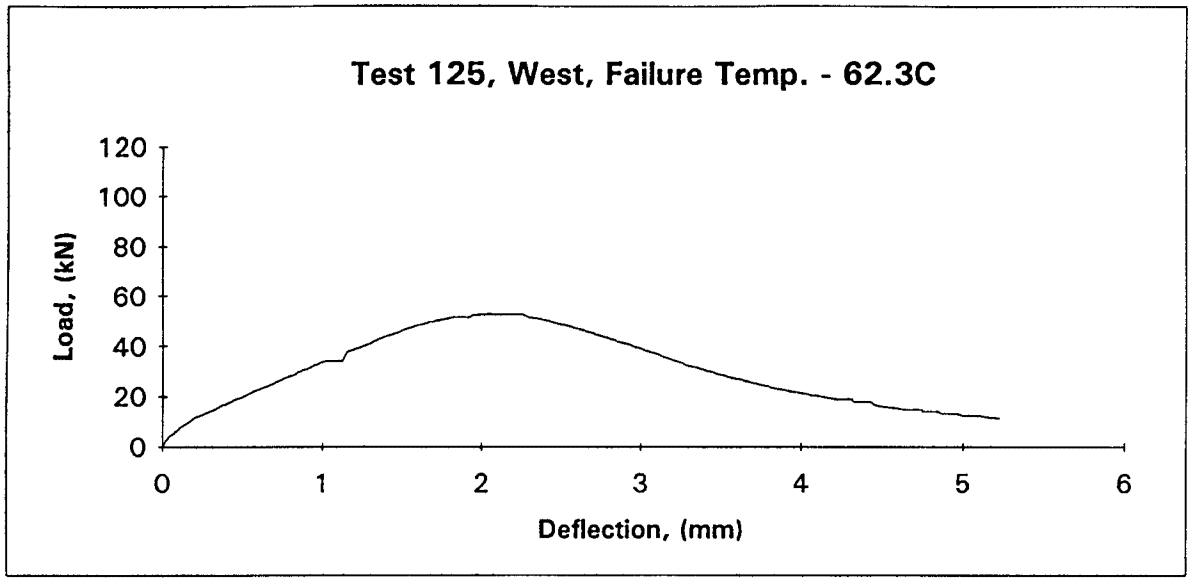
Test 125, West, Failure Temp. - 62.3C
Load, (kN)
120
100
80
60
40
20
0
0
1
2
3
4
5
6
Deflection, (mm)

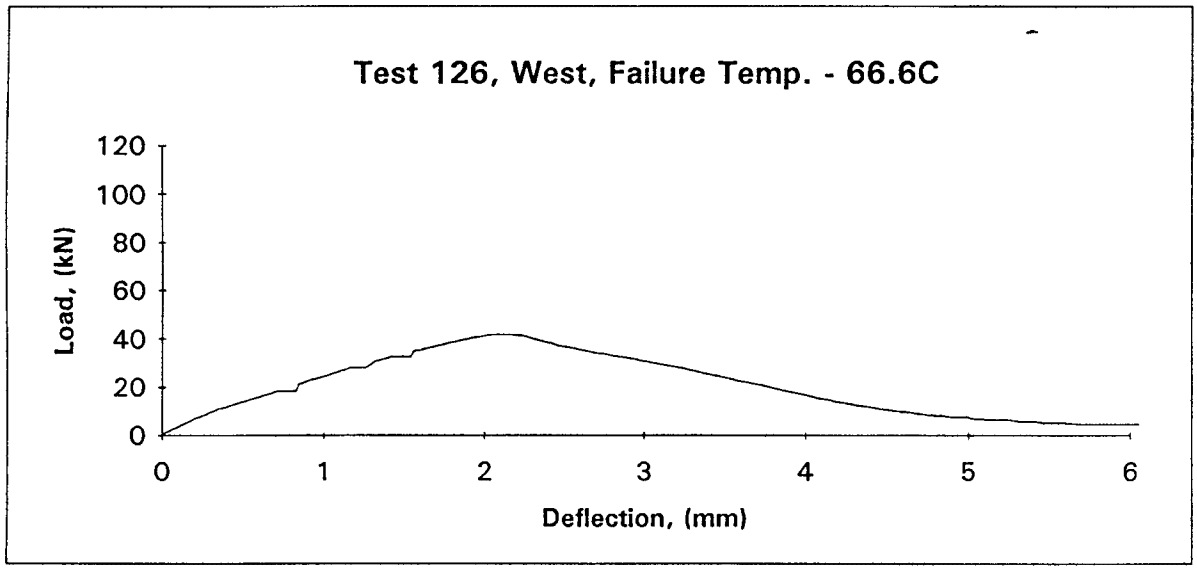
Test 126, West, Failure Temp. - 66.6C
Load, (kN)
120
100
80
60
40
20
0
0
1
2
3
4
5
6
Deflection, (mm)

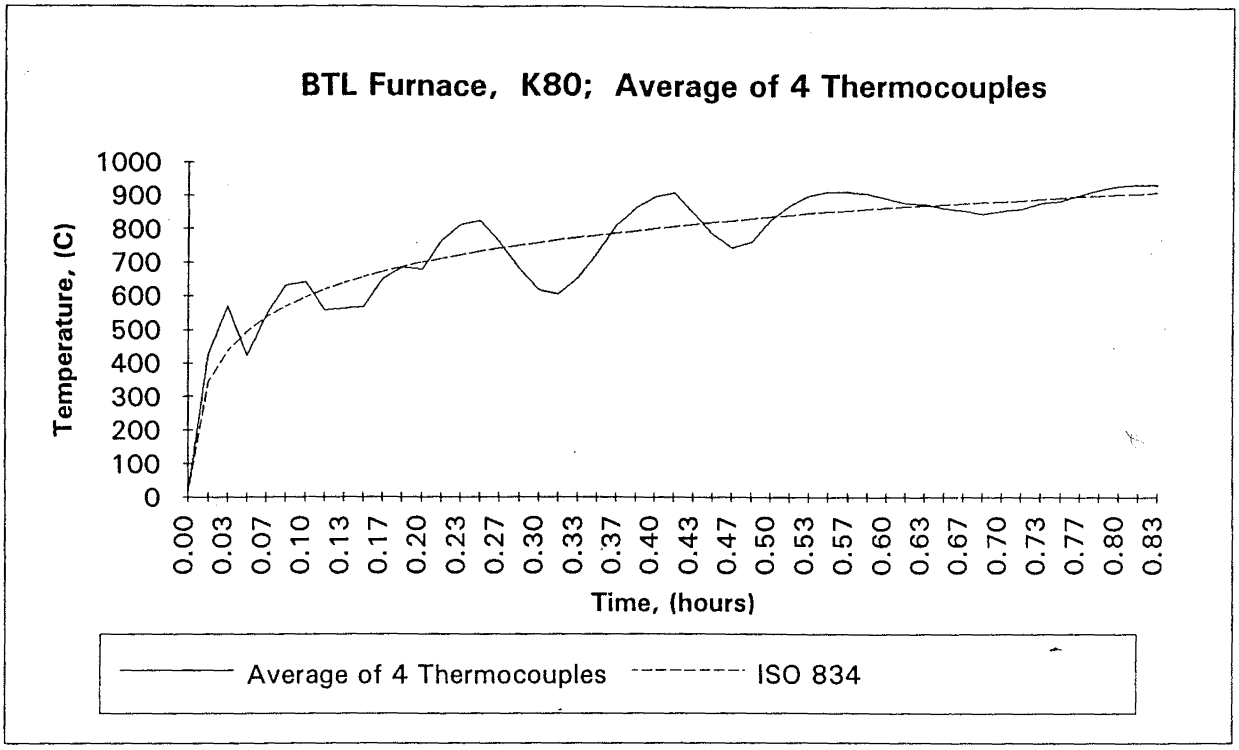
BTL Furnace, K80; Average of 4 Thermocouples
Temperature, (C)
1000
900
800
700
600
500
400
300
200
100
0
0.00
0.03
0.07
0.10
0.13
0.17
0.20
0.23
0.27
0.30
0.33
0.37
0.40
0.43
0.47
0.50
0.53
0.57
0.60
0.63
0.67
0.70
0.73
0.77
0.80
0.83
Time, (hours)
Average of 4 Thermocouples
ISO 834

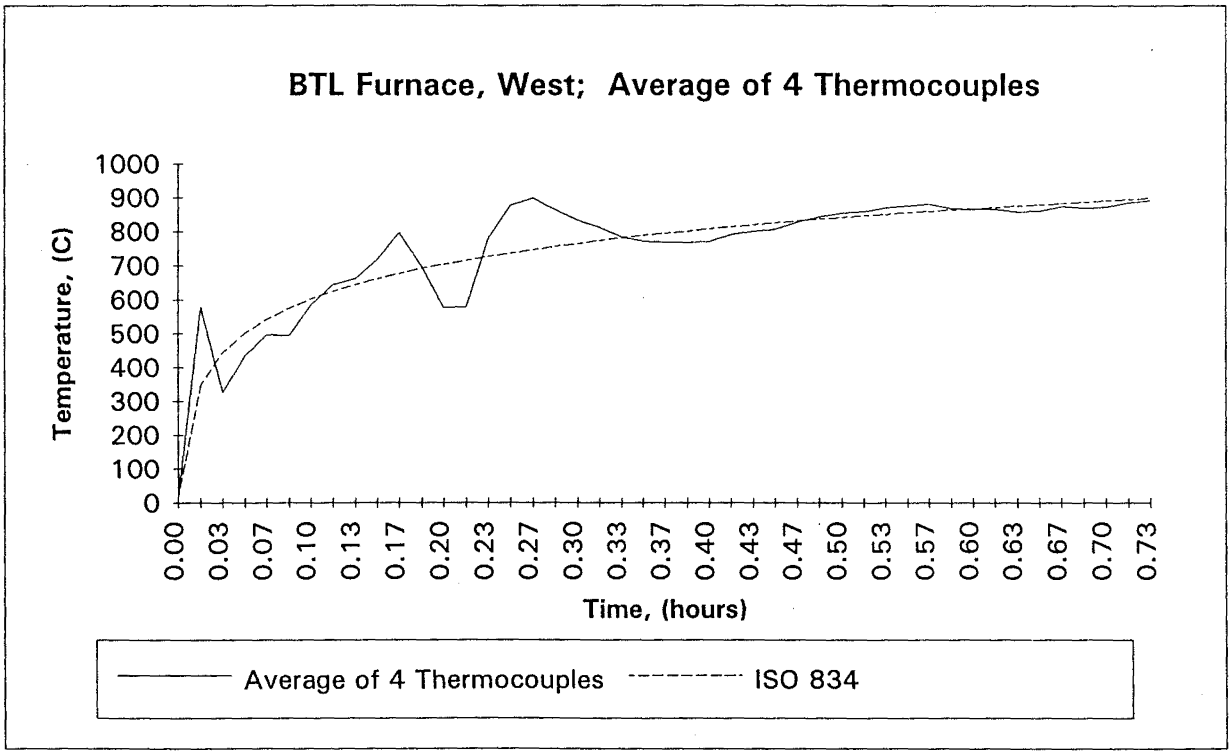
BTL Furnace, West; Average of 4 Thermocouples
Temperature, (C)
1000
900
800
700
600
500
400
300
200
100
0
0.00
0.03
0.07
0.10
0.13
0.17
0.20
0.23
0.27
0.30
0.33
0.37
0.40
0.43
0.47
0.50
0.53
0.57
0.60
0.63
0.67
0.70
0.73
Time, (hours)
Average of 4 Thermocouples
ISO 834